Molecular Mechanisms of Reovirus Oncolysis

by

Da Pan

Submitted in partial fulfilment of the requirements
for the degree of Doctor of Philosophy

at

Dalhousie University
Halifax, Nova Scotia
October 2011

DALHOUSIE UNIVERSITY

DEPARTMENT OF MICROBIOLOGY AND IMMUNOLOGY

The undersigned hereby certify that they have read and recommend to the Faculty of Graduate Studies for acceptance a thesis entitled "Molecular Mechanisms of Reovirus Oncolysis" by Da Pan in partial fulfillment of the requirements for the degree of Doctor of Philosophy.

Dated: October 26th, 2011

External Examiner: _____

Research Supervisor: _____

Examining Committee: _____

_____

_____

Departmental Representative: _____

DALHOUSIE UNIVERSITY

DATE: October 26th, 2011

AUTHOR: Da Pan

TITLE: Molecular Mechanisms of Reovirus Oncolysis

DEPARTMENT OR SCHOOL: Department of Microbiology and Immunology

DEGREE: PhD CONVOCATION: May YEAR: 2012

_____

Signature of Author

Table of Contents

List of Tables

List of Figures

Abstract

Mammalian reovirus is a naturally benign virus that preferentially replicates in cancer cells (reovirus oncolysis) and has been tested as a potential cancer therapy *in vitro*, *in vivo* and in clinical trials for treating cancers from a wide range of origins.

Reovirus-induced apoptosis has been shown to be important for reovirus oncolysis. The tumor suppressor protein p53 plays vital roles in mediating host apoptosis but its effect on reovirus oncolysis has not been fully understood and hence investigated. Data here show that p53 does not affect reovirus replication or reovirus-induced apoptosis in human cancer cells. However, significant enhancement of the reovirus-mediated apoptosis is induced by addition of p53 accumulators/activators such as a MDM2 antagonist Nutlin-3a or sub-lethal concentrations of chemotherapy drugs. This enhanced cell death is p53-dependent, requires NF-κB activation and p53 target genes *p21* and *bax*. Furthermore, a combination of reovirus and p53 accumulators/activators directly results in significantly higher level of reovirus dissemination and spread. One of the hurdles for current chemotherapy in patients is the side effects caused by high concentrations of cytotoxic drugs. Hence, a therapeutic regime using the combination of reovirus and sub-lethal (lower concentrations of) chemotherapeutics that induce p53 activation/accumulation potentially can both enhance tumor regression and reduce the side effects in patients.

Ras mutation, one of the most prevalent mutations in human cancer, has been implicated to determine the susceptibility of cancer cells to reovirus infection. However, the underlying mechanism of reovirus preferential replication needs to be further delineated. Quantitative analysis was used to compare individual steps of reovirus replication between non-transformed and Ras-transformed NIH 3T3 cells. Contrary to previous reports, reoviral protein synthesis is shown to be comparable between non-Ras and Ras-transformed cells. Meanwhile, although reovirus binding and internalization is not affected by Ras-transformation, reovirus uncoating is enhanced in Ras-transformed cells. Ras-transformation also enables reovirus to better spread to neighboring cells through apoptosis. Furthermore, reovirus infection of Ras effector mutant cells that activate specific Ras effector pathways indicate that sub-Ras pathways play different roles in enhancing reovirus preferential replication in Ras-transformed cells and therefore provide additional targets for cancer therapy.

List of Abbreviations Used

5-FU: 5-Fluorouracil

AA: antibiotic-antimycotic

ActD: Actinomycin D

AIF: apoptosis inducing factor

ATCC: American Type Culture Collection

ATP: Adenosine 5′-triphosphate

Bax: Bcl-2 associated X protein

Bcl-2: B cell lymphoma 2

BSA: Bovine serum albumin

Chk: Checkpoint kinase

CNS: central nervous system

DC: Dentritic cell

Dox: Doxorubicin

DTT: Dithiothreitol

EGTA: Ethylene glycol-bis(2-aminoethylether)-*N,N,N′,N′*-tetra-acetic acid

EMSA: electrophoretic mobility shift assay

Etp: Etoposide

FACS: fluorescence-activated cell sorting

FADD: Fas-associated Death Domain

FBS: fetal bovin serum

GAP: GTPase-activating protein

GTP: Guanosine 5′-triphosphate

IAPs: inhibitor of apoptosis proteins

IFN: interferon

IκBs: inhibitors of NF-κB

IKK: IκB kinase

i.p.: intraperitoneal

IPS-1: IFN-β promoter stimulator 1

IR: Ionizing radiation

IRF-3: interferon regulatory factor 3

ISVP: intermediate subviral particles

i.t.: intratumoral

JAM: junctional adhesion molecule

JMEM: Joklik's modified Eagle's medium

MDA5: melanoma differentiation-associated protein 5

MDM2: murine double minute 2

MEF: mouse embryonic fibroblast

MEM: modified Eagle's medium

MOI: multiplicity of infection

NARA: neutralizing anti-reovirus antibodies

NF-κB: Nuclear Transcription Factor κB

NOD-SCID: non-obese diabetic (NOD)-severe combined immune-deficient

NT: no treatment

PBS: phosphate buffered saline

PCR: polymerase chain reaction

pfu: particle forming unit

PI: propidium iodide

PKR: double-stranded RNA activated protein kinase

PUMA: p53 upregulator of apoptosis

RIG-I: retinoic acid-inducible gene I

RITA: Reactivation of p53 and induction of tumor cell apoptosis

rpm: revolutions per minute

RT: room temperature

s.c.: subcutaneously

SDS-PAGE: dodecyl sulfate polyacrylamide gel electrophoresis

Smac/DIABLO: second mitochondria-derived activator of caspase/direct binding of inhibitor of apoptosis protein (IAP) with low isoelectric point, PI

SPAK/JNK: stress activated c-jun N-terminal kinase

TBK1: Tank Binding Kinase 1

TLRs : Toll-like receptors

TSC2: tuberous sclerosis complex 2

UV: ultroviolet

Acknowledgements

I want to give my sincere thank you to my supervisor Dr. Patrick W.K. Lee for giving me this life-changing opportunity to work in his lab and to be able to grow independently as a scientist with his guidance and support. Patrick, you made me realize how passionate a scientist should be, and that to thrive in any career, passion and hard work are the keys. You also showed me how a positive attitude can be transforming in a negative situation. Without the enthusiasm and excitement you show us everyday, the lab would not be the "LEE LAB"!

I also want to thank two of my best friends I made since coming to the lab: Drs. Paola Marcato and Maya Shmulevitz. I cannot imagine a lab experience without you! Little by little, you girls implanted me with logical thinking as well as techniques required to complete this thesis work. I also feel as if I grew under your wings. I don't know how many times I cried to you girls and sought not only suggestions but shoulders to lean on and a source of courage to carry on. Life can be difficult, but friends make it wonderful! I am so lucky I met and worked with you. I would not be me today without you.

I want to thank the rest of the Lee lab: Pan, thank you so much for introducing me to this lab and being so patient with me throughout the years. I don't know how many times I asked for protocols, plasmids, chemicals, etc. from you. You are one of the most generous persons I have ever met! Cheryl, thank you for being such a great friend and being so understanding. I will miss you so much! Katy, what a rich soul you are. I envy your energy and enthusiasm about life you show almost everyday. I love sharing my little secrets with you here and there. We gradually found that we had a lot in common. I hope

we will be friends for a long time. Rich and Drew, thank you very much for all the late-night discussions in the lab at the beginning of this journey and all the drinks we had those days. Remember the first time the lab brought me out for my birthday and I slept on the table? Good times☺ Christine and Laura, thank you for organizing the girls' nights and invited me out for social events and including me into many "Canadian" activities. You helped me learn this country and culture that I have become very fond of it! Daniel, welcome again to the Lee lab. I think you are such a great addition to the lab. Your honesty and humor are amazing and good luck with the research. Shashi, Shashi, why do I put you last in this list? Because you are all the possibilities! You really showed me how possible life can be as far as we can think! Inside the box or outside the box, our brain is our power box! Don, thank you so much for getting the EM images of reovirus and ISVP for me. Such a good quality control☺ I also want to thank you for all the snacks and support you offered throughout the years. You are a good friend!

I also want to thank my supervisory committee members: Drs. Duncan, Singer and Ridgeway. Thank you for all the suggestions, discussions and recommendations. I will not be able to complete this work without your support.

Last but certainly not the least, I want to thank my dear husband, my family and my extended family. Without your love, I would not be able to do this. Greg, how lucky I am to have met you in this journey and you fill my life with love and excitement. Your support makes today possible. I am so looking forward to the new life ahead of us.

Chapter 1 Introduction

1.1. Reovirus

Reoviridae is a family of non-enveloped double-stranded RNA (dsRNA) viruses that ubiquitously infect vertebrates, invertebrates, and plants. *Reoviridae* currently consists of twelve virus genera (for the most updated list of viruses belonging to *Reoviridae*, see *ICTVdB-The Universal Virus Database, version 4.* http://www.ncbi.nlm.nih.gov/ICTVdb/ICTVdB/). Mammalian reovirus (*r*espiratory, *e*nteric, *o*rphan virus) belongs to the *Reoviridae* family and was so named because of its isolation from human respiratory and gastrointestinal tracts and its lack of connection to any severe disease state (Sabin 1959). The mammalian reovirus isolates that have been studied in the laboratory for decades are serotype 1 strain Lang (T1L), serotype 2 strain Johns (T2J), serotype 3 strain Dearing (T3D) and strain Abney (T3A) (Ramos-Alvarez and Sabin 1958; Sabin 1959; Rosen et al. 1960). These strains are only associated with mild, subclinical symptoms. However, one case of acute respiratory disease in human caused by a reovirus was discovered in 2007, which was caused by a previously unknown, bat-origin reovirus that is serologically unrelated to the commonly isolated mammalian reovirus strains (Chua et al. 2007). A few other new reovirus strains such as type 2 Winnipeg (Hermann et al. 2004; Jiang et al. 2006), serotype 1 (Johansson et al. 1996), serotype 3 (T3C96) (Tyler et al. 2004), and MRV2Tou05 (Ouattara et al. 2011) were also identified from patient samples of young children who were diagnosed with meningitis, necrotizing encephalopathy or other central nervous system (CNS) pathological symptoms.

Extensive studies with reovirus over the years have defined the general process of its replication. However, since the recent discovery that T3D reovirus preferentially replicates in cancer cells (reovirus oncolysis), the focus of much research has shifted to defining the cellular characteristics of cancer cells which make them intrinsically permissive to reovirus infection, as well as applying reovirus as a cancer therapeutic agent. Therefore, I focus here on reovirus infection in the context of cancer and highlight the signaling pathways of cancer cells that make them highly infectible by reovirus. Henceforth, unless otherwise stated, I refer to T3D reovirus as reovirus in this chapter.

1.2. Biology of Reovirus: Structure and Replication

Reovirus has a segmented, double-stranded RNA genome consisting of ten double-stranded RNA segments which are grouped into three size classes: small, medium or large (S, M and L). Each segment of the genome encodes one viral protein, with the exception of the S1 segment that encodes two proteins (σ1 and σ1S). Eight of the eleven viral proteins are structural proteins that appear in the viral particles, and the remaining non-structural proteins are essential players in completing the replication of reovirus. The dsRNA reovirus genome is surrounded by two concentric protein shells: the inner and outer capsids. The inner capsid consists of λ1, λ3, μ2, σ2, and the outer capsid consists of μ1, σ1, σ3, and λ2. Protein μ1 (76 kDa) undergoes autocleavage, yielding a small 4.2-kDa fragment μ1N and the complementary fragment μ1C. Proteins μ1N, μ1C and a small amount of μ1 all appear to be components of the mature virions (Smith et al. 1969; Pett et al. 1973; Jayasuriya et al. 1988). However, Nibert *et al.* (Nibert et al. 2005) recently showed that using certain conditions (high pH, absence of reducing agent and low

temperature) to disrupt reovirus for protein separation on polyacrylamide gel, a high percentage of intact μ1 protein could be recovered, suggesting that μ1 autocleavage might be an important process for virus disassembly during reovirus entry. Reovirus virions are converted into two distinct types of subviral particles during infection, the intermediate subviral particles (ISVPs) (Borsa et al. 1973), and cores (Smith et al. 1969). Both subviral particles are isolatable and can be generated *in vitro* (Bodkin et al. 1989).

As illustrated in Fig. 1.1, reovirus infection begins with virus binding to cell surface receptors, such as sialic acid and/or the junctional adhesion molecule (JAM) (Paul et al. 1989; Barton et al. 2001). Following binding, reovirus enters cells through receptor-mediated endocytosis. Beta-integrin plays a role in mediating reovirus internalization following attachment, possibly through its interaction with λ2 protein (Maginnis et al. 2006). Once in acidified endosomes or lysosomes, reovirus uncoating/disassembly (digestion of σ3 protein and cleavage of μ1/μ1C into δ) occurs in a protease-dependent manner, and ISVPs are formed (Sturzenbecker et al. 1987). ISVPs can be generated naturally by intestinal proteases as well as by trypsin and chymotrypsin *in vitro* (Bodkin et al. 1989). In addition, cysteine proteases are indicated to be important for reovirus uncoating (Baer et al. 1999; Ebert et al. 2002). It has been postulated that ISVP can penetrate membranes such as the plasma membrane as well as lysosomal membranes, and as a result viral particles enter the cytosol (Borsa et al. 1979; Chandran et al. 2002), where the remaining reovirus replication cycle occurs until virus release. During the process of penetration, σ1 proteins are shed off the particles and transcriptionally active cores are formed with conformational changes of the reovirus particles (Mendez et al. 2008). Subsequently, reovirus mRNAs are transcribed in the cores by reovirus RNA-dependent RNA polymerase λ3 independently of host cell machinery and are released into the

cytoplasm (primary transcription). Like all other viruses, reovirus mRNAs are translated into proteins using host protein translation machinery. Concordantly, newly transcribed mRNAs and certain viral proteins form cytoskeleton-associated structures "viral factories" (Sharpe et al. 1982), where new core particles will assemble. Nonstructural proteins μNS, σNS, and the structural protein μ2 form the framework for the viral factories and are crucial in recruiting viral transcripts and proteins and initiating assembly of virus particles (Kobayashi et al. 2006). Following progeny virus core formation, secondary transcription begins. Minus strand RNAs are synthesized within the assembled cores, using the plus strand RNAs as templates (Schonberg et al. 1971). At a later stage of the reovirus life cycle outer capsid proteins are added to the cores, halting transcription and completing the assembly of mature virus particles (Nibert et al. 2001). These mature virion particles are released from the cells, which can be mediated by apoptosis (Oberhaus et al. 1997). During the reovirus replication cycle, viral mRNA and proteins are exposed to the intracellular environment and can potentially trigger host signaling pathways. Studies in recent years reveal that reovirus exploits the deregulated Ras-signaling pathways in transformed cells for its own replication.

1.3. Cell Signaling Events in Cancer that Assist Reovirus Infection

In 1977, Hashiro *et al.* found that reovirus type 2 (T2J) infected tumor cells and certain spontaneously transformed cells, but that normal cells were resistant to infection (Hashiro et al. 1977). Later, Duncan *et al.* discovered that WI-38 cells (human embryonic lung cells) transformed by SV40 displayed drastically enhanced susceptibility to T3D reovirus infection (Duncan et al. 1978). However, it was not until the 1990s that a distinct

connection between reovirus and oncolysis was made, when it was shown that preferential replication of reovirus in transformed cells was dependent on having an activated Ras-signaling pathway (Strong et al. 1998). Further studies showed that a single injection of reovirus could induce tumor regression in a mouse xenograft model (Coffey et al. 1998). It was estimated that Ras mutations occur in more than 30% of human cancers (Rodenhuis 1992). When sub-Ras pathways are taken into consideration, a higher percentage of cancers would potentially be susceptible to reovirus. Since this discovery, studies of reovirus as a potential anti-cancer therapy have been aggressively pursued and reovirus is currently being tested in several clinical trials including a phase III clinical study of head and neck cancer (Bell 2010). Results of completed clinical trials are summarized in the following sections.

1.3.1. The Ras Signaling Pathway is Usurped by Reovirus

In 1993, the importance of epidermal growth factor receptor (EGFR) for increased susceptibility to reovirus was demonstrated (Strong et al. 1993). Following this observation, it was found that the *v-erbB* oncogene, which encodes a mutated EGFR homolog that lacks the extracellular ligand domain but has a constitutively active intracellular effector domain, confers enhanced cellular susceptibility to reovirus infection (Strong and Lee 1996). This finding indicated that successful reovirus production in transformed cells requires the intrinsic signaling events initiated by EGFR. Furthermore, cells that were transformed by activated *son of sevenless (sos)* or *ras*, both of which are key factors in Ras signaling pathways downstream of EGFR, are significantly more susceptible to reovirus compared to normal cells (Strong et al. 1998). These findings link the Ras signaling pathway to the preferential replication of reovirus in transformed cells.

1.3.2. Ras Signaling

Small GTP-binding proteins (G-proteins) comprise a superfamily of proteins that contribute to numerous cellular and physiological processes. These proteins can be structurally classified into sub-families such as Ras, Rho, Rab, Ran and Arf (Takai et al. 2001). Ras family proteins are small GTP-binding proteins and are at the hub of convergent signaling pathways activated by extracellular stimuli (Shields et al. 2000). Being GTPases, activation of Ras proteins is tightly regulated by a group of guanine nucleotide exchange factors, such as *sos*, and GTPase activating proteins, such as necrosis factor 1 (NF1). These factors control the cycling of Ras between its active GTP-bound state and its inactive GDP-bound state. In its GTP-bound state, Ras initiates signaling through numerous downstream cascades, which as shown in Fig. 1.2, control a plethora of cellular functions, such as trafficking, transcription, translation, cell cycle progression, differentiation and apoptosis (Malumbres and Pellicer 1998; Shields et al. 2000; Shaw and Cantley 2006). Constitutively activated Ras is insensitive to GAP (GTPase-activating protein) regulation and causes deregulation in signaling pathways. Activating mutations in Ras isoforms (H-, K- and N-Ras) are found in different human tumors and are among the most prevalent mutations in human cancer (Bos 1989; Rodenhuis 1992; Wittinghofer 1998).

Three of the main downstream signaling pathways regulated by Ras are the Raf/MEK/Erk pathway, the PI3K/Akt pathway and the RalGEFs/Ral pathway. Among the sub-Ras effectors, Raf is the most studied and is extensively targeted in cancer therapies that employ Raf-specific pharmaceutical inhibitors (Schreck and Rapp 2006; Gollob et al. 2006; Reddy and Bukowski 2006; Roberts and Der 2007). Activated Ras

interacts with Raf through a Ras-binding domain (RBD) and recruits Raf onto the plasma membrane where Raf is activated. Activated Raf then phosphorylates and activates MEK1/2 which in turn phosphorylates and activates p42 and p44 Erk1/2. Activated Erk1/2 can phosphorylate a group of substrates including p90 ribosomal S6 kinase (RSK) and TSC2 (tuberous sclerosis complex, also known as hamartin) (Ma et al. 2005). It also controls cell proliferation, transcription, translation and the apoptosis aspects of transformation (Malumbres and Pellicer 1998). Lysosomal proteases like cathepsin L (Baer et al. 1999; Ebert et al. 2002), cathepsin B (Ebert et al. 2002) and neutrophil elastase (Takai et al. 2005) are responsible for reovirus uncoating. The production and activity of cathepsin L is up-regulated by the activated Raf pathway in murine fibroblast cells. However, in epithelial cells, all three main sub-Ras pathways are needed (Collette et al. 2004), indicating that the downstream pathways activated by Raf may be cell-type dependent.

The next most extensively studied sub-Ras pathway is PI3K/Akt. Phosphatidylinositol 3-kinase (PI3K), catalyzes the conversion of phosphatidylinositol (4,5)-biphosphate (PtdIns[4,5]P_2) to phosphatidylinositol (3,4,5)-triphosphate (PtdIns[3,4,5]P_3) in response to growth factors and cytokines. PI3K and its lipid second-messenger products PtdIns[3,4,5]P_3 and PtdIns[4,5]P_2 control cell proliferation, cell survival, cell-cycle regulation and cell metabolism (Shaw and Cantley 2006). The most important downstream effector of PI3K is Akt (also known as protein kinase B, PKB). PtdIns[3,4,5]P_3 can directly interact with Akt and cause the translocation of Akt to the plasma membrane followed by the activation of this kinase. Activated Akt regulates a numerous downstream effectors such as glycogen synthase kinase-3 (GSK-3) and TSC2. Since functional GSK-3 is linked to inhibitions of the cell cycle and Akt phosphorylation

of GSK-3 can inhibit its function, activation of Akt is believed to cause abnormal cell growth and has repeatedly been shown to be important for Ras-mediated transformation (Datta et al. 1997; Kauffmann-Zeh et al. 1997).

The third so called "orphan" sub-Ras effector pathway is RalGEFs/Ral. RalGEFs represent a group of guanine exchange factors that stimulate the GDP/GTP exchange of Ral and activate the protein in a Ras-dependent manner (Urano et al. 1996). Activated Ral binds to its downstream effectors such as Cdc42/Rac, phospholipase D and Ral binding protein (RalBP1, also known as RIP1 or RLIP76) (Feig 2003; Camonis and White 2005) and is closely associated with cell functions such as vesiclular formation and Golgi trafficking. RalGEFs have been shown to be essential components of Ras-mediated transformation (Hamad et al. 2002; Rangarajan et al. 2004). There are two isoforms of human Ral proteins, RalA and RalB. The two isoforms were shown to collaborate to both enhance proliferation and limit cell death (Chien and White 2003). Moreover, RalB is able to directly recruit and activate the atypical IκB kinase family member Tank Binding Kinase 1 (TBK1) to activate NF-κB and support survival in cancer cells (Henry et al. 2000; Chien et al. 2006). Although RalB-dependent activation of TBK1 is dispensable for normal cells, it helps respond to dsRNA virus infection (Chien et al. 2006). It was also shown that the RalGEFs/Ral pathway plays a role in the metastasis of prostate cancer to bone (Yin et al. 2007), further indicating the importance of this sub-Ras pathway in tumorigenesis.

Other Ras effector pathways, such as the Tiam and the Rho/Rac pathways, control many aspects of cell transformation mediated by Ras, and cross-talk between different sub-Ras pathways is common (Malumbres and Pellicer 1998). Pathways initiated by Ras-

transformation may signal in a cooperative fashion to enable preferential reovirus replication and cell killing in transformed cells. It is therefore important to determine the specific steps of reovirus replication that are enhanced by Ras-transformation and which sub-Ras pathway might contribute to the augmentation of individual steps.

1.4. Reovirus-triggered Apoptosis in Host Cell

By analyzing the morphological changes and fragmentation of cellular DNA of reovirus infected cells, it was found that reovirus causes the host cell to undergo apoptosis (Tyler et al. 1995). One of the important tools used in reovirus studies is reovirus reassortment. When host cells are infected with two different strains of reovirus, the progeny virus generated from the infected cells may have genomes composed from both parent genomes. Newly assembled viruses will contain a mixture of the ten double-stranded RNA segments from the two genomes of the two infecting virions. Using reovirus reassortants, strain-specific signaling pathways induced by reovirus infection can be mapped to certain viral genes. Using reovirus reassortments, the reovirus S1 and M2 gene segments, which encode σ1 and μ1 proteins respectively, were found to be critical for reovirus-mediated apoptosis (Tyler et al. 1995; Liemann et al. 2002). Reovirus infection also triggers host cell signaling events such as the activation of the stress-activated c-jun N-terminal kinase (SAPK/JNK) pathways, and the activation of Nuclear Transcription Factor κB (NF-κB) pathway. These pathways are critical players in reovirus-triggered apoptosis. Meanwhile, S1 and M2 genes are implicated to be important for triggering these host pathways (Clarke et al. 2001b; Clarke and Tyler 2007). The exact nature of involvement of these proteins in activating the host signaling pathways is not clear. Genome-wide analysis of gene expression changes upon reovirus infection

(DeBiasi et al. 2003) revealed that altered gene transcripts are highly clustered in cellular apoptosis and DNA repair pathways. Recently, the long-awaited plasmid based reverse genetics system for double-stranded RNA viruses has been successfully produced (Kobayashi et al. 2007), enabling reovirus researchers to precisely mutate individual genes and incorporate them into infectious viral particles. This technology will help us better understand the roles individual reoviral proteins play in triggering host signaling pathways, including the apoptotic pathways.

1.4.1. Reovirus-triggered Apoptosis

It was first observed that apoptosis triggered by reovirus infection of human embryonic kidney HEK293 cells could be drastically decreased by interfering with TNF-related apoptosis-inducing ligand (TRAIL)-receptor interaction, including pretreatment using anti-TRAIL (TRAIL1/2) antibodies, overexpression of decoy death receptors DcR1/2, or incubation with soluble TRAIL receptors such as DR5 (Clarke et al. 2000; Clarke et al. 2001a). Antibodies against Fas or soluble TNF receptor had no effect on reovirus-triggered apoptosis, indicating Fas and TNF are likely not involved in reovirus-triggered apoptosis. Downstream adapter protein Fas-associated Death Domain (FADD) mediates the downstream activation of caspases following ligand-receptor interactions. When a dominant negative (DN) FADD mutant was expressed, reovirus-triggered apoptosis was reduced significantly (Clarke et al. 2000). Moreover, treatment with caspase-8 inhibitor was shown to abrogate reovirus-triggered apoptosis (Rodgers et al. 1997). These findings suggest that an extrinsic apoptosis pathway is triggered by reovirus through TRAIL/death receptor/FADD and caspase-8 (Fig. 1.3A).

It was later shown that the mitochondrial pathway also plays an important role in reovirus-triggered apoptosis (Kominsky et al. 2002a). Release of cytochrome c and Smac/DIABLO (second mitochondria-derived activator of caspase/direct binding of inhibitor of apoptosis protein (IAP) with low isoelectric point, PI) but not apoptosis inducing factor (AIF), and cleavage of pro-apoptotic protein Bid were observed following reovirus infection (Rodgers et al. 1997; Kominsky et al. 2002a; Kominsky et al. 2002b). Overexpression of DN-FADD could block the release of cytochrome c and cleavage of Bid, indicating that activation of caspase-8 is critical to initiate the mitochondria-dependent pathway after reovirus infection (Rodgers et al. 1997; Kominsky et al. 2002a). Overexpression of B cell lymphoma 2 (Bcl-2) inhibited release of cytochrome c or Smac/DIABLO and activation of effector caspases-3 and -7, implicating the mitochondrial apoptosis pathway involved in reovirus-mediated apoptosis (Rodgers et al. 1997; Kominsky et al. 2002a). Meanwhile, expression of a dominant negative form of caspase-9 did not prevent the activation of caspase-3 and the resulting cleavage of Poly(ADP-ribose) polymerase (PARP), suggesting that activation of caspase-9 is dispensable to reovirus-mediated apoptosis (Kominsky et al. 2002b). As a result of Smac/DIABLO release induced by reovirus infection, anti-apoptotic inhibitor of apoptosis proteins (IAPs) including XIAP, c-IAP1 and survivin were downregulated while c-IAP2 level remained relatively the same throughout the reovirus replication cycle (Kominsky et al. 2002b), indicating the reovirus infection triggers selective downregulation of cellular IAPs. These results suggest that reovirus-triggered apoptosis involves both extrinsic and intrinsic apoptosis pathways (Fig. 1.3A).

It was also observed that reovirus infection caused release of TRAIL from host cells (Clarke et al. 2000). In addition, reovirus could sensitize cells to TRAIL-induced

apoptosis (Clarke et al. 2000; Clarke et al. 2001a; Clarke and Tyler 2007). Several cancer cell lines were tested for TRAIL sensitivity and it was shown that reovirus and TRAIL could synergistically kill cancer cells and this effect is TRAIL-dependent and caspase-8 mediated (Clarke et al. 2001a; Clarke and Tyler 2007). Reovirus infection of ovarian cancer cells showed that expression of cFLIP, a negative mediator of apoptosis initiated by TRAIL, decreased after infection. Downregulation of cFLIP by RNA interference could render cancer cells more sensitive to TRAIL-induced apoptosis after reovirus infection (Clarke and Tyler 2007). The combination of reovirus and TRAIL may represent a novel cancer therapy for TRAIL-resistant cancer.

1.4.2. Activation of NF-κB by Reovirus Infection

One of the early signaling events following reovirus infection is the activation of NF-κB, which is important to reovirus-mediated apoptosis (Connolly et al. 2000; Clarke et al. 2003). NF-κB is a transcription factor that regulates cellular functions such as immune response, inflammation and cell survival in response to different signals. Deregulated NF-κB has been implicated in human diseases including cancer (Siebenlist et al. 1994; Thanos and Maniatis 1995; Baeuerle and Baltimore 1996; Karin 2006; Inoue et al. 2007). NF-κB transcription factors are assembled through dimerization of the five Rel/NF-κB proteins: RelA(p65), c-Rel, RelB, NF-κB1(p50/p105) and NF-κB2(p52/p100) (Baldwin, Jr. 1996). Proteins p50 and p52 are proteolytic products of p105 and p100 respectively. Latent NF-κB is retained in the cytoplasm by the bindings of inhibitors of NF-κB (IκBs) for RelA and c-Rel, or NF-κB2p100 for RelB. NF-κB activation involves its translocation from the cytoplasm to the nucleus. In a canonical NF-κB activation

pathway, site-specific phosphorylation of IκBs by the IκB kinase (IKK) complex results in ubiquitination and proteasomal degradation of these NF-κB inhibitor proteins (Palombella et al. 1994; Chen et al. 1995; Traenckner et al. 1995; Baldwin, Jr. 1996; Whiteside et al. 1997; Heusch et al. 1999), and this allows the prototypical NF-κB, which contains p50/RelA dimers, to translocate into the nucleus. The IKK complex contains two catalytic subunits, IKKα and IKKβ, and two regulatory subunits, IKKγ/NEMO and ELKS (Karin and Ben-Neriah 2000; Ghosh and Karin 2002; Ducut Sigala et al. 2004). IKKβ is essential for NF-κB activation in the canonical pathway in the presence of IKKγ/NEMO. In an alternative NF-κB activation pathway, IKKα is phosphorylated by NF-κB-inducing kinase (NIK) and in turn phosphorylates NF-κB2p100 (Yamaoka et al. 1998; Schomer-Miller et al. 2006), targeting NF-κB2p100 for ubiquitination and degradation. NF-κB dimers containing RelB or p52 are then released and translocate into nucleus. A third pathway of NF-κB activation involves IκBα phosphorylation by CK2, followed by ubiquitination and degradation (Yamaoka et al. 1998; Schomer-Miller et al. 2006).

It was determined in electrophoretic mobility shift assays (EMSA) that NF-κB was activated (bound to its DNA consensus sequence) following reovirus infection in HeLa, HEK293, L and Madin-Darby canine kidney (MDCK) cells (Connolly et al. 2000; Clarke et al. 2003). In HeLa cells, activation of NF-κB starts as early as 4 hours post infection (hpi), peaks at 10 hpi and starts to decline at 12 hpi (Connolly et al. 2000), indicating that NF-κB activation is an early event triggered by the infecting reovirus. Activation of NF-κB by reovirus infection results in the translocation of p65 and p50 into the nucleus. Reovirus-triggered apoptosis requires NF-κB activation because reovirus-induced apoptosis can be significantly blocked by: (a) a proteasome inhibitor which blocks degradation of IκBs; or (b) transient expression of a dominant-negative form of

IκBα which lacks the sites for ubiquitination and degradation and quenches activation of NF-κB (Connolly et al. 2000). Regulation of inhibitor protein IκBα, but not IκBβ or IκBε, is essential for reovirus-mediated NF-κB regulation. Blocking the activity of IKKα instead of IKKβ diminished translocation of RelA protein and as a result blocked the activation of NF-κB. In addition, reovirus-mediated apoptosis and NF-κB regulation both depend on IKKγ/NEMO, since cells lacking IKKγ/NEMO underwent a lower level of apoptosis after reovirus infection compared to normal cells (Hansberger et al. 2007). These results suggest that reovirus infection triggers the activation of NF-κB through an IKKα- and IKKγ/NEMO-dependent pathway (Fig. 1.3B).

In HEK293 cells, however, NF-κB activation was observed at an early time post infection but this activation was blocked at later times through inhibition of IκBα degradation (Clarke et al. 2003). Reovirus infection blocked NF-κB activation through stopping IκBα from being degraded at a later stage of the infection (Clarke et al. 2003). This downregulation of NF-κB sensitized HEK293 cells to TRAIL- or TNF-induced apoptosis. This study indicates that reovirus can both activate and inhibit NF-κB activation and that this regulation can be cell-type dependent. It is also possible that this cell-type dependent activation of NF-κB is a result of various signaling pathways activated in different cell lines.

In order to identify downstream events that are activated by NF-κB in reovirus infected cells, human HeLa cells were engineered to express a degradation-resistant mutant of IκBα in an inducible manner (O'Donnell et al. 2006). Expression of 112 genes under the activation of NF-κB was altered upon reovirus infection. Most of these genes have roles in the innate immune response and cell death programs. It will be interesting to identify how certain genes that are activated by NF-κB upon reovirus infection can

contribute to reovirus-triggered apoptosis, and which specific pathways are involved.

It was shown recently that reovirus activates interferon (IFN) regulatory factor-3 (IRF-3), an important factor in host immune response, and that IRF-3 is activated at a similar time when NF-κB is activated (Holm et al. 2007). Activation of IRF-3 requires retinoic acid-inducible gene-I (RIG-I) and interferon-β promoter stimulator-1 (IPS-1, also known as CARDIF, MAVS or VISA). Moreover, IPS-1 and IRF-3 are also required for reovirus-triggered apoptosis, indicating the involvement of apoptosis in anti-viral responses following reovirus infection (Fig. 1.3D). However, IPS-1 and IRF-3 are dispensable for activation of NF-κB, indicating that NF-κB activation might be mediated by signaling pathways other than RIG-I signaling.

1.4.3. JNK is Activated during Reovirus Infection

An important kinase in pathways that transduce extracellular stress-related signals, SAPK/JNK, was found to be activated after reovirus infection (Clarke et al. 2001b). Strain differences in inducing JNK activation were mapped to S1 and M2 viral genes which are also critical for reovirus-triggered apoptosis. Activity of JNK closely correlated with reovirus-induced apoptosis and c-jun was phosphorylated after reovirus infection (Clarke et al. 2001b). This was further confirmed by using an inhibitor of JNK which blocked reovirus-induced apoptosis, but not virus yield (Clarke et al. 2004). Furthermore, inhibition of JNK delayed the release of cytochrome c and Smac/DIABLO, with the latter an essential effector for reovirus-mediated apoptosis (Clarke et al. 2004). Using mouse embryonic fibroblast cells harboring either wild-type or no MEKK, an upstream kinase that activates JNK (Yujiri et al. 2000), it was shown that reovirus-induced caspase-3

activation was diminished in MEKK null cells, an effect similar to that caused by the JNK inhibitor (Clarke et al. 2004). These results suggest that JNK plays an important role in reovirus-induced apoptosis (Fig. 1.3C). Whether the activation of JNK and NF-κB in reovirus-mediated apoptosis is interconnected remains unclear at present.

1.4.4. Reovirus-triggered Host Signaling and Reovirus Uncoating/Disassembly

It was shown that reovirus-mediated apoptosis requires virus uncoating/membrane penetration, but not virus replication. Uncoating inhibitors such as ammonium chloride (NH_4Cl) and E64, both of which stop reovirus uncoating by inactivating proteases, can abolish reovirus-triggered apoptosis. On the other hand, *in vitro* generated ISVPs can infect cells and trigger apoptosis and are unaffected by these inhibitors (Connolly and Dermody 2002). Activation of NF-κB and JNK correlate with reovirus uncoating and reovirus-triggered apoptosis (Clarke et al. 2001b; Clarke and Tyler 2007). The importance of virus disassembly might indicate that the uncoating process of reovirus replication can release signals necessary to be recognized by host sensors. It will be of great interest to determine which host proteins or processes are able to recognize and respond to reovirus disassembly. As mentioned above in this chapter, reovirus μ1 protein is indicated to be important for reovirus-triggered apoptosis. Mutations in the μ1 protein that reduce the penetration efficiency of reovirus diminish activation of NF-κB as well as reovirus-induced apoptosis (Danthi et al. 2008b). Interestingly, mutations in the δ fragment (N terminus) of μ1C protein affect both penetration and reovirus-induced apoptosis (Danthi et al. 2008b), while plasmid-based expression of the φ fragment (C terminus) of μ1C protein is sufficient to induce apoptosis (Coffey et al. 2006). Using the reverse genetics

methodology, reovirus particles containing different single substitutions in the φ fragment of μ1C protein were created. It was discovered that the pro-death activation and the membrane penetration functions of μ1φ could be uncoupled (Danthi et al. 2008a). Since reovirus particles containing the penetration proficient μ1φ mutant could not induce apoptosis, it is possible that apoptosis is triggered subsequent to reovirus penetration and that the delivery of μ1φ fragment might serve as a signal to initiate reovirus-induced apoptosis (Danthi et al. 2008a). Therefore, it will be interesting to determine the cellular binding partner(s) of μ1φ fragment to determine how apoptotic signals are sent to NF-κB or JNK.

1.4.5. p53 and Reovirus Oncolysis

The role of the Ras signaling pathway has been extensively studied in reovirus oncolysis. However, p53, another important protein that plays vital roles in tumorigenesis, especially in mediating apoptosis, was not as thoroughly studied in reovirus oncolysis.

Since its discovery, p53 has been extensively studied as a tumor suppressor protein which is essential in deciding cell fate between DNA repair, cell cycle arrest and apoptosis upon damage. The most studied function of p53 is its role in transcriptional activation.

In a normal cell, the protein level of p53 is low due to its fast turnover, which is mediated by ubiquitination by MDM2 (or HDM2 in human) followed by proteasomal degradation. The Mdm2 gene is also a downstream transcription target of p53. Thus, activation of p53 can upregulate the expression of Mdm2, which in turn negatively regulates the stability and activity of p53, forming an autoregulatory feedback loop

(Mandinova and Lee 2011). Upon DNA damage, p53 is activated and undergoes extensive posttranslational modifications such as phosphorylation, methylation and acetylation. Activated p53 can then bind to its target DNA sequences in a sequence-specific manner and regulate the expression of genes involved in cell cycle arrest or apoptosis (Kern et al. 1991).

As a transcription activator, p53 can activate the transcription of target genes involved directly in both intrinsic (most notably) and extrinsic apoptotic pathways (Yu and Zhang 2004). For inducing the intrinsic apoptotic pathways, genes encoding proapoptotic Bcl-2 family proteins such as Bax (Bcl-2 associated X protein), PUMA (p53 upregulator of apoptosis), Noxa, and Bid were discovered to be downstream transcriptional targets regulated by p53 and their expression is upregulated by p53 upon DNA damage (Miyashita and Reed 1995; Oda et al. 2000; Nakano and Vousden 2001; Thornborrow et al. 2002; Jeffers et al. 2003). Proteins that are important for triggering extrinsic apoptotic pathways, such as the death receptor proteins DR4, DR5 and the Fas protein, were also demonstrated to be upregulated by p53 upon DNA damage (Sheikh et al. 1998; Muller et al. 1998; Liu et al. 2004). Meanwhile, the inhibition of damaged cells from entering the proliferation phase before DNA repair is also an important mechanism by which p53 ensures the integrity of the genome. p53 can upregulate genes that are involved in G1 or G2 cell cycle arrest, which include p21, Gadd45 and 14-3-3σ.

Previous studies demonstrated that p53 is induced in response to viral infection mediated by type I interferon (IFN) signaling, and can induce apoptosis upon RNA virus infection (Takaoka et al. 2003). Huang *et al.* tested whether reovirus-induced apoptosis was affected by the status of p53 in human cancer cells and demonstrated the level of cell death induced by reovirus was not affected by the lack of p53 (Huang et al. 2004).

Recently, Kim *et al.* demonstrated that cell death was enhanced by reovirus infection in p53-deficient mouse embryonic fibroblasts (MEFs) compared to wild-type p53 cells. The difference between the two studies may be due to the cell types used. In addition, the possible role of p53 in other steps of reovirus replication was not studied in either of these studies. The important role of p53 in tumorigenesis makes it a good target for cancer therapy. Since the successful identification of Nutlins and their tumor regression functions tested *in vivo* and *in vitro*, drugs that can restore p53 functions in tumor cells (p53 activators) have been developed. These drugs have also been tested alone or in combination with other chemotherapy drugs *in vitro* and *in vivo* (Brown et al. 2011). Therefore, further studies on the possible role of p53 in reovirus oncolysis and its effect on the combination therapy of reovirus and p53-activators are needed.

1.5. Reovirus in Cancer Therapy

1.5.1. Animal Tumor Models for Reovirus Therapy

The linkage of reovirus infection to activated Ras signaling led to extensive experiments to test the potential of applying reovirus as a cancer treatment. Thus far, human colon, ovarian, breast, pancreatic and bladder cancer cell lines or *ex vivo* human tumor surgical specimens have been tested with reovirus infection and showed effective cancer killing (Hirasawa et al. 2002; Norman et al. 2002; Etoh et al. 2003; Hanel et al. 2004). Animal models using tumor cell implants have also been tested and nearly complete tumor regression occurred after intratumoral (*i.t.*) injection of reovirus (Hirasawa et al. 2002; Etoh et al. 2003; Yang et al. 2004; Hingorani et al. 2011). Generally, tumors implanted in immunocompromised animals need only a single

injection of reovirus, while immunocompetent animals require multiple injections of reovirus or in combination with immunosuppressive drugs to induce tumor suppression (Smakman et al. 2006b). Systemic intravenous (*i.v.*) therapy with reovirus not only regressed pediatric sarcoma xenografts but also inhibited metastatic tumor growth and improved the survival rate of the animals, raising the possibility of using reovirus to attack metastatic tumors in inaccessible locations (Yang et al. 2004; Smakman et al. 2006b; Hingorani et al. 2011). Although Ras mutations are rare in lymphoid malignancies, when lymphoid cell lines were tested for the efficacy of reovirus therapy, several cell lines were found to be susceptible to infection (Alain et al. 2002), possibly due to activation of Ras pathways through activating mutations upstream or downstream of Ras in these cell lines. Lymphoma cells implanted subcutaneously (*s.c.*) in mice regressed after a single injection of live reovirus. Furthermore, of the 27 human lymphoma specimens, 21 of them were susceptible to reovirus, suggesting that reovirus can be used in the treatment of some lymphoma (Alain et al. 2002).

Concerns are raised that long term exposure to reovirus infection might cause resistance of tumors to reovirus and select for persistently infected (PI) cancer cells. Raji lymphoid cells were infected with reovirus and the surviving cells were cultured and re-infected to create persistently infected cell lines (PI Raji cells) (Alain et al. 2006). PI Raji cells could be treated by anti-reovirus antibodies so that the cured Raji cells would no longer release reovirus. It was found that PI Raji cells were nontumorigenic, while cured Raji cells, which were resistant to reovirus infection *in vitro*, formed tumors but were susceptible to reovirus infection *in vivo*. Further study showed that the proteases such as cathepsins present in the microenvironment of the tumor augmented the uncoating efficiency of reovirus and thus enhanced reovirus oncolysis. Following this study, the

same group further compared a range of cell lines susceptible or resistant to reovirus infection and discovered that proteolytic stripping of the outer capsid protein of reovirus virions (i.e. the uncoating step) is critical for reovirus oncolysis (Alain et al. 2007a). Although Ras activation is not found in every susceptible cell line, a pathway downstream of Ras might be activated. Consistent with this, it was discovered that Ras-transformation enhances reovirus uncoating, rendering Ras-transformed cells more susceptible to reovirus infection (Marcato et al. 2007). On the other hand, the uncoating process is essential for reovirus-induced apoptosis (Connolly and Dermody 2002), indicating that apoptosis caused by reovirus infection might be affected by upregulation of proteases caused by Ras activation.

Kim *et al.* also demonstrated that a fibrosarcoma cell line (HT1080) develops resistance (HTR1) to reovirus infection *in vitro* and that the cured HTR1 cells are more highly tumorigenic (Kim et al. 2007). Furthermore, HTR1-resistant cells had lower levels of cathepsin B activity compared to parental cells. However, whether the highly tumorigenic cured cell could be killed by re-challenge of reovirus *in vivo* was not addressed in this study. Nonetheless, co-implantation of persistently infected HTR1 and cured HTR1 cells did not show tumor formation, indicating that residual reovirus released by the HTR1 cells might be able to infect and kill the tumor cells *in vivo*. Meanwhile, the cured cells could be triggered to undergo apoptosis by other apoptosis-inducing reagents such as camptothecin, indicating the reovirus-resistant tumors might be susceptible to a combination therapy.

Most of the current animal models of reovirus oncolysis were tested with tumors formed by established tumor cell lines or transformed cells. Colon cancer induced by azoxymethane, which resembles natural tumor development, was recently tested for

reovirus oncolysis (Alain et al. 2007b). Reovirus-treated animals showed a significantly lower level of tumor formation and metastases.

1.5.2. Reovirus Targets Breast Cancer Stem Cells

Increasing evidence suggests that only a small fraction of the cancer cells are responsible for tumorigenesis. This subpopulation of cancer cells are named cancer stem cells (CSCs) because of their shared properties with the normal stem cells of self-renewal and pluripotency (Al-Hajj et al. 2003; Dalerba et al. 2007). CSCs have also been indicated to be responsible for chemoresistance and radioresistance of a cancer cell population (Dean et al. 2005; Diehn et al. 2009). Therefore, drugs that target CSCs could have a better clinical outcome by preventing relapse in patients. The ability of reovirus to target CSCs was tested using breast cancer as a model (Marcato et al. 2009). Breast cancer stem cells were isolated according to the cell surface marker ($CD24^{-}CD44^{+}$) or a functional marker ($ALDH1^{+}$). It was shown that not only did reovirus induce tumor regression of primary cancer-patient xenografts established in non-obese diabetic-severe combined immune-deficient (NOD-SCID) mice, but reovirus targeted both non-cancer stem cells and CSCs equally well *in vivo*. Therefore, reovirus can serve as a potential alternative treatment for cancers that develop resistance to radiotherapy or chemotherapies.

1.5.3. Human Clinical Trials with Reovirus

With promising results showing that reovirus preferentially kills cancer cells *in vitro* and *in vivo*, reovirus is undergoing phase I, II and III clinical trials. Currently, there have been 14 trials completed and 12 trials ongoing, including one phase III clinical trial

in the USA, the UK, Canada and Belgium (for updates on clinical trials for reovirus, search in www.clinicaltrials.gov with Reolysin). Results of the clinical trials that have been published are summarized below.

Both intratumoral (*i.t.*) and intravenous (*i.v.*) administrations of reovirus at dosages ranging from 1 x 10^7 to 1 x 10^9 tissue culture infective dose ($TCID_{50}$) for *i.t.* injections or to 1 x 10^7 to 3 x 10^{10} for *i.v.* injections have been tested in phase I clinical trials (Forsyth et al. 2008; Vidal et al. 2008; Gollamudi et al. 2010). None of these phase I clinical trials reached the maximum toxicity for reovirus and the administrations of reovirus were well tolerated. Minor adverse events related to reovirus administrations such as fever, fatigue and cold-like symptoms were observed in certain patients within the first week of administration but did not extend into later weeks (Gollamudi et al. 2010). Although reovirus shedding was observed in patients after reovirus administration, an increase in neutralizing anti-reovirus antibodies (NARA) was detected as well and probably accounts for the safe administration of reovirus through *i.t.* or *i.v.* routes. On the other hand, analysis of post-treatment tumor biopsy samples indicated that reovirus was present in the tumor site after treatments. Therefore, it is clear that reovirus is able to reach the tumor through *i.v.* administration without harming normal tissues (Vidal et al. 2008). Although phase I clinical trials aim at testing toxicity and tolerance of patients to reovirus, these studies also showed that certain patients experienced a partial response or kept a stable disease state (Gollamudi et al. 2010), suggesting the potential clinical benefit of using reovirus as a cancer therapeutic. Interestingly, the overall clinical benefit rate was higher in patients with virus shedding than those without (Gollamudi et al. 2010), suggesting that reovirus replication and spreading might be beneficial for treating cancer.

Despite successful phase I clinical studies which showed positive patient tolerance to reovirus administration, the limited data published so far also suggest that reovirus might not be an efficient therapy if administered alone. Therefore, combination therapy using reovirus and either radiotherapy or chemotherapy might be needed for improved clinical outcome. A combination of reovirus and radiotherapy was tested *in vitro*, *in vivo* and then in patients in a phase I clinical trial. The *in vitro* studies demonstrated that reovirus was not significantly inactivated by gamma irradiation (IR), but enhanced cytotoxicity in human cancer cell lines was observed when a wide range of reovirus doses are combined with IR (Twigger et al. 2008). Furthermore, *i.t.* injection of reovirus enhanced the efficacy of IR in animal models *in vivo* (Twigger et al. 2008).

The promising *in vitro* and *in vivo* data lead to a phase I clinical study testing the safety and feasibility of combining reovirus and palliative radiation therapy in patients with advanced cancer (Harrington et al. 2010a). The treatment was divided into two stages, with a lower and then a higher dose of radiation combined with various doses of reovirus *i.t.* injections. The combination therapy was well tolerated with limited toxicity. Moreover, the presence of reovirus in the tumor sites was confirmed and responses to the combination therapy, including a partial response as well as a stable disease state, were observed in patients tested. Therefore, the combination of reovirus and palliative radiotherapy was proved to be safe and warrants a further study to determine the possible enhanced efficacy in patients with advanced cancer.

Combinations of reovirus and chemotherapeutic drugs were tested *in vitro*, *in vivo* and in clinical trials. For *in vitro* models of combination therapy, human as well as murine melanoma cell lines were infected with reovirus at various dosages with or without the addition of chemotherapy drugs (cisplatin, carboplatin, paclitaxel, DTIC/

dacarbazine and Gemcitabine) (Pandha et al. 2009). Synergistic cytotoxicity was observed when chemotherapy drugs were supplemented with reovirus infection *in vitro*. Furthermore, the combination of reovirus and cisplatin enhanced tumor growth delay as well as improved survival in two immunocompetent murine models of malignant melanoma. Human prostate cancer cell lines were also treated with a combination of reovirus and docetaxel and the results indicated an enhancement of reovirus-induced cell death in these cancer cells *in vitro* and were further confirmed by *in vivo* animal models (Heinemann et al. 2011).

These *in vitro* and *in vivo* results lead to phase I clinical trials of combination therapy using reovirus and chemotherapy drugs. In a completed phase I trial with reovirus combined with gemcitabine, a dose combination of 1×10^{10} $TCID_{50}$ of reovirus on day 1 and full dose of gemcitabine at 1000 mg/m^2 on day 1 and day 8 of a 21-day cycle was preliminarily determined to be suitable for further phase II clinical trial testing (Lolkema et al. 2011). Partial responses are observed in certain patients using this combination in the phase I clinical trial. Common toxicity similar to the phase I clinical trials were observed and the concurrent administration of reovirus and gemcitabine caused a rise in liver enzymes (a common side effect caused by gemcitabine alone), although this liver enzyme change was reversible.

Addition of gemcitabine to reovirus administration attenuated the induction of neutralizing anti-reovirus antibodies as well as the peak values compared to clinical trials using reovirus alone. This attenuation could have two contrasting effects: increase the exposure of normal tissue to reovirus infection, or allow reovirus enough time to replicate in patients in order to efficiently reach tumor sites. Therefore, the combination of reovirus and gemcitabine needs to be further tested despite the relatively safe profile of co-

administration. Unpublished clinical trials testing the combination of reovirus and cisplatin or paclitaxel were also reported in reviews (Harrington et al. 2010b) and were indicated to be well tolerated by patients. These successful phase I clinical trials of combining reovirus and chemotherapy drugs warrant phase II and III clinical trials. A combination of reovirus and paclitaxel or carboplatin is currently being tested in several phase II trails in a variety of cancers as well as a phase III clinical trial for head and neck cancer.

1.5.4. Reovirus Oncolysis and Tumor Immune Evasion

Tumors have developed strategies to reduce the anti-tumor immunity of the host and avoid subsequent elimination by the immune system (Whiteside 2006; Rabinovich et al. 2007; Stewart and Abrams 2008). These evasion strategies involve a wide range of immunologic abnormalities-associated with the tumor microenvironment which either inhibit the priming of antitumor adaptive immunity (such as downmodulation of tumor-antigen presentation) or trigger antigen-specific T-cell anergy (Staveley-O'Carroll et al. 1998; Lee et al. 1999; Ohlen et al. 2002; Lyman et al. 2004). Thus, a better immunotherapy for treating cancer would be composed of biological therapies attempting to activate the host immunity towards cancer as well as approaches to reverse the immune dysfunction caused by the tumor (Whiteside 2006). A body of reports has demonstrated that reovirus could induce host innate as well as adaptive immune responses to facilitate its oncolytic activity, as demonstrated in both murine models and in a clinical trial (Errington et al. 2008; Prestwich et al. 2008; White et al. 2008; Prestwich et al. 2009a; Prestwich et al. 2009b; Steele et al. 2011). These data indicate that reovirus-induced

tumor suppression may benefit from both direct tumor cell lysis and activation of the immune system to target cancer.

Recently, our lab further demonstrated that administration of reovirus not only promotes host immune responses (such as proinflammatory cytokine expression, lymphoid cell migration, Dentritic cell (DC) activation and T cell activation), but also exposes the otherwise inaccessible tumor antigen for processing and presentation (Gujar et al. 2010; Gujar et al. 2011). Furthermore, the co-administration of reovirus and anti-tumor DC or T cells significantly enhanced the survival of tumor-bearing animals and the reovirus-activated anti-tumor immune response was shown to protect the host against subsequent tumor challenge. Therefore, complementation of immunotherapies with reovirus oncolysis can potentially lead to better efficacy and long-term survival.

It is noteworthy that immunosuppressive drugs such as cyclophosphamide were suggested to be used along with reovirus administration in order to prevent NARA from blocking reovirus reaching the tumor sites. Indeed, fine-tuning the administration of cyclophosphamide reduced the levels of NARA and facilitated reovirus access to tumor sites and enhanced tumor regression in an immunocompetent animal model without causing severe toxicity (Qiao et al. 2008). However, the use of immunosuppressive drugs can potentially reduce the antitumor immune responses induced by reovirus oncolysis and thus need to be further examined.

1.6. Objectives

Reovirus has been used as a tool to understand virus-host interactions. Comprehensive studies on reovirus-induced apoptosis suggest that a network of host

signaling pathways is involved in reovirus infection. The Ras signaling pathway has been implicated preferential in reovirus replication in cancer cells. However, the role of the tumor suppressor protein p53 in reovirus oncolysis was not thoroughly determined. I wanted to determine whether p53 and p53-mediated apoptosis play any role in reovirus replication in cancer cells, as well as the effect of p53 in combination therapy with reovirus and p53 activators.

Although the Ras-signaling pathway was indicated to be essential in reovirus oncolysis, the detailed mechanisms involved need to be further delineated. Especially, the sub-Ras pathways which may provide advantages for individual steps of reovirus replication need to be identified. By delineating the molecular mechanisms of reovirus oncolysis, we may be better able to apply reovirus to target cancer cells that are from different origins but share similar signaling activation. Currently, reovirus is undergoing clinical trials in Canada, the United States, the United Kingdom and Belgium. Knowledge of reovirus oncolysis will help us to further identify targets for cancer therapy, especially for combination therapies with reovirus.

Fig. 1.1. Overview of reovirus replication cycle. Reovirus infection steps include: interaction of σ1 protein with receptors such as sialic acid and JAM, receptor-mediated endocytosis, virus uncoating/disassembly, penetration of subviral particles (ISVPs) through the endosomal membrane, formation of core particles, primary transcription of viral mRNA, viral protein synthesis, assembly of virus cores containing viral transcripts and proteins in viral factories, secondary viral transcription and translation, virion maturation, and virus release mediated by apoptosis. Refer to text for more details. Figure modified from "RNA Virus: Host Signaling Responses to reovirus Infection", Da Pan, Paola Marcato, Maya Shmulevitz, Patrick W.K. Lee, edited by Decheng Yang, copyright @ 2009 by World Scientific Publishing Co. Pte. Ltd.

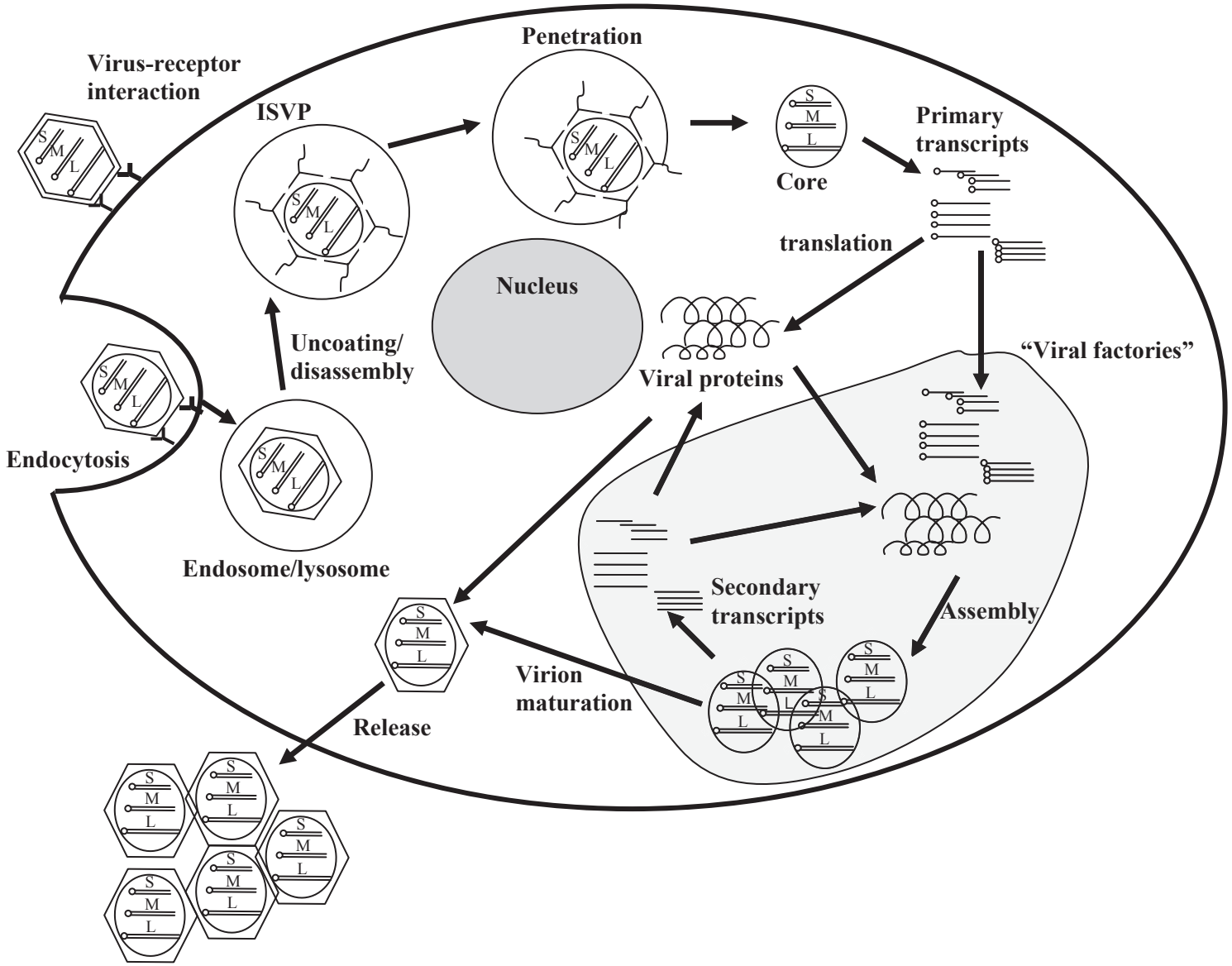
Virus-receptor interaction
ISVP
Penetration
Core
Primary transcripts
translation
Nucleus
Uncoating/ disassembly
Viral proteins
"Viral factories"
Endocytosis
Endosome/lysosome
Secondary transcripts
Assembly
Virion maturation
Release
S
M
L

Fig. 1.2. Activation of the oncogenic Ras and its main effector pathways. Upon binding of the epidermal growth factor (EGF) to the receptor, EGFR, the intrinsic tyrosine kinase activity of the receptor is activated. This causes phosphorylation of tyrosine residues in the cytoplasmic domain of the receptor, which are then recognized by the Grb2 adaptor protein. The association of the Grb2:Sos complex with the activated EGFR allows Sos (guanine nucleotide exchange factor) to activate Ras. Activated Ras then interacts with its effectors and activates downstream signaling pathways. The three main Ras-effector pathways are shown: Raf/MEK/ERK, RalGEFs/Ral, PI3K/Akt pathways. Figure from "RNA Virus: Host Signaling Responses to reovirus Infection", Da Pan, Paola Marcato, Maya Shmulevitz, Patrick W.K. Lee, edited by Decheng Yang,

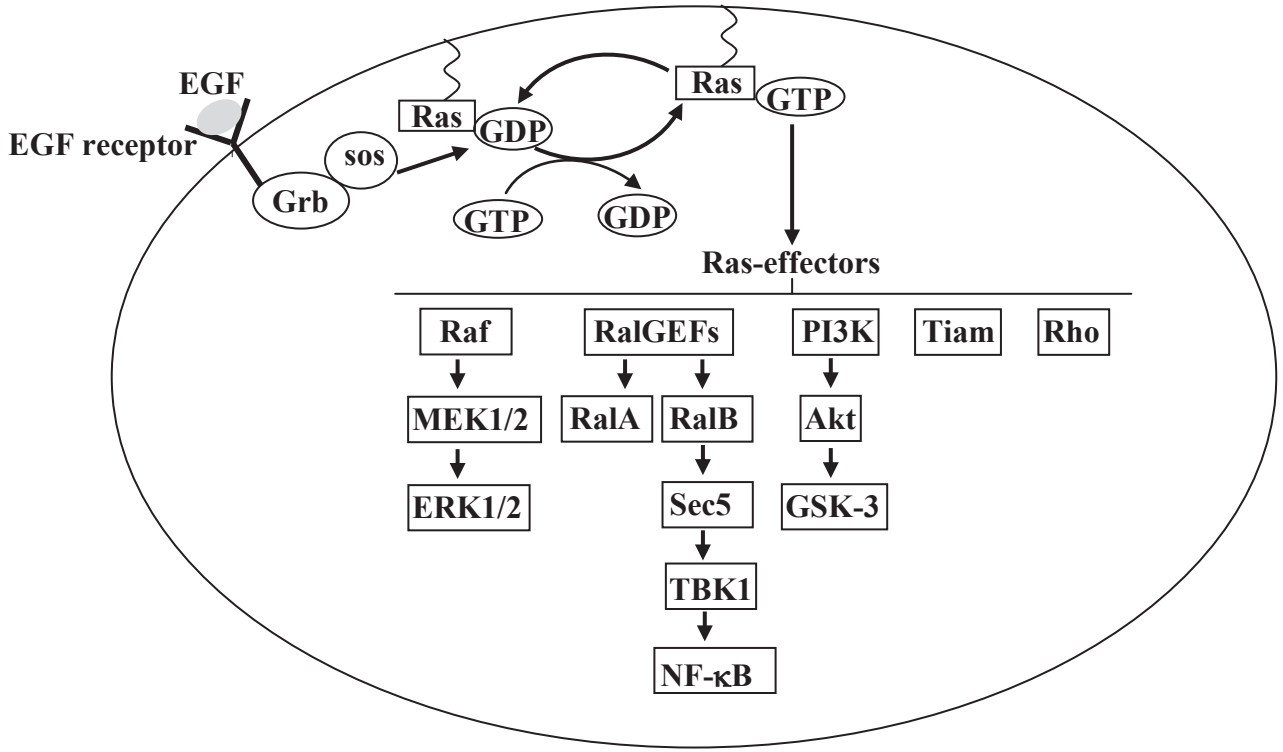
EGF
EGF receptor
Grb
sos
Ras
GDP
GTP
GDP
Ras
GTP
Ras-effectors
Raf
RalGEFs
PI3K
Tiam
Rho
MEK1/2
RalA
RalB
Akt
ERK1/2
Sec5
GSK-3
TBK1
NF-κB

Fig. 1.3. Schematic demonstration of apoptotic pathways that are triggered by reovirus infection. A. Reovirus triggers apoptosis through both cytoplasmic and mitochondrial pathways. The cytoplasmic pathway that functions in a caspase-8 dependent manner can be inhibited with by cFLIP. Activation of the mitochondrial pathway depends on selective release of Smac/DIABLO, which selectively neutralizes apoptosis inhibitor proteins (AIPs) including XIAP, survivin and c-AIP1. Cleavage of Bid by caspase-8 serves to connect the cytoplasmic and mitochondrial apoptosis pathways. Reovirus infection also triggers **B.** activation of JNK (in the grey balloon), as well as **C.** activation of NF-κB. **D.** RIG-1 and IPS-1 are important for reovirus-mediated apoptosis but are dispensable for activation of NF-κB. Bold lines show pathways that are involved in reovirus-induced apoptosis. Dashed lines represent pathways that are dispensable for reovirus-mediated apoptosis. Figure from "RNA Virus: Host Signaling Responses to reovirus Infection", Da Pan, Paola Marcato, Maya Shmulevitz, Patrick W.K. Lee, edited by Decheng Yang, copyright @ 2009 by World Scientific Publishing Co. Pte. Ltd.

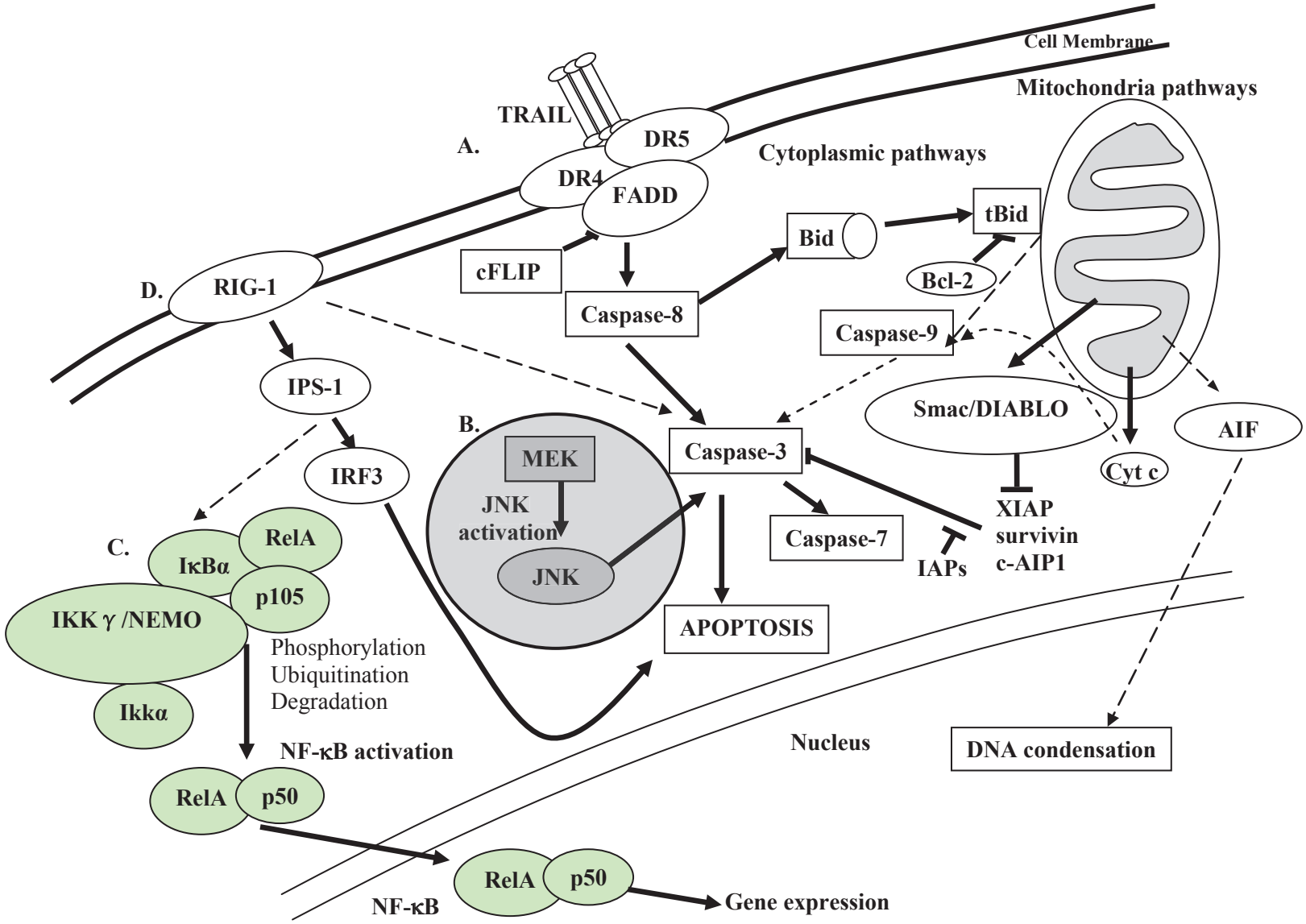
Cell Membrane
Mitochondria pathways
TRAIL
A.
DR5
DR4
FADD
Cytoplasmic pathways
cFLIP
Bid
tBid
Bcl-2
D.
RIG-1
Caspase-8
Caspase-9
IPS-1
B.
MEK
JNK activation
JNK
Caspase-3
Smac/DIABLO
AIF
Cyt c
IRF3
Caspase-7
XIAP
survivin
c-AIP1
IAPs
C.
RelA
IκBα
p105
IKK γ /NEMO
Phosphorylation
Ubiquitination
Degradation
Ikkα
APOPTOSIS
NF-κB activation
Nucleus
DNA condensation
RelA
p50
RelA
p50
NF-κB
Gene expression

Chapter 2 Materials and Methods

2.1. Cell culture and Virus

2.1.1 Cells and Virus

L-929, NIH-3T3, U2OS, A549 and TRAMP-C1 cells were purchased from American Type Culture Collection (ATCC, Manassas, VA) and cultured as instructed by ATCC. HCT116 (parental p53+/+, p53-/-, PUMA-/-, Bax-/-, p21-/-, PUMA-/-p21-/- and Bax-/-p21-/-) cells were gifts from Dr. Bert Volgelstein (Johns Hopkins University, Baltimore, MD) and were maintained in McCoy's 5A supplemented with 10% fetal bovine serum (FBS) and 1% antibiotic-antimycotic (AA). All cells were maintained at 37^{o}C in a 5% CO_2 humidified incubator. All media (except Joklik's modified Eagles' medium, JMEM), FBS and AA were purchased from Invitrogen (Life technologies, Carlsbad, CA).

Reovirus (Dearing strain, T3D) was propagated in a L-929 suspension culture in JMEM (Sigma-Aldrich Canada, Oakville, ON, Canada) supplemented with 5% horse serum, 1% AA and sodium pyruvate (110 mg/L). Reovirus was purified following established procedures (Smith et al. 1969; Mendez et al. 2000; Berard and Coombs 2009) and reovirus infectivity was determined by standard plaque titration.

2.1.2 Molecular Constructs

The coding sequence of human p53 was reverse-transcribed from U2OS total RNA and subcloned into pcDNA3 (pcDNA3-p53) by Dr. Lu-Zhe Pan. Reovirus gene S4 as well as control eGFP gene were reverse-transcribed and subcloned into pcDNA3 by Dr. Maya Shmulevitz (pcDNA3-eGFP and pcDNA3-S4). pSMP vectors containing either

scrambled sequence or a *p53*-specific shRNAmir sequence were obtained from Open Biosystems (Thermo Fisher Scientific Inc., Huntsville, AL). An online program (Cold Spring Harbor Laboratories, the Hannon Lab), was used to select Noxa-specific shRNAmir sequences (see http://katahdin.cshl.org/siRNA/RNAi.cgi?type=shRNA). These sequences were used as templates for polymerase chain reaction (PCR) using specific primers (SMP-PCR-F and SMP-PCR-R; see List of primers) containing BamHI and XhoI restriction sites and *Noxa*-specific shRNAmir sequences were subcloned into pSMP vectors. All constructs were sequenced in both directions to verify the sequences.

2.1.3. Retroviral and Lentiviral Infection and Generation of Cell Lines

Plasmids were transfected with Lipofectamine^{TM} 2000 (Lipo) transfection reagent (Invitrogen) at a 1:3 ratio of DNA: Lipofectamine^{TM} 2000 according to manufacture instructions. Specifically, 1.6 μg of pcDNA3 (Invitrogen) or pcDNA3-p53 was transfected into HCT116 cells in the absence of AA. To create a knockdown cell line specific to a certain gene, the same ratio of DNA: Lipo was used to transfect retroviral vector pSMP with either scrambled sequence or sequence-specific shRNAmir sequences into the Pheonix packaging cell line (Dr. Garry P. Nolan, Stanford University). The resulting retrovirus supernatants were applied to recipient cells with 2 μg/mL Sequa-brene (Sigma-Aldrich) for 6 hours. Stable cells were selected by addition of 2 μg/mL puromycin at 48-hour post retrovirus infection. Similarly, pBabepuro vectors containing activated H-Ras or its effector mutants (RasV12S35, RasV12C40 and RasV12G37, gifts from Dr. Channing Der, Lineberger Comprehensive Cancer Center, University of North Carolina) (Rodriguez-Viciana et al. 1997; Fiordalisi et al. 2001) were transfected into a packaging cell line and the retrovirus supernatants were applied to NIH3T3 cells with 8

μg/mL Sequa-brene. Stable cells were selected similarly. All cells were maintained for no longer than three weeks for experiments.

Lentivirus vector pLKO.1-puro (control) and Noxa-kd plasmids were purchased from Sigma-Aldrich (TRCN0000150554 for Noxa-kd1 and TRCN0000150555 for Noxa-kd2). Lentivirus clones (including control, Noxa-kd2 and Noxa-kd2) were produced similarly as retrovirus, and stable cells lines were created by being infected by retrovirus followed by selection with puromycin.

2.1.4. Chemotherapeutic Drugs

Nutlin-3a and Nutlin-3b were provided by Hoffmann-La Roche Inc. (Nutley, NJ, USA). RITA was purchased from Calbiochem (Merk in Canada, Toronto, ON, Canada; Cat# 506149). Actinomycin D (cat# A9415), Etoposide (cat# E1383), Doxorubicin (cat# D1515) and 5-fluorouricial (cat# F6627) were purchased from Sigma-Aldrich Canada.

2.2. Inhibitors

Caspase inhibitors and NF-κB inhibitors were purchased from Calbiochem: Caspase inhibitor I Z-VAD(OMe)-FMK (ZVAD) (cat# 627610); caspase 2 inhibitor Z-VD(OMe)VAD(OMe)-FMK (cat# 218744); caspase 3 inhibitor II Ac-DEVD-CHO (cat# 264155); caspase 8 inhibitor I (cat# 218773); caspase 9 inhibitor I Z-LE(OMe)HD(OMe)-FMK (cat# 218761). NF-κB inhibitor: InSolution^{TM} NF-κB activation inhibitor (N) (cat# 481407) and InSolution^{TM} BAY 11-7082 (B) (cat# 196817).

2.3. Western Blotting and Antibodies

Cells were collected at the indicated time-points and lysed using RIPA buffer (50 mM Tris-HCl, pH 7.4, 150 mM NaCl, 0.5% Na-deoxycholate, 1% IGEPAL®CA-630) supplemented by 1x protease inhibitor cocktail (Sigma-Aldrich). Cell lysates were passed through a 26-gauge needle 10 times and then centrifuged at 10,000 rpm (revolutions per minute) for 5 minutes (min) to collect soluble supernatant. Protein concentration was determined by a Coomassie (Bradford) Protein Assay Kit (Thermo Scientific, Rockford, IL). Cell lysates were subjected to sodium dodecyl sulfate-polyacrylamide gel electrophoresis (SDS-PAGE) and western blotting following standard protocols. Generally, blots were incubated with blocking buffer (TBST: Tris-buffered saline, TBS supplemented with 5% Bovine serum albumin, BSA and 1% Tween®80) for 1 h at room temperature (RT) and then subjected to proper dilution of primary antibodies. Blots were then washed with TBST three times and incubated with secondary antibodies for 1 h at RT, followed by three washes of TBST. Blots were developed using ECL plus western blotting detection reagents and images were obtained using Typhoon™ 9400 system (GE healthcare life science, Piscataway, NJ).

Antibodies used in experiments are listed here. Santa Cruz Biotechnology (Santa Cruz, CA, USA): p53 (DO-I) (sc-126), p21 F5 (sc-6246), p65 (sc-71677), β-actin (sc-81760), cathepsin L (C-18, sc-6498), p-ERK (E-4, sc-7383), ERK-1 (K-23, sc-94). Cell Signaling Technology (Danvers, MA, USA): PUMA (4976), Bax (2772), p-p65 (3033).

2.4. Ras-activation Assay

Ras activation was measured using a Ras Activation Assay Kit (Upstate Biotechnology, Temecula, CA, USA) as per manufacture instructions. Specifically, this

kit consists of an agarose-conjugated GST-fusion protein corresponding to the human Ras Binding Domain (RBD, residues 1-149) of Raf-1. The RBD specifically binds to and precipitates Ras-GTP from cell lysates. The precipitated Ras is then detected by western blotting using anti-Ras antibody provided in the kit.

2.5. Apoptosis Assay, Sub-G1 Profiling and Fluorescence-Activated Cell Sorting (FACS) Analysis

Unless otherwise indicated, at 24 hpi, cells cultivated in the presence or absence of inhibitors were harvested and stained with Annexin V-FITC and 7-AAD (BD pharmingen, Oakville, ON, Canada) according to manufacturer's instructions. Cell death was quantified by flow cytometry using a FACScan flow cytometer (BD Biosciences, San Jose, CA) and analyzed using WinMDI Version 2.8 (Scripps Research Institute).

For sub-G1 profiling, cells were fixed with 70% ice-cold ethanol for 30 min, washed with phosphate-buffered saline (PBS) and then stained with PI staining buffer (50 μg/mL of PI, 20 μg/mL RNase A and 0.5% BSA) for 30 min. Two million cells were sorted and quantified by FACS.

To determine the percentage of reovirus infected cells using FACS analysis, collected cells were fixed, blocked, and permeabilized in 5% bovine serum albumin, 0.1% Triton X-100 in phosphate-buffered saline, and probed with anti-reovirus rabbit antibody followed by staining with goat anti-rabbit immunoglobulin G conjugated with Cy2. Washed cells were quantified with a FACScan flow cytometer.

2.6. Detection of Reovirus Internalization

Cells were pre-chilled for one hour before reovirus was added. After one hour of binding, cells were washed three times with ice-cold PBS. Cells were then either incubated with EZ-Link Sulfo-NHS-SS-Biotin (Pierce, Rockford, IL, USA) as per the manufacturer's instructions, or incubated at 37^{o}C for 20, 40 or 60 min before biotinylation. At each time-point after biotinylation, cells were collected and lysed in RIPA buffer. Equal quantities of total cell lysates were then incubated with streptavidin-conjugated magnetic beads (Invitrogen). Following extensive washing, immunoprecipitated biotinylated reovirus proteins were detected by Western blotting.

2.7. Metabolic Radiolabeling

Cells were metabolically labelled with EasyTag [^{35}S]methionine (Perkin Elmer, Waltham, MA, USA) in methionine-free DMEM (Invitrogen) for one hour. Cells were then washed with ice-cold PBS and solubilized in RIPA buffer. Proteins were separated by SDS-PAGE (10% w/v), and detected by autoradiography on a Typhoon 9400 imager (GE Healthcare Bio-Sciences Corp., Piscataway, NJ, USA).

2.8. *In vitro* Transcription of Control and Viral RNAs

RNA templates (eGFP and reovirus S4 gene) for *in vitro* translation were *in vitro* transcribed using RiboMax^{TM} large scale RNA production system-SP6 and T7 (Promega) as per manufacturer's instructions with or without the addition of a Ribo m^{7}G cap-analog (Promega) using restriction enzyme digested pcDNA3-eGFP, pcDNA3-S4 and pcDNA3-M1 as DNA templates, which contain the T7 promoter. The *in vitro* transcribed RNA fragments were then digested with RNase-free DNase I (Invitrogen) and purified with PureLink^{TM} RNA mini column (Invitrogen).

2.9. Preparation of Cell Extracts from Adherent Cells for *In Vitro* Translation

Cell lysates were prepared for *in vitro* translation reactions as described using RNase-free reagents (Favre and Trepo 2001). Specifically, cells were seeded the day before the experiment to obtain a culture at 70% confluency the next day. On the day of the experiment, cells were washed with PBS and then cultured in methionine-free DMEM supplemented with 10% FBS (Invitrogen) at 37^{o}C in a 5% CO_2 humidified incubator for one hour. Cells were then left on ice for 15 min before the medium was removed. Cells were washed once with wash buffer (20 mM Hepes-KOH, pH 7.4, 150 mM sucrose, 33 mM NH_4Cl, 7 mM KCl). Wash buffer with 200 μg/mL cell-permeable reagent L-palmitoyl-lysophosphatidylcholine (Sigma-Aldrich) was then added to cells and left on ice for 60 seconds. The buffer was quickly removed and drained. Cells were scraped into extraction buffer at 192 μL per 1 x 10^7 cells (Extraction buffer: 100 mM Hepes-KOH, pH 7.4, 120 mM KOAc, pH 7.4, 2.5 mM $Mg_2(OAc)_2$, 1 mM dithiothreitol (DTT), 2.5 mM adenosine 5′-triphosphate (ATP), 1 mM guanosine 5′-triphosphate (GTP), 100 μM S-adenosyl-methionine, 1 mM spermidine, 20 mM fresh creatine phosphate, and 100 mM sucrose). Cells were passed through a 25-gauge needle until the nuclei were stained blue with Trypan-Blue (Sigma-Aldrich) but still intact. Cells were then centrifuged at 800 x g for 2 min at 4 ^{o}C and the aqueous phase and the floating lipids were removed from the pellet. Micrococcal nuclease (Sigma-Aldrich) was added to the supernatant (2 units per 1 x 10^7 cells) with 1 mM $CaCl_2$ and incubated at RT for 7 min. The reaction was then stopped with 2.5 mM ethylene glycol-bis(2-aminoethylether)-*N,N,N′,N′*-tetra-acetic acid (EGTA), pH 7. The protein concentration of the lysates was quantified and lysates were diluted to the same concentration, aliquoted, flash-frozen and stored at -80 ^{o}C until use.

At the time of *in vitro* translation reaction, activated creatine phosphokinase was dissolved in activating buffer (50 mM Tris-HCl, pH 7.4, 40 mM DTT) to a final concentration of 50 mg/mL and left at RT for 1 hour. A reaction mixture of 40 μM of amino acids minus methionine (Promega), *in vitro* translation grade [^{35}S]-Methionine (GE) at 0.5 mCi/mL, RNase inhibitor (Ambion) combined with 0.6 μg of each *in vitro* transcribed RNA was incubated at 30 ^{o}C for 90 min. RNA was then degraded with 500 ng/mL RNase (Invitrogen) at 30 ^{o}C for 10 min. Proteins were separated by SDS-PAGE (10% w/v) and detected by autoradiography on a Typhoon 9400 imager (GE).

2.10. RNA Extraction and Quantitative Real-time Polymerase Chain Reaction

RNAs were extracted from cells with TRIzol® and residual cDNAs were removed by DNase I and cleared on PureLink™ RNA mini-columns (Invitrogen). Messenger RNAs were reverse transcribed using the Superscript II reverse transcriptase kit (Invitrogen) according to manufacturer instructions. QuantiFast SYBR RT-PCR kit (Qiagen, Mississauga, ON, Canada) with gene-specific primers (see List of primers) was used to quantify gene expression as per manufacturer instructions. Up to 40 amplification cycles of 95°C for 10 seconds and 60°C for 30 seconds preceded by a 3 min 95°C denaturation step were completed using the Mx3000P real-time PCR instrument (Stratagene, Agilent Technologies Canada Inc. Mississauga, ON). Standard curves were generated to calculate relative levels of mRNA of the gene of interest compared to internal standard control (GAPDH mRNA).

2.11. Dual Luciferase Assay

pNFκB-luc (3.1 μg, Clontech Laboratories Inc., Mountain View, CA) and pGL4.74 (0.08 μg, Promega, Madison, WI) were transfected into HCT116 cells in 6-well plates (1 x 10^6 cells/well) 24 hrs prior to Nutlin-3a treatment. At 6-h post transfection, cells were divided into ¼, seeded into 12-well plates and allowed to settle for 18 hrs. The transfected cells were treated with vehicle (DMSO) or Nutlin-3a for 6 hrs and then infected by reovirus. Cells were then lysed with passive lysis buffer (Dual luciferase assay kit, Promega) and the collected lysates were flash-frozen and stored in –80^{o}C until use. Luciferase activity was measured by a GloMax Luminometer (Promega).

2.12. Immunostaining for Detecting NF-κB p65 Localization

Cells grown overnight on gelatin-coated cover slides were infected with reovirus at a multiplicity of infection (MOI) of 1 in the presence or absence of actinomycin D (0.63 nM), etoposide (1.6 μM) or 6-h pretreatment of Nutlin-3a. At 12-h post infection (hpi), cells were fixed with 4% paraformaldehyde (in PBS) and then stained with anti-p65, anti-reovirus antibodies, followed by Cy3-AffiniPure goat anti-mouse IgG (Jackson ImmunoResearch Laboratories Inc., West Grove, PA, USA), Alexa Fluor 488 F(ab')$_2$ fragment of goat anti-rabbit IgG (H + L) and To-Pro-3 (Invitrogen Canada, Burlington, ON, Canada) for nuclear staining. Images were captured with a Zeiss LSM 510 laser scanning confocal microscope (Carl Zeiss Canada Ltd., Toronto, ON, Canada).

2.13. Plaque Size Analysis

Cells cultured to 90% confluency were infected with serial dilutions of reovirus in a volume of 100 μL in 12-well plates for one hour at 37^{o}C. FBS and AA were

supplemented to 2 x MEM (modified Eagle's medium) to a final concentration of 10% FBS and 2 x AA to make the 2 x MEM mixture. After one hour of reovirus attachment, the 100 μL of reovirus solutions was removed and an equal volume of 2 x MEM mixture and 2% agar were mixed and applied to cells with or without the proper concentration of chemicals. After the mixture solidified, plates were placed with the solid agar side up in a 37^{o}C incubator for 7 days (for HCT116, U2OS cells) or 5 days (for NIH 3T3 cells). Cells were then fixed with 10% formaldehyde at RT for 10 min and the agar layer was taken off. Cells were fixed with methanol for 5 min, washed with PBS three times and incubated with blocking buffer (PBS supplemented with 5% BSA and 0.1% Triton X-100) for 1 hour at RT. Rabbit polyclonal anti-reovirus antibody was diluted with blocking buffer at a concentration of 1:10,000 and applied to cells for 1 hour at RT after blocking. Cells were washed three times with PBS + 0.1% Triton X-100 and secondary antibody with 1:1000 goat anti-rabbit antibody conjugated with alkaline phosphatase (Jackson ImmunoResearch Laboratories, Ltd., West Grove, PA) was applied to cells and incubated at RT for 30 min. After three times of washing with PBS + 0.1% Triton X-100, reovirus plaques were developed using BCIP/NBT Alkaline Phosphatase Substrate Kit IV (Vector Laboratories Ltd., Burlingame, CA). The size was quantified by measuring the diameter of the plaques.

2.14. *In Vivo* Tumor Treatment with Reovirus

Male NOD-SCID mice (7-8 weeks old) were bred and maintained in the Carlton Animal Facility at Dalhousie University. Tumor xenografts were established following a protocol approved by the University Committee on Laboratory Animals at Dalhousie University. For experiments using combinations of reovirus and chemotherapy drugs,

mice were injected with either actinomycin D or etoposide to accumulate p53 with or without a one-time *i.t.* injection of reovirus (1 x 10^7 pfu in 50 μL PBS) on the first day of injection. Mice were monitored daily and tumor size was measured three times per week until 21 days post injection. Tumor volume was calculated using a formula: $V= (a^2 \text{ x } b)/2$, where *a* is the width and *b* was the maximum length.

Chapter 3 Effects of Nutlin-3a on Reovirus-induced Apoptosis and Virus Spread

3.1. Introduction

The tumor suppressor protein p53 plays a pivotal role in dictating the cell fate upon diverse stress conditions. In response to stress, p53 mainly functions as a transcriptional activatorfor its target genes such as *p21* and *puma*, which is responsible for a variety of cellular functions including cell cycle arrest and apoptosis. Due to its vital function of guarding genomic integrity, p53 is also one of the most mutated proteins in cancer: over 50% of cancer cells contain p53 mutations (Dey et al. 2008). Even among the half of the tumor cells that contain wild-type p53, the tumor suppressive downstream pathways are partially abrogated (Brown et al. 2011). Therefore, p53 has been a major therapeutic target for cancer treatment, and developing drugs that can restore p53 functions in cancer cells is an ongoing effort in cancer research.

MDM2 (murine double minute 2) is one of the key negative regulators of p53. MDM2 functions as an E3 ligase and marks p53 with ubiquitin for proteasomal degradation. MDM2 is also directly regulated by p53 transcription activity. Therefore, MDM2 and p53 form a negative feedback loop so that no untimely apoptosis or cell cycle disruption would occur due to accumulation of p53 (Mandinova and Lee 2011). MDM2 can also interact with p53 and inhibits the transcription activation by preventing its interaction with the transcription machinery (Vousden and Lane 2007). In many tumor cells that contain wild-type p53, MDM2 is over-expressed (Momand et al. 1998; Freedman et al. 1999) and therefore inhibits p53 accumulation upon cellular stress. Nutlin-3, a *cis*-imidazoline, was the first small molecule MDM2 antagonist discovered to show *in vivo* effectiveness (Vassilev et al. 2004). Nutlin-3a is the active enantiomer of

Nutlin-3 and binds to MDM2 to interrupt its interaction with p53, preventing MDM2 from ubiquitinating p53 and therefore accumulating p53. Nutlin-3a has been shown to effectively accumulate p53 and thus induce apoptosis or cell cycle-arrest in cancer cells containing wild-type p53 and inhibit tumor growth *in vivo* (Vassilev et al. 2004; Tovar et al. 2006). Since the discovery of Nutlin-3a and the proof of its effectiveness in activating p53 in cancer cells, many different small molecules were designed or selected for disrupting the MDM2/p53 interaction in order to re-activate p53 functions in tumors. Some of these MDM2 antagonists include RITA (Issaeva et al. 2004) (reactivation of p53 and induction of apoptosis), benzodiazepine (Grasberger et al. 2005), MI-219 (Ding et al. 2006), etc.

p53 is a homo-tetrameric protein of subunits that contain a N-terminal transactivation domain, a DNA-binding core domain, a tetramerization domain and a C-terminal regulatory domain (Ho et al. 2006). The majority of p53 mutations occur in the DNA-binding core domain of the protein (Hainaut and Hollstein 2000), implicating the importance of p53 transcription-activation function. These mutations can be categorized as either contact or structural (Bullock and Fersht 2001). Contact mutations locate at the interface of p53 and DNA so as to disrupt the transcription activation function of p53, but do not affect protein folding. In contrast, structural mutations can either destabilize the local structure of the p53 core domain or destabilize the entire protein. These destabilizing mutations furthermore give dominant negatives (gain-of-function) to p53, which can drive new oncogenic properties (Milner and Medcalf 1991; Milner et al. 1991; Levine et al. 1995; Strano et al. 2007). Therefore, developing small molecules or peptides that can re-stabilize the structure of p53 so as to restore the binding activity of p53 to its DNA targets has been another strategy for restoring p53 wild-type activity. A few of the

successful examples include CP31398 (Foster et al. 1999), Prima-1 (Bykov et al. 2002) and CBD3 (Friedler et al. 2002).

Reovirus preferentially kills cancer cells (reovirus oncolysis), and Ras-transformation in tumor cells provides advantages for reovirus replication in tumor cells compared to in normal cells (Hashiro et al. 1977; Duncan et al. 1978; Strong et al. 1998; Coffey et al. 1998). Reovirus-induced apoptosis was shown to be significantly enhanced in Ras-transformed cells, which increased the levels of reovirus release and therefore infection of neighbour cells (Smakman et al. 2005; Smakman et al. 2006a; Marcato et al. 2007). Therefore, it is rational to propose that reovirus oncolysis might be helped by an enhancer of apoptosis so that the levels of reovirus spread would be increased. Indeed, it has been shown that combining reovirus with ionizing radiation (IR) or certain chemotherapeutic drugs could enhance the efficacy of tumor regression *in vitro* (Twigger et al. 2008; Pandha et al. 2009; Sei et al. 2009).

While the involvement of Ras signaling in reovirus oncolysis has been thoroughly investigated, the role of p53 in reovirus oncolysis is still relatively unknown (Huang et al. 2004; Kim et al. 2010). In order to study the possible role of p53 in reovirus oncolysis, a pair of human colorectal cancer cell lines (HCT116 p53+/+ and p53-/-) were compared in terms of reovirus replication and reovirus-induced apoptosis. Since p53 is a major transcription activator and enhancement of apoptosis might benefit reovirus oncolysis, a p53 activator/accumulator Nutlin-3a was used in combination with reovirus to determine whether activation/accumulation of p53 could enhance reovirus-induced apoptosis.

3.2. Results

3.2.1. p53 Stabilization by Nutlin-3a Enhances the Release of Progeny Reovirus

Virions

The paramount function of p53 in regulating apoptosis raised the possibility that p53 status might influence reovirus replication. To address this question, reovirus was used to infect HCT116 p53+/+ and p53-/- cells and total virus titre was compared. As shown in Fig. 3.1A, by 18-hour post infection (hpi), reovirus production from HCT116 p53+/+ cells was comparable to that from HCT116 p53-/- cells, indicating that the deletion of p53 did not affect reovirus replication.

To test whether accumulation/activation of p53 can alter reovirus production in cancer cells, HCT116 p53+/+ cells were treated with the MDM2 antagonist Nutlin-3a and then infected with reovirus. As shown in Fig. 3.1C, 5 μM Nutlin-3a induced almost immediate (as early as 3-hour post treatment) and significant accumulation of p53. As well, p21 and PUMA were accumulated upon Nutlin-3a treatment; p21 upregulation occurred as early as 3-h post treatment, while PUMA upregulation being within 6-h post treatment. HCT116 p53+/+ cells were therefore treated with 5 μM of Nutlin-3a and then infected with reovirus. Total reovirus production was measured at 18 hpi. As shown in Fig. 3.1A, the levels of p53 were increased in the presence of Nutlin-3a regardless of reovirus infection. Moreover, p53 accumulation/activation induced by Nutlin-3a did not affect reovirus production. Overall, the extent of virus production in a single round of replication was impervious to the status of p53 in HCT116 cells.

Virus oncolysis depends not only on efficient virus production in cancer cells, but also on the efficient killing of infected cells, which facilitates release of progeny virus for cell-to-cell spread. Experiments were therefore performed to determine if p53 affects reovirus release. In the absence of Nutlin-3a, the titres of released (i.e. extracellular) reovirus were similar in p53+/+ and p53-/- HCT116 cells, suggesting that cell death and

subsequent virus release were unaffected by p53 deletion in HCT116 cells (Fig. 3.1B). However, the titres of extracellular reovirus were significantly increased following Nutlin-3a treatment of infected p53+/+ cells, but not p53-/- cells (Fig. 3.1B). Therefore, accumulation of p53 induced by Nutlin-3a does not affect reovirus replication but significantly increased the level of reovirus release.

The enhanced release of reovirus from infected p53+/+ cells following Nutlin-3a treatment was also accompanied by a significant increase in cytotoxicity (Fig. 3.1D). Cytotoxicity was dependent on productive reovirus replication, as cells treated with UV-inactivated reovirus and Nutlin-3a were relatively healthy (data not shown). However, the enhanced cytotoxicity induced by the combination of reovirus and Nutlin-3a was not due to increased reovirus production in Nutlin-3a treated cells since there was no significant difference in reovirus production in the presence or absence of Nutlin-3a treatment (Figs. 3.1A and 3.2A). Altogether, accumulation of p53 by Nutlin-3a in reovirus-infected cancer cells facilitates cell death and hence the release of progeny virions.

3.2.2. Nutlin-3a Significantly Enhances Reovirus-induced Cell Death in Cancer Cells Containing Wild-type p53

The effects of Nutlin-3a on the cytotoxicity of reovirus-infected cells were further characterized using Annexin V and 7-AAD staining to quantify the extent of early-apoptosis and cell death. Nutlin-3b is the inactive enantiomer of the Nutlin-3. When Nutlin-3b was used to treat the HCT116 p53+/+ cells, the level of cell death was similar to that of the vehicle (DMSO) treated cells in the presence or absence of reovirus infection (Fig. 3.2B). Therefore, I used DMSO as a no-treatment control in the follow-up experiments. HCT116 p53+/+ were treated with Nutlin-3a for 6 hrs before being infected

by reovirus at MOI of 1. Cells were harvested at 12, 15, 18, 24, 36 and 48 hpi. As shown in Fig. 3.2C, at every time-point collected, the level of cell death in cells that were treated by the combination of reovirus and Nutlin-3a was significantly increased compared to that of cells infected by reovirus alone, indicating that Nutlin-3a indeed significantly increased the reovirus-induced cell death of HCT116 p53+/+ cells.

In order to further prove that Nutlin-3a could enhance reovirus-induced cell death in cells that contain wild-type p53, two other cell lines that contain wild-type p53 (U2OS human osteosarcoma cells and A549 human lung non-small cell carcinoma cells) were treated with Nutlin-3a and then infected by reovirus. As shown in Fig. 3.2D and E (U2OS cells and A549 cells, respectively), the combination of reovirus and Nutlin-3a could induce significantly higher levels of apoptosis compared to Nutlin-3a alone or reovirus alone, indicating that Nutlin-3a indeed could enhance reovirus-induced apoptosis in cancer cell lines that contain wild-type p53. Moreover, the percentage of cell death induced by the combination of reovirus and Nutlin-3a was significantly higher than the added value of either treatment alone, suggesting a synergistic cytotoxic effect between Nutlin-3a and reovirus.

3.2.3. Enhanced Cell Death Induced by the Combination of Reovirus and Nutlin-3a is due to Increased Level of Apoptosis

Apoptosis is a programmed mode of cell death. Apoptosis of mammalian cells is accompanied by various morphological changes including nuclear condensation, DNA fragmentation and cell surface changes (Wyllie et al. 1980; Cohen et al. 1992). As well, soon after the initiation of apoptosis, mammalian cells translocate phosphatidylserine (PS) from the inner face of the plasma membrane to the cell surface. Because Annexin V has a

strong affinity to PS, when coupled with the use of a viability marker (e.g. 7-AAD), the staining of live cells with Annexin V could not only differentiate early from late apoptosis (dead cell) and damaged cells (necrosis), but help to detect the transition of cells from early to late apoptosis (Zhang et al. 1997; van England et al. 1998). As shown in Fig. 3.3A, each lower right quadrant of a dotplot represents early apoptotic cells and each upper right quadrant represents late apoptotic cells. Non-treated (NT) cells had very low levels of either early or late apoptotic cells. On the contrary, for HCT116 p53+/+ cells that were infected with reovirus in the presence of Nultin-3a, the percentage of early apoptotic cells increased with time until 48 hpi when the majority of cells were at the late stage of apoptosis. The transition of early apoptosis towards cell death indicated that the enhanced cell death observed in the reovirus and Nutlin-3a combination treatment was due to higher level of apoptosis. Reovirus infection alone also induced the transition from early apoptosis towards cell death although the levels of early as well as late apoptosis are significantly lower (data not shown).

To further determine whether cell death induced by reovirus and Nutlin-3a co-treatment was a consequence of increased apoptosis, the extents of early apoptosis and cell death were quantified in the presence or absence of the caspase inhibitor I Z-VAD(OMe)-FMK (ZVAD). ZVAD treatment caused significant reduction of apoptotic and dead cells following reovirus infection alone (Fig. 3.3B). Cell death caused by the combination of reovirus and Nutlin-3a was also inhibited by ZVAD, suggesting that p53 accumulation causes increased caspase-dependent apoptosis of reovirus-infected cells (Fig. 3.3B). I then used relatively more specific caspase inhibitors to treat HCT116 p53+/+ cells before Nutlin-3a or reovirus treatment (listed in 2.2. Inhibitors). In this experiment, the enhanced apoptosis induced by the combination of reovirus and Nutlin-3a

was reduced by treatment with caspase-2, -8 and -9 inhibitors. Specifically, the caspase-3 inhibitor reduced the level of cell death induced by combined reovirus and Nutlin-3a to the lowest level among all the inhibitors tested. Interestingly, caspase-9 was shown to be dispensable for reovirus-mediated apoptosis (Kominsky et al. 2002b) while in my study blocking capspase-9 activity inhibited the enhancement of apoptosis induced by the combination of reovirus and Nutlin-3a. Since caspase-3 is the executer caspase of the caspase cascade downstream of caspase-2, -8 and -9, and at late stage of apoptosis, the extent of apoptosis might have been escalated by autocleavage and cleavage of caspases. This result further confirmed that p53 accumulation induced by Nutlin-3a treatment enhanced caspase-dependent apoptosis induced by reovirus.

3.2.4. Enhanced Apoptosis Caused by the Combination of Reovirus and Nutlin-3a is p53-dependent

In HCT116 cells, the enhancement of reovirus-induced cell death by Nutlin-3a was significantly higher in p53+/+ cells than p53-/- cells (Fig. 3.4A). Therefore, the augmentation of apoptosis in HCT116 p53+/+ cells induced by the combination of Nutlin-3a and reovirus is likely mediated directly through p53 rather than potential non-specific targets in HCT116 cells. To further prove the p53 dependence of the combination effect of reovirus and Nutlin-3a, A549 cells were transduced by either shRNA vector control or shRNA specific for the p53 gene sequence and then subjected to reovirus infection in the absence or presence of Nutlin-3a treatment. Nutlin-3a had no effects on reovirus-induced apoptosis when p53 was knocked-down in A549 cells (Fig. 3.4B), indicating that the enhancement of apoptosis in the presence of Nutlin-3a is p53-dependent. Conversely, transient over-expression of p53 in HCT116 p53-/- cells using a

p53-expression plasmid resulted in significantly higher levels of reovirus-induced apoptosis (Fig. 3.4C). These studies show that p53 accumulation, whether by Nutlin-3a treatment or by transient over-expression, is responsible for enhanced apoptosis of cancer cells induced by reovirus.

Another small molecule MDM2 antagonist RITA (reactivation of p53 and induction of tumor cell apoptosis), was also used to induce p53 accumulation. RITA inhibits specific interactions between MDM2 and p53, similar to Nutlin-3a but unlike Nutlin-3a, RITA binds directly to p53 rather than to MDM2 (Issaeva et al. 2004). As shown in Fig. 3.4D, treatment of HCT116 p53+/+ cells with RITA induced accumulation of p53, which significantly enhanced apoptosis compared to reovirus infection alone. However, the enhancement of apoptosis induced by the combination of reovirus and RITA was not observed in HCT116 p53-/- cells. These results suggest that reovirus oncolysis could be enhanced by RITA, Nutlin-3a, or other prospective drugs that promote p53 accumulation/activation.

3.2.5. Enhanced Apoptosis Induced by the Combination of Nutlin-3a and Reovirus Requires *bax* and *p21*

Since the enhancement of apoptosis induced by the combination of Nutlin-3a and reovirus is p53-dependent, I wanted to determine whether the combination of Nutlin-3a and reovirus could increase expression of p53 target genes. RNA samples were collected at 24 hpi and subjected to quantitative real-time PCR (qRT-PCR) using primers specific for *noxa*, *puma*, *bax* and *p21* (see List of primers). As expected, Nutlin-3a treatment alone induced expression of *puma*, *bax* and *p21* but not *noxa*. *Puma* and *noxa* were upregulated

by reovirus infection alone. When Nutlin-3a and reovirus were combined, expression levels of proapoptotic genes *noxa*, *puma* and *bax* were further increased in p53+/+ cells (Fig. 3.5A, B and C). Since reovirus alone had minimal effect on *p21* expression, it is not surprising that the already elevated level of anti-apoptotic *p21* by Nutlin-3a treatment alone was not further enhanced by the combination treatment (Fig. 3.5D). Therefore, the combination of Nutlin-3a and reovirus had a more pronounced effect on the expression of pro-apoptotic genes (*puma*, *bax* and *noxa*) than the pro-arrest gene (*p21*) at 24 hpi when apoptosis was the desirable outcome.

In order to further characterize p53 target genes that are important for the enhancement of apoptosis induced by the combination of Nutlin-3a and reovirus, I used a panel of knockout cells derived from HCT116 (p53+/+) that were obtained from Dr. Vogelstein (Fig. 3.6A). HCT116 p53+/+ cells were also transduced with lentivirus constructs that contain either scrambled (vector) or Noxa-specific shRNA (Noxa-kd1 and Noxa-kd2), to knock down *noxa* expression in HCT116 cells (Fig. 3.7, left panel). These cells were treated with Nutlin-3a, reovirus or the combination of the two and apoptosis was assayed using Annexin V and 7-AAD staining as described before. The status of *puma* or *noxa* did not affect the enhancement of apoptosis induced by Nutlin-3a and reovirus (Fig. 3.6B and Fig. 3.7), since apoptosis was not significantly decreased in PUMA-/- or Noxa-kd cells compared to HCT116 p53+/+ cells. Interestingly, although levels of cell death induced by reovirus alone did not significantly vary among all the knockout cells compared to p53+/+ cells (Fig. 3.6B), the levels of apoptosis induced by the combination of Nutlin-3a and reovirus were significantly decreased in Bax-/- and p21-/- cells. A further decrease in the apoptosis level was observed in Bax-/-p21-/- cells (Fig. 3.6B), indicating that both *bax* and *p21* are required for the p53-dependent enhancement

of apoptosis induced by Nutlin-3a and reovirus. The upregulation of pro-arrest *p21* by Nutlin-3a might have blocked apoptosis at earlier times to allow reovirus to efficiently replicate whereas enhanced *bax* expression by Nutlin-3a and reovirus combined at later times would promote apoptosis for virus release.

3.2.6. The Enhancement of Apoptosis Induced by Nutlin-3a and Reovirus Requires NF-κB Activation

It was previously demonstrated that reovirus infection causes NF-κB activation. Furthermore, NF-κB was shown to be necessary for reovirus-induced apoptosis, as inhibition of NF-κB activation through blockage of IκB degradation diminished reovirus-induced apoptosis. As well, cells deficient for either p50 or p65 subunits of NF-κB were found to be resistant to reovirus infection (Connolly et al. 2000; Clarke et al. 2003). Using a dual-luciferase reporter assay, I found that reovirus infection alone caused the activation of NF-κB transcription in both p53+/+ and p53-/- cells, while Nutlin-3a alone had a negligible effects on NF-κB activation (Fig. 3.8A and B). When cells were challenged by the combination of reovirus and Nutlin-3a, however, the level of NF-κB transcription activation was further increased in p53+/+ cells (wild-type HCT116 and U2OS cells) but not in p53-/- HCT116 cells, indicating that the enhancement of NF-κB activation caused by Nutlin-3a and reovirus is p53-dependent. In accordance with the dual-luciferase reporter assay results, immunostaining of the NF-κB subunit p65 (Fig. 3.8C) showed that Nutlin-3a itself did not affect p65 localization (p65 was exclusively cytoplasmic) while reovirus infection clearly induced nuclear translocation of p65 in both p53+/+ and p53-/- cells. However, the addition of Nutlin-3a significantly enhanced the nuclear localization

of p65 in reovirus-infected p53+/+ cells but not in p53-/- cells, further confirming that the combination of reovirus and Nutlin-3a could induce significantly higher levels of NF-κB activation and this enhancement is p53-dependent.

Furthermore, when NF-κB activation was prevented by NF-κB activation inhibitors, as evidenced by the blockage of p65 nuclear translocation (Fig. 3.9A), cell death was significantly reduced in p53+/+ HCT116 cells that were co-treated with reovirus and Nutlin-3a (Fig. 3.9B and C). These results suggest that the cytotoxicity caused by the combination of reovirus and Nutlin-3a is mediated through activation of NF-κB signaling pathways.

I then determined the RNA levels of representative p53 target genes with or without treatment with the NF-κB inhibitor N. As shown in Fig. 3.10, the enhanced expression of these genes upon combined treatment with reovirus and Nutlin-3a was clearly suppressed by NF-κB inhibition. Therefore, p53-dependent NF-κB activation likely plays a role in controlling the upregulation of p53-target genes, indicating a link between NF-κB activation and the augmentation of apoptosis in Nutlin-3a and reovirus treated cells.

3.2.7. Apoptosis Induced by Nutlin-3a and Reovirus is not due to Activation of the TRAIL Signaling Pathway

Clark et al. showed that reovirus-induced apoptosis requires pro-apoptotic signaling through extracellular TRAIL and its receptors DR4 and DR5 in certain cell types (Clarke et al. 2000). Since Nutlin-3 can upregulate the expression and externalization of the TRAIL receptor DR5 (Hori et al. 2010), the involvement of TRAIL

was investigated. Anti-TRAIL antibody and competitive soluble DR4 and DR5 ligands were used to subdue the extrinsic TRAIL response and prevented cell death caused by the exogenously added TRAIL (Fig 3.11A). However, anti-TRAIL antibody and competitive DR4 and DR5 soluble ligands did not prevent apoptosis induced by either reovirus or the combination of reovirus and Nutlin-3a (Fig. 3.11B). Therefore, the extrinsic TRAIL-mediated pathway does not play a major role in reovirus and Nutlin-3a-induced apoptosis.

3.2.8. Nutlin-3a Significantly Increases Reovirus-induced Cytotoxicity to Cancer Cells and Promotes Virus Dissemination

Since the combination of Nutlin-3a and reovirus is significantly more cytotoxic to cancer cells, I wanted to explore the possibility of using reovirus and Nutlin-3a as a combination therapy for cancers with wild-type p53. To investigate whether Nutlin-3a could improve the efficacy of reovirus, different doses of reovirus were used to infect HCT116 cells in the presence or absence of 5 μM Nutlin-3a and IC50 of reovirus was calculated accordingly. As shown in Fig. 3.12A, Nutlin-3a significantly reduced the IC50 of the input reovirus (from 1.4 MOI to 0.22 MOI) in HCT116 p53+/+ cells while having negligible effect on p53-/- cells. Therefore, the combination of reovirus and Nutlin-3a has potential as a combination therapy in p53+/+ cancer.

In addition to cytotoxicity, viral oncolysis relies on efficient cell-to-cell spread of virus to overcome the growing tumor. The increased cytotoxicity of reovirus-infected cells and augmented release of new progeny virions by Nutlin-3a suggests that Nutlin-3a could facilitate both cytoxicity and rapid viral dissemination among tumor cells. Virus cell-to-cell spread can be easily visualized with a virus plaque assay, where the agar

overlay restricts virus infection to only neighbouring cells. The size of the plaque reflects the extent of virus dissemination over several rounds of replication, release, and re-infection (Marcato et al. 2007). As shown in Fig. 3.12B, reovirus plaques formed on Nutlin-3a treated HCT116 p53+/+ cells were significantly bigger than the ones on vehicle-treated cells, indicating that Nutlin-3a could enhance the spread of reovirus to the neighboring cells. The enlargement of reovirus plaques by Nutlin-3a was also observed in U2OS control cells but not the p53-shRNA knockdown cells (Fig. 3.12C). Taken together, these results suggest that Nutlin-3a co-treatment confers two important advantages for viral oncolysis: Nutlin-3a supports increased killing of p53+/+ cancer cells and subsequently also permits rapid reovirus dissemination.

3.3. Discussion

My study is the first to report that the combination of reovirus and a drug that causes p53-accumulation (Nutlin-3a) can enhance cytotoxicity in cancer cells. Although the status of p53 in HCT116 tumor cells does not affect reovirus production, the intact function of p53 in cancer cells can be utilized to promote reovirus-mediated, caspase-dependent apoptosis of cancer cells.

Recently, Kim et al. reported that the lack of p53 in certain cells renders them susceptible to reovirus infection (Kim et al. 2010). Our data showed that there was no significant difference between the HCT116 p53+/+ and p53-/- cells in reovirus production within at least the first round of reovirus infection (18 hpi, Fig. 3.1A), and that the level of apoptosis induced by reovirus was not significantly different between p53+/+ and p53-/- HCT116 cells or between A549 control and p53 knockdown cells (Fig. 3.4A and B). Therefore, p53-dependent resistance of tumor cells might be cell type-dependent.

Moreover, for less susceptible cancer cells (e.g. U2OS), when combined with reovirus, Nutlin-3a treatment clearly induced higher levels of apoptosis and reovirus spread (Figs. 3.2D and 3.12C). Therefore, our results indicate that irrespective of the effects of wild-type p53 on reovirus infection, p53 *accumulation* due to Nutlin-3a treatment ultimately promotes reovirus-mediated cancer cell killing.

The transcription factor NF-κB plays an important role in regulating apoptosis and appears to be involved in a mechanism by which reovirus and Nutlin-3a synergize to increase cancer cell killing. NF-κB was clearly induced by the combination of reovirus and Nutlin-3a in a p53-dependent manner, and induction of NF-κB was required for the full cytotoxic potential of reovirus and Nutlin-3a co-treatment. It was previously reported that NF-κB is essential for p53-dependent apoptosis and that p53 can enhance the activation of NF-κB (Ryan et al. 2000; Ryan et al. 2004). In my study, we showed that certain p53 target genes were upregulated by the combination of Nutlin-3a and reovirus, among which *p21* and *bax* seem to play more important role in promoting cell death induced by the combination of the two agents, since p21-/-, Bax-/- and Bax-/-p21-/- HCT116 cells had a significantly decreased level of apoptosis. Moreover, inhibition of NF-κB activation with NF-κB inhibitors suppressed the upregulation of p53 target genes by reovirus and Nutlin-3a, further confirming the link between the enhancement of NF-κB activation and increased in cytotoxicity induced by combination of p53 accumulation and reovirus infection.

Most existing chemotherapy reagents function by causing damage to cells, with the premise that highly dividing cancer cells are more prone to the cytotoxic effects. Unfortunately, chemotherapy reagents also damage normal cells and result in various side

effects that reduce the quality of life for cancer patients. Attempts are ongoing to reduce unwanted side-effects of cancer therapies through alternative cancer treatments and/or through combinations of distinct cancer therapeutics at reduced dosages. Concurrently, reovirus and other oncolytic viruses are being tested as cancer therapeutics. Reovirus is a promising anti-cancer therapy and phase I clinical trials of Reolysin^{TM} showed limited toxicity towards patients (Forsyth et al. 2008; Vidal et al. 2008; Harrington et al. 2010a). Nutlin-3a was also found to exhibit no pathological effect in *in vivo* murine studies (Vassilev et al. 2004). According to our results, the combination of the two low-toxic reagents (reovirus and Nutlin-3a) could be an alternative way of inducing cancer regression without exposing cancer patients to unwanted side-effects and warrants further *in vivo* testing for safety and efficacy.

Fig. 3.1. p53 stabilization by Nutlin-3a enhances reovirus-associated cytoxicity and the release of progeny virions. (A) Upper panel: Human colon cancer HCT116 p53+/+ and p53-/- cells were pretreated with 5 μM Nutlin-3a for 6 h and then infected at an MOI of 1. Total virus samples were collected at 18 hpi and quantified by plaque titration (±*s.e.m.*, n=3). Lower panel: western blot analysis to determine levels of p53 upon reovirus or Nutlin-3a treatment at 24 hpi. (B) Percentage of reovirus released into the medium was determined by dividing reovirus titres from cell media by the total reovirus titre (released reovirus titre/total reovirus titre) (±*s.e.m.*, n=3). (C) p53 accumulation after Nutlin-3a treatment in p53+/+ cells. HCT116 cells were treated with Nutlin-3a, collected at different time-points and subjected to western blotting using p53, p21 and PUMA-specific antibodies. (D) p53-dependent cytotoxicity enhancement caused by the combination of reovirus and Nutlin-3a. HCT116 p53+/+ or p53-/- cells were mock infected or infected at an MOI of 1 in the presence or absence of 5 μM Nutlin-3a. Images were taken at 24 hpi. Unless otherwise indicated, no treatment indicates that they were treated with dimethyl sulfoxide (DMSO, vehicle). Student's *t*-test was used to compare two groups of data; NS: not significant, **P*<0.05, ***P*<0.001 and ****P*<0.0001.

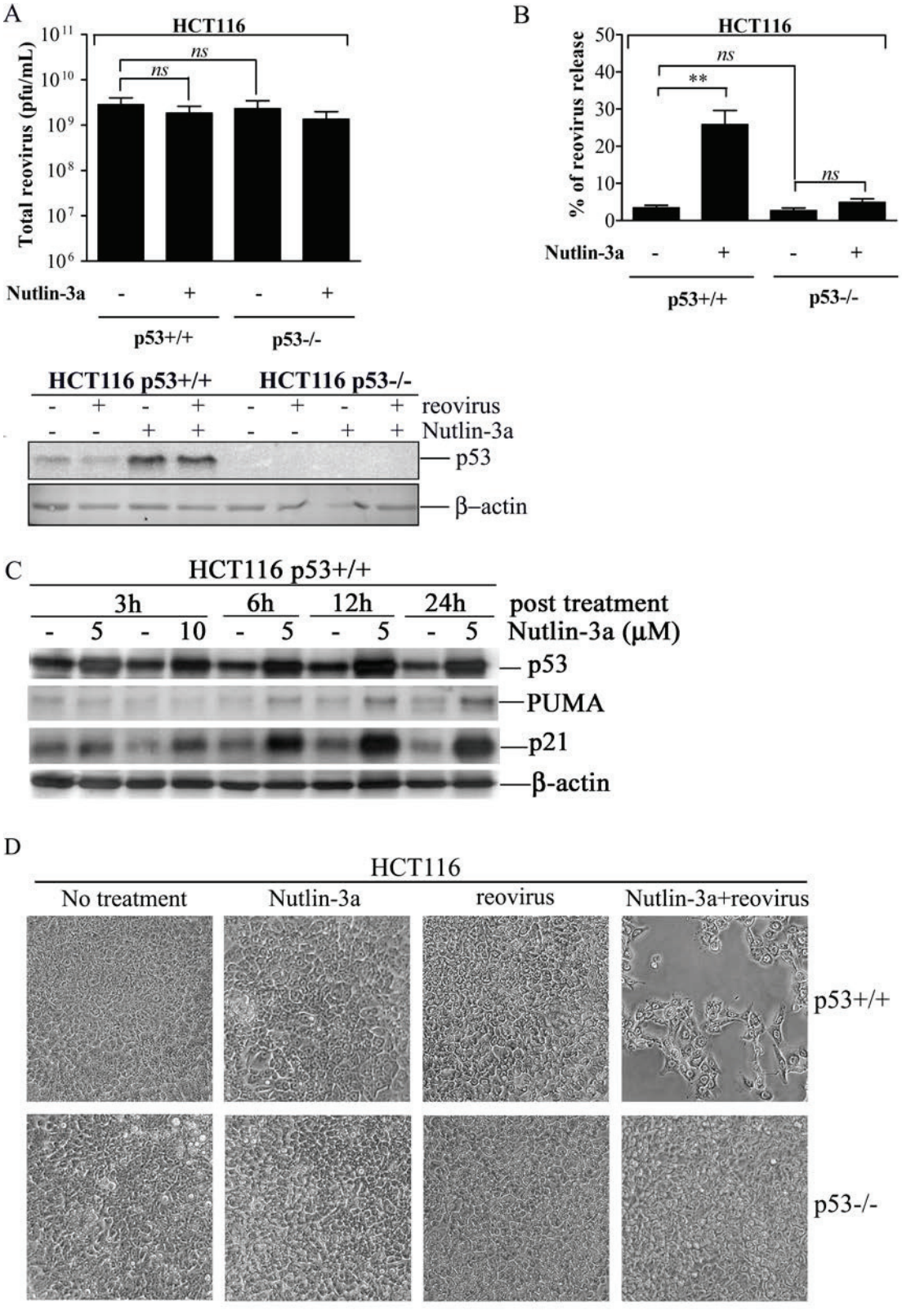
A
HCT116
Total reovirus (pfu/mL)
ns
ns
Nutlin-3a
p53+/+
p53-/-
B
HCT116
% of reovirus release
ns
**
ns
Nutlin-3a
p53+/+
p53-/-
HCT116 p53+/+
HCT116 p53-/-
reovirus
Nutlin-3a
p53
β–actin
C
HCT116 p53+/+
3h
6h
12h
24h
post treatment
Nutlin-3a (μM)
p53
PUMA
p21
β-actin
D
HCT116
No treatment
Nutlin-3a
reovirus
Nutlin-3a+reovirus
p53+/+
p53-/-

Fig. 3.2. Nutlin-3a treatment induces significantly higher level of cell death in reovirus-infected p53+/+ tumor cells without affecting reovirus replication. (A) Reovirus production in HCT116 p53+/+ cells in the presence or absence of 5 μM Nutlin-3a. Total titre samples were collected at different time-points and reovirus production was determined by plaque titration. Representative of two independent experiments (±*s.e.m.*, n=2). (B) Effects of Nutlin-3b (inactive enantiomer of Nutlin-3) on mock or reovirus-infected HCT116 p53+/+ cells. Cells were infected at an MOI of 1 with or without the pre-treatment using Nutlin-3b or DMSO control. Cells were harvested at 12, 15, 18, 24, 36 and 48hpi and stained with Annexin V and 7-AAD to determine the levels of cell death. The apoptotic fraction was calculated as the sum of Annexin V-positive live cells and dead cells (upper and lower right quadrants). (C) Percentage of cell death in HCT116 p53+/+ cells caused by reovirus, Nutlin-3a, or the combination of the two quantified by Annexin V and 7-AAD staining. (D) and (E) Cell death in U2OS (±*s.e.m.*, n=3) or in A549 (±*s.e.m.*, n=3) cells. A549 and U2OS cells were infected at an MOI of 100 and 500 respectively. Samples were collected at 24 and 48 hour respectively for Annexin V and 7-AAD staining. The right-most bar in (D) and (E) represents mathematical addition of eat treatment alone. Student's *t*-test was used to compare two groups of data; NS: not significant, **P*<0.05, ***P*<0.001.

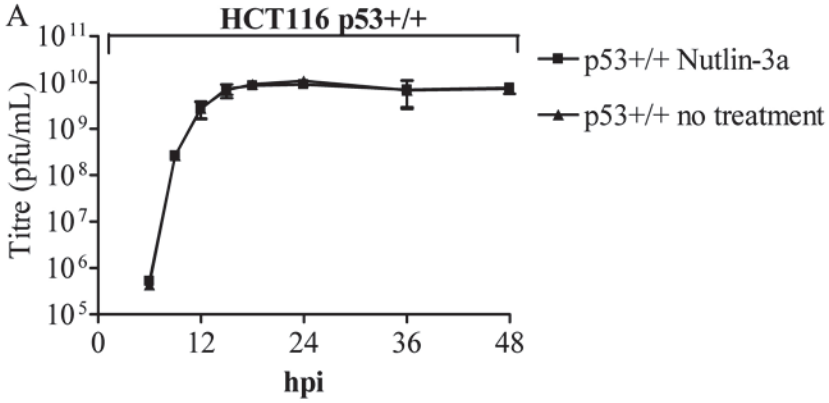
A
HCT116 p53+/+
Titre (pfu/mL)
hpi
p53+/+ Nutlin-3a
p53+/+ no treatment

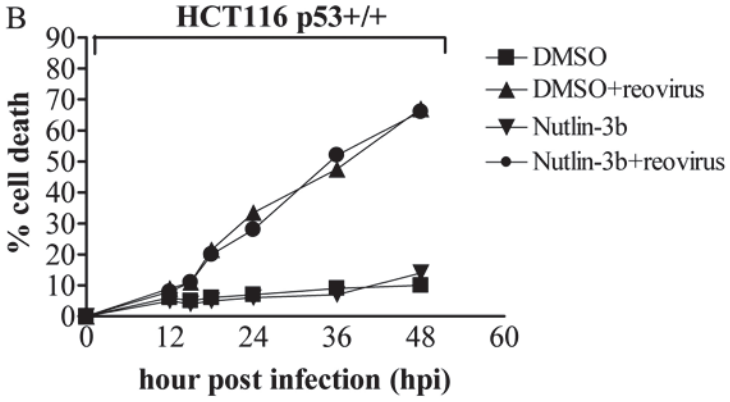
B
HCT116 p53+/+
% cell death
hour post infection (hpi)
DMSO
DMSO+reovirus
Nutlin-3b
Nutlin-3b+reovirus

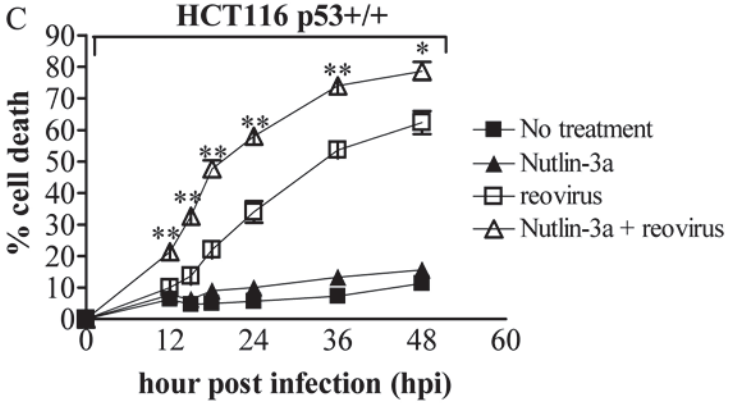
C
HCT116 p53+/+
% cell death
hour post infection (hpi)
No treatment
Nutlin-3a
reovirus
Nutlin-3a + reovirus

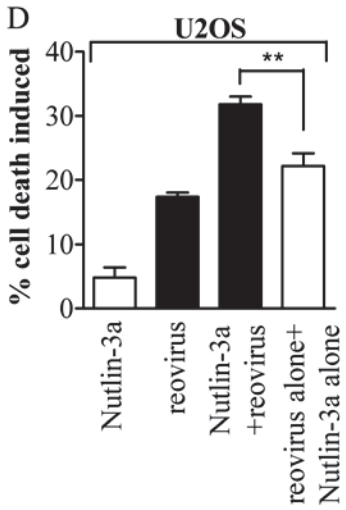
D
U2OS
% cell death induced
Nutlin-3a
reovirus
Nutlin-3a +reovirus
reovirus alone+ Nutlin-3a alone

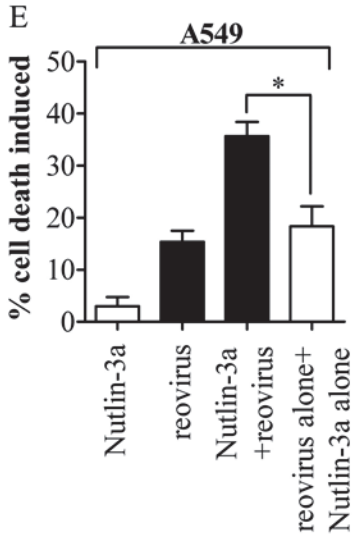
E
A549
% cell death induced
Nutlin-3a
reovirus
Nutlin-3a +reovirus
reovirus alone+ Nutlin-3a alone

Fig. 3.3. The enhancement of cell death caused by the combination of reovirus and Nutlin-3a is due to higher level of apoptosis. (A) Dot-plot diagrams of Annexin V and 7-AAD stained HCT116 p53+/+ cells that were treated with the combination of reovirus and Nutlin-3a. Cells were collected at 12, 15, 18, 24, 36, 48 hpi. Percentages of early (lower right quadrant) and late (upper right quadrant) apoptotic cells were quantified and indicated. Samples are from one of three independent experiments. NT: no treatment. (B) Caspase inhibitor ZVAD blocked apoptosis induced by reovirus or the combination of Nutlin-3a and reovirus. Cells were treated with ZVAD (50 μM) at the same time as Nutlin-3a treatment and throughout infection (±*s.e.m.*, n=4). (C) Various caspase inhibitors blocked apoptosis induced by the combination of reovirus and Nutlin-3a. Cells were treated with caspase-2 inhibitor I (30 μM), Caspase-8 inhibitor I (30 μM), Caspase-9 inhibitor I (30 μM) or Caspase-3 inhibitor II (30 μM) at the same time as Nutlin-3a treatment and throughout infection. Cell death in (B) and (C) was determined by Annexin V and 7-AAD staining. Student's *t*-test was used to compare two groups of data; NS: not significant and $*P<0.05$.

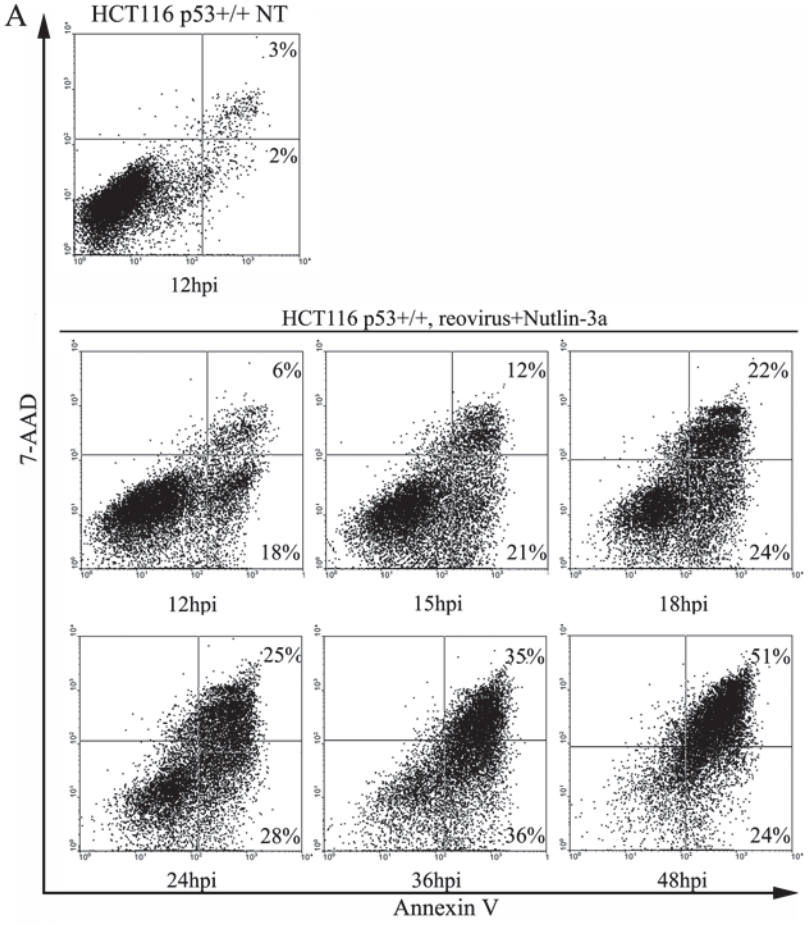
A
HCT116 p53+/+ NT
3%
2%
12hpi
HCT116 p53+/+, reovirus+Nutlin-3a
7-AAD
6%
18%
12hpi
12%
21%
15hpi
22%
24%
18hpi
25%
28%
24hpi
35%
36%
36hpi
51%
24%
48hpi
Annexin V

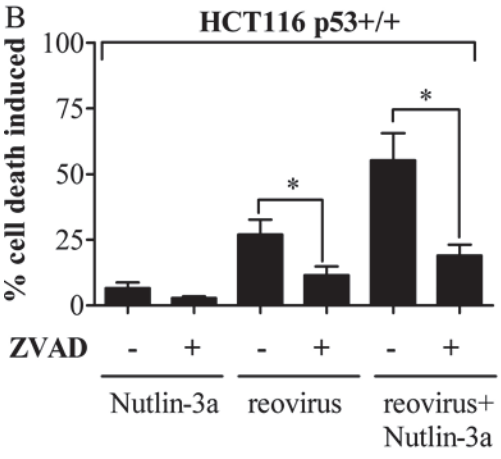
B
HCT116 p53+/+
% cell death induced
100
75
50
25
0
*
*
ZVAD - + - + - +
Nutlin-3a
reovirus
reovirus+
Nutlin-3a

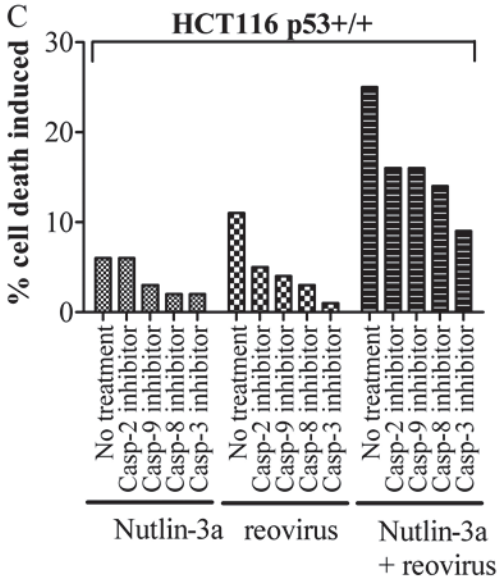
C
HCT116 p53+/+
% cell death induced
30
20
10
0
No treatment
Casp-2 inhibitor
Casp-9 inhibitor
Casp-8 inhibitor
Casp-3 inhibitor
Nutlin-3a
reovirus
Nutlin-3a
+ reovirus

Fig. 3.4. The enhanced cell death induced by the combination of Nutlin-3a and reovirus is dependent on p53. (A) The combination of reovirus and Nutlin-3a caused significantly higher levels of cell death in HCT116 p53+/+ but not p53-/- cells. HCT116 p53+/+ and p53-/- were either mock infected or infected with reovirus at an MOI of 1. Cells were collected at 24 hpi, subjected to Annexin V and 7-AAD staining and quantified by FACS analysis. (±*s.e.m.*, n=4). (B) Extent of cell death of A549 p53 knockdown cells (A549 p53shRNA) and non-silencing control cells (A549 control) induced by Nutlin-3a, reovirus (MOI of 100) or the combination of the two reagents (upper panel). p53 levels after Nutlin-3a treatment (lower panel) were determined by western blotting. (C) Extent of cell death in reovirus-infected HCT116 p53-/- cells weretransfected with either p53-expression (pcDNA3-p53) or control (pcDNA3) plasmid. HCT116 p53-/- were transfected by pcDNA3-p53 or pcDNA3 plasmids and mock infected or infected with reovirus at an MOI of 1. (D) Induction of p53 protein accumulation at different concentrations of RITA (left panel) and percentage of apoptosis in reovirus-infected HCT116 p53+/+ cells and p53-/- cells with or without 0.63 μM RITA treatment (right panel) (±*s.e.m.*, n=3). Student's *t*-test was used to compare two groups of data; NS: not significant, $^{**}P<0.001$ and $^{***}P<0.0001$.

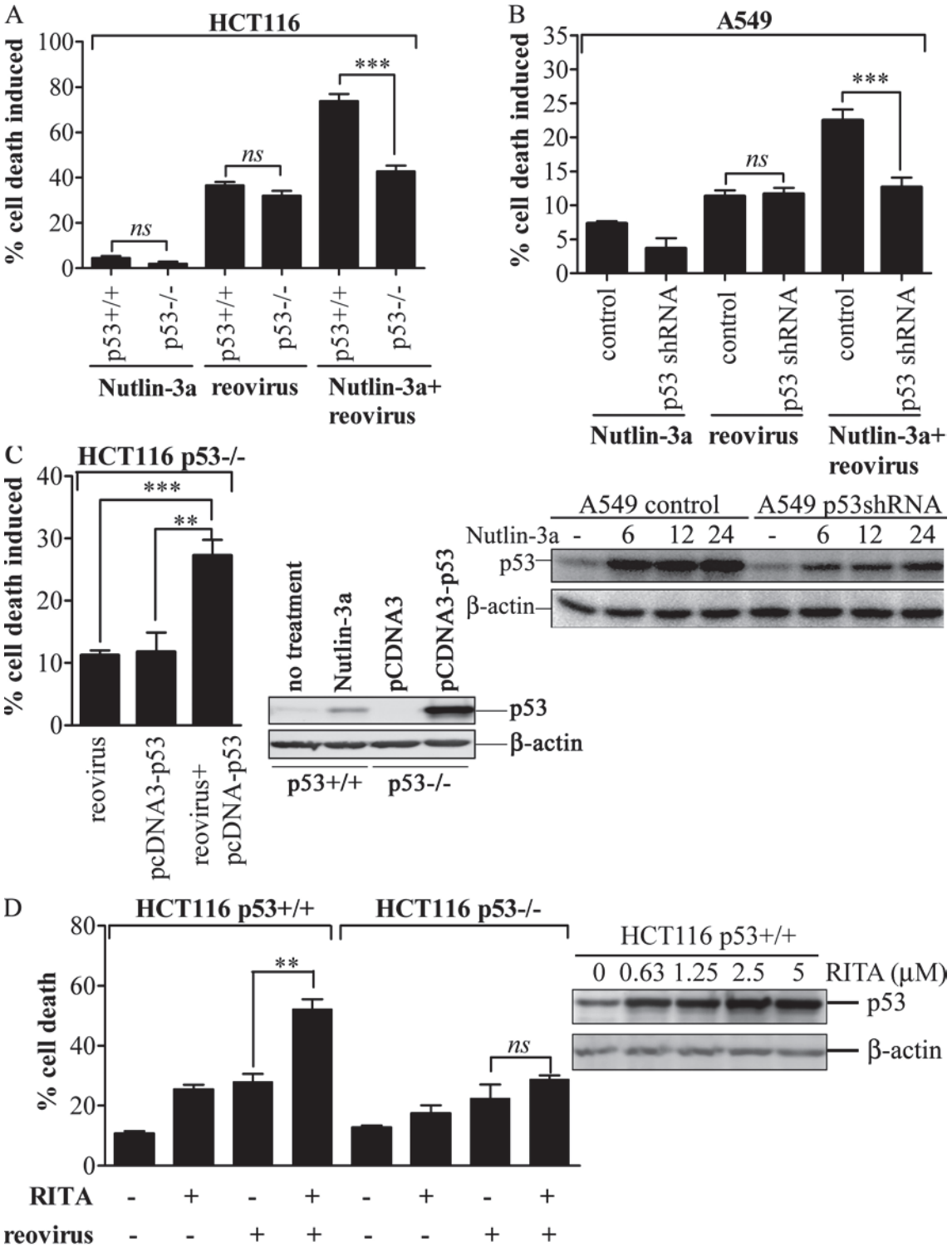
A
HCT116
% cell death induced
100
80
60
40
20
0
***
ns
ns
p53+/+
p53-/-
p53+/+
p53-/-
p53+/+
p53-/-
Nutlin-3a
reovirus
Nutlin-3a+ reovirus
B
A549
% cell death induced
35
30
25
20
15
10
5
0
***
ns
control
p53 shRNA
control
p53 shRNA
control
p53 shRNA
Nutlin-3a
reovirus
Nutlin-3a+ reovirus
C
HCT116 p53-/-
% cell death induced
40
30
20
10
0
***
**
reovirus
pcDNA3-p53
reovirus+ pcDNA-p53
no treatment
Nutlin-3a
pCDNA3
pCDNA3-p53
p53
β-actin
p53+/+
p53-/-
A549 control
A549 p53shRNA
Nutlin-3a - 6 12 24 - 6 12 24
p53
β-actin
D
HCT116 p53+/+
HCT116 p53-/-
% cell death
80
60
40
20
0
**
ns
RITA - + - + - + - +
reovirus - - + + - - + +
HCT116 p53+/+
0 0.63 1.25 2.5 5 RITA (μM)
p53
β-actin

Fig. 3.5. Differential expression levels of p53 target genes (A) *noxa*, (B) *puma*, (C) *bax* or (D) *p21*, induced by reovirus, Nutlin-3a or the combination of the two. Total RNA was extracted from HCT116 p53+/+ or p53-/- cells treated with Nutlin-3a, reovirus or the combination of the two at 24 hpi (as indicated). Expression levels of *GAPDH*, *noxa*, *puma*, *bax* and *p21* were determined by real-time (RT) qPCR. Levels of transcripts were normalized to those of the house keeping-gene *GAPDH*. Student's *t*-test was used to compare two groups of data; NS: not significant, **P*<0.05 and ***P*<0.001.

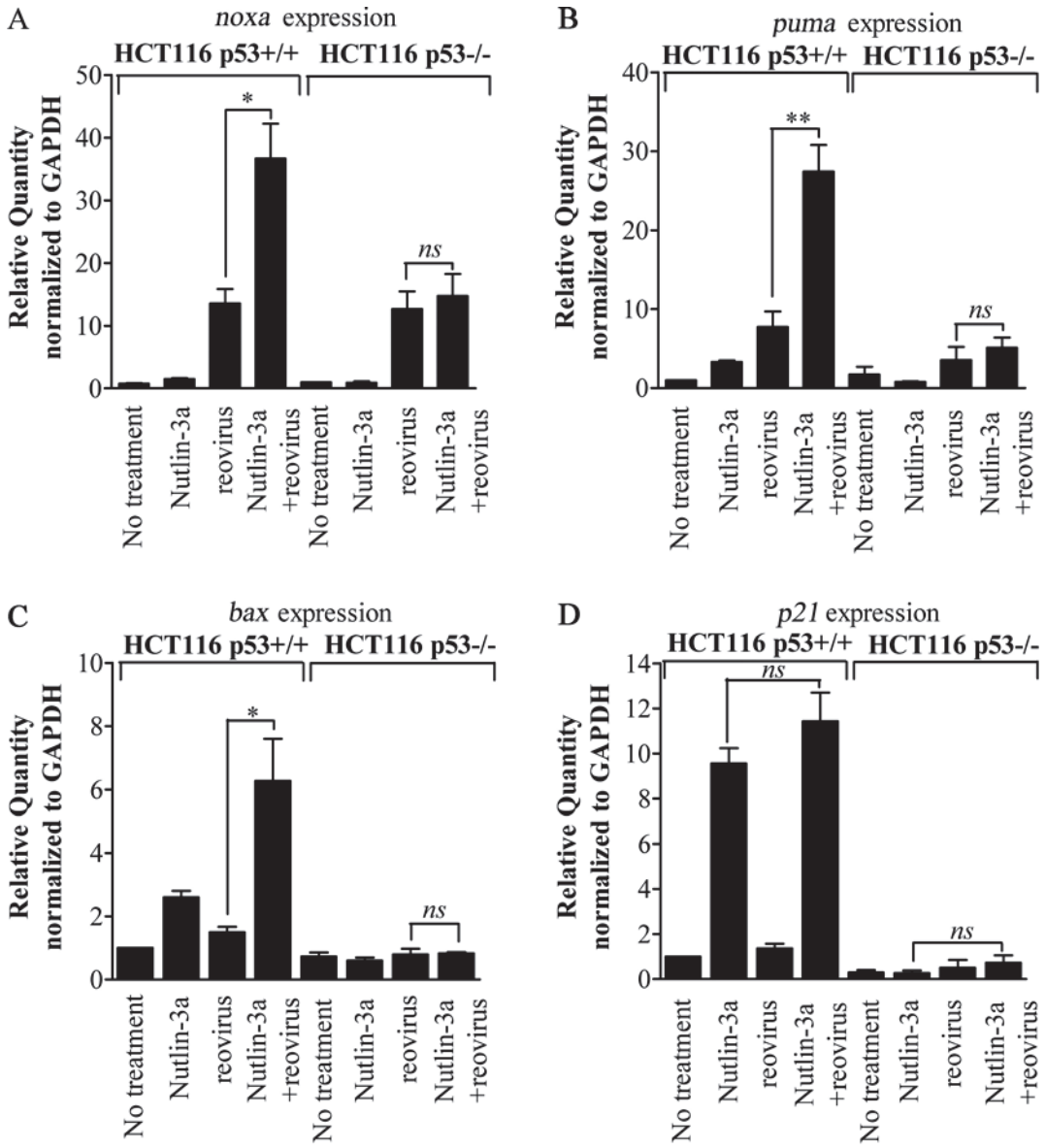
A
noxa expression
HCT116 p53+/+
HCT116 p53-/-
Relative Quantity normalized to GAPDH
50
40
30
20
10
0
*
ns
No treatment
Nutlin-3a
reovirus
Nutlin-3a +reovirus
No treatment
Nutlin-3a
reovirus
Nutlin-3a +reovirus
B
puma expression
HCT116 p53+/+
HCT116 p53-/-
Relative Quantity normalized to GAPDH
40
30
20
10
0
**
ns
No treatment
Nutlin-3a
reovirus
Nutlin-3a +reovirus
No treatment
Nutlin-3a
reovirus
Nutlin-3a +reovirus
C
bax expression
HCT116 p53+/+
HCT116 p53-/-
Relative Quantity normalized to GAPDH
10
8
6
4
2
0
*
ns
No treatment
Nutlin-3a
reovirus
Nutlin-3a +reovirus
No treatment
Nutlin-3a
reovirus
Nutlin-3a +reovirus
D
p21 expression
HCT116 p53+/+
HCT116 p53-/-
Relative Quantity normalized to GAPDH
14
12
10
8
6
4
2
0
ns
ns
No treatment
Nutlin-3a
reovirus
Nutlin-3a +reovirus
No treatment
Nutlin-3a
reovirus
Nutlin-3a +reovirus

Fig. 3.6. *Bax* and *p21* are required for the enhanced apoptosis induced by the combination of reovirus and Nutlin-3a. (A) Western blot analysis for HCT116 cells (p53+/+, p53-/-, PUMA-/-, Bax-/-, PUMA-/-p21-/- and Bax-/-p21-/-). (B) Levels of cell death induced by Nutlin-3a, reovirus or the combination of the two in HCT116 knockout cells (±*s.e.m.*, n=4). Student's *t*-test was used to compare two groups of data; NS: not significant, **P*<0.05 and ***P*<0.001.

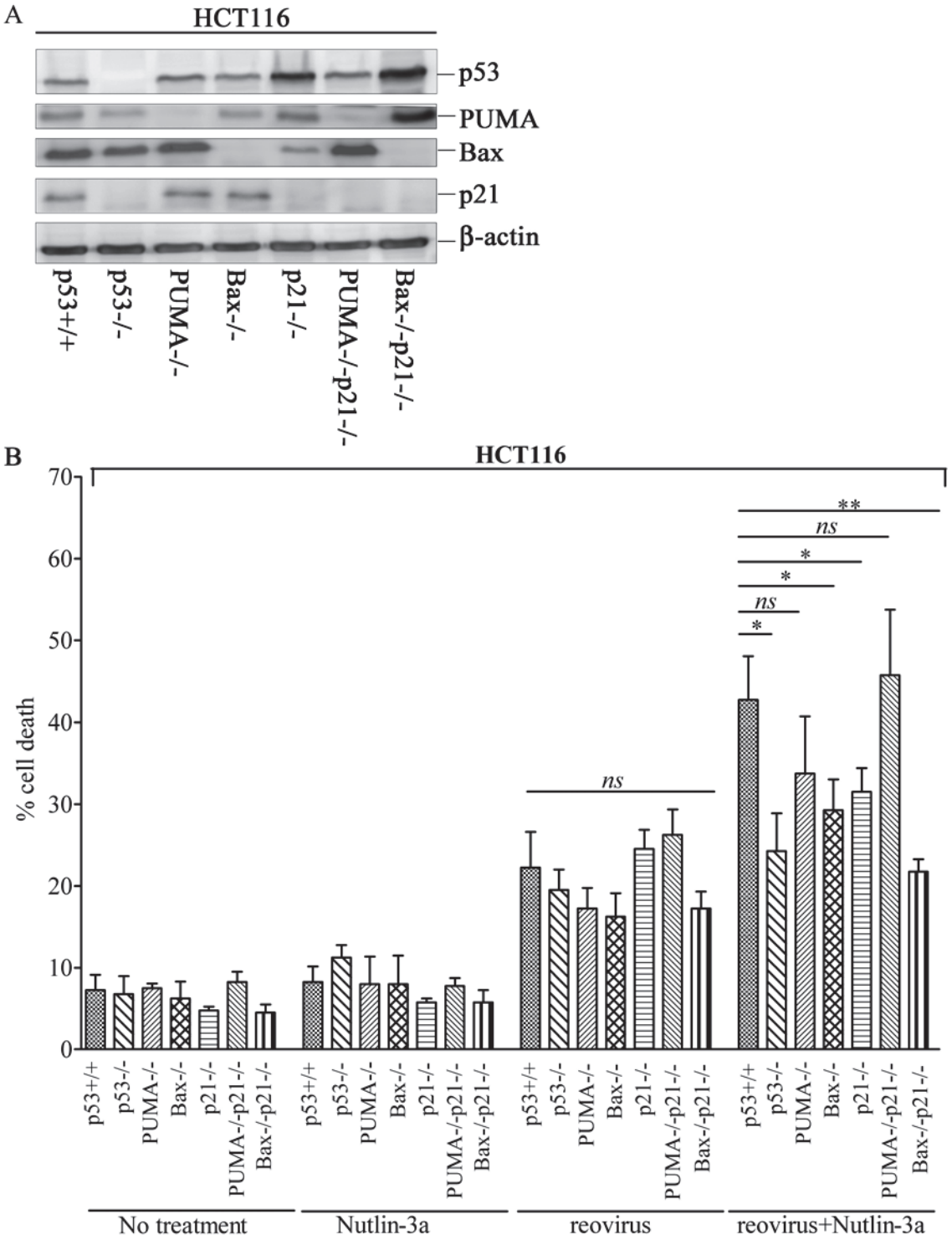
A
HCT116
p53
PUMA
Bax
p21
β-actin
p53+/+
p53-/-
PUMA-/-
Bax-/-
p21-/-
PUMA-/-p21-/-
Bax-/-p21-/-
B
HCT116
% cell death
70
60
50
40
30
20
10
0
ns
**
ns
*
*
ns
*
No treatment
Nutlin-3a
reovirus
reovirus+Nutlin-3a

Fig. 3.7. *Noxa* status does not significantly affect the apoptosis levels of HCT116 cells. (A). RNA levels for *noxa* were determined by real-time PCR (left panel). (B). Vector control cells and Noxa knockdown (kd) cells were subjected to treatment with Nutlin-3a, reovirus or the combination of the two. Levels of cell death were determined by Annexin V and 7-AAD staining (right panel, ±*s.e.m.*, n=2).

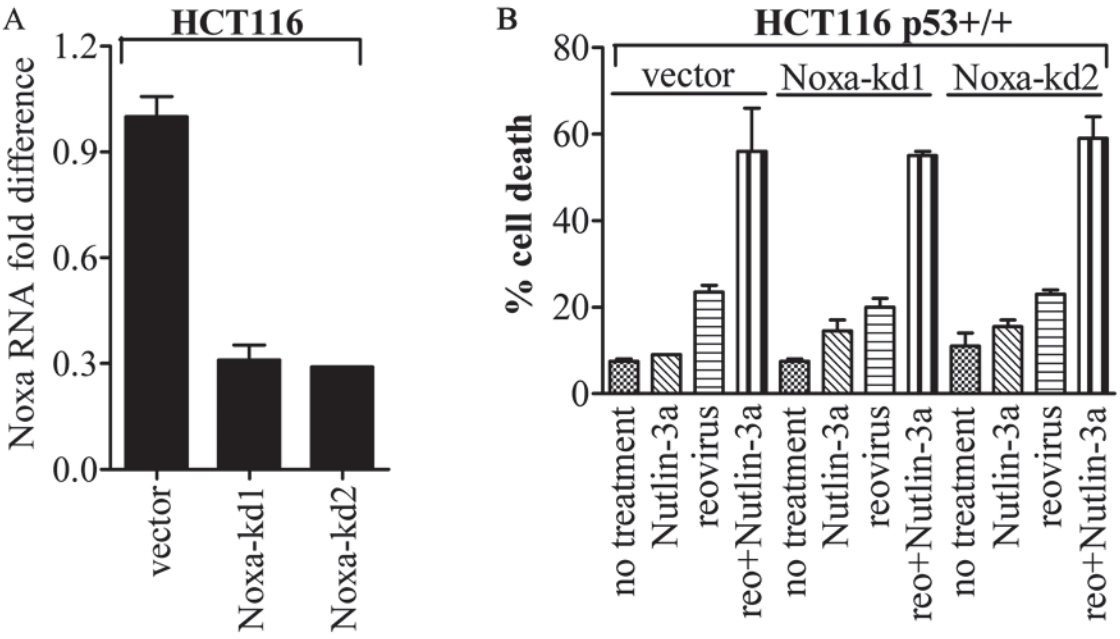
A
HCT116
Noxa RNA fold difference
1.2
0.9
0.6
0.3
0.0
vector
Noxa-kd1
Noxa-kd2
B
HCT116 p53+/+
% cell death
80
60
40
20
0
vector
Noxa-kd1
Noxa-kd2
no treatment
Nutlin-3a
reovirus
reo+Nutlin-3a

Fig. 3.8. A combination of reovirus and Nutlin-3a induces higher levels of NF-κB activation compared to reovirus infection alone. Levels of NF-κB transcription activity after reovirus infection in (A) HCT116 p53+/+ cells and (B) U2OS cells (both ±*s.e.m.*, n=4). HCT116 cells were infected at an MOI of 1 and lysates were collected at 12 hpi. U2OS cells were infected at MOI of 500 and lysates were collected at 48 hpi. NF-κB activation was determined by a dual-luciferase reporter assay. (C) Nutlin-3a treatment enhanced levels of NF-κB p65 nuclear translocation. Arrows point to infected cells. Student's *t*-test was used to compare two groups of data; NS: not significant and **P*<0.05.

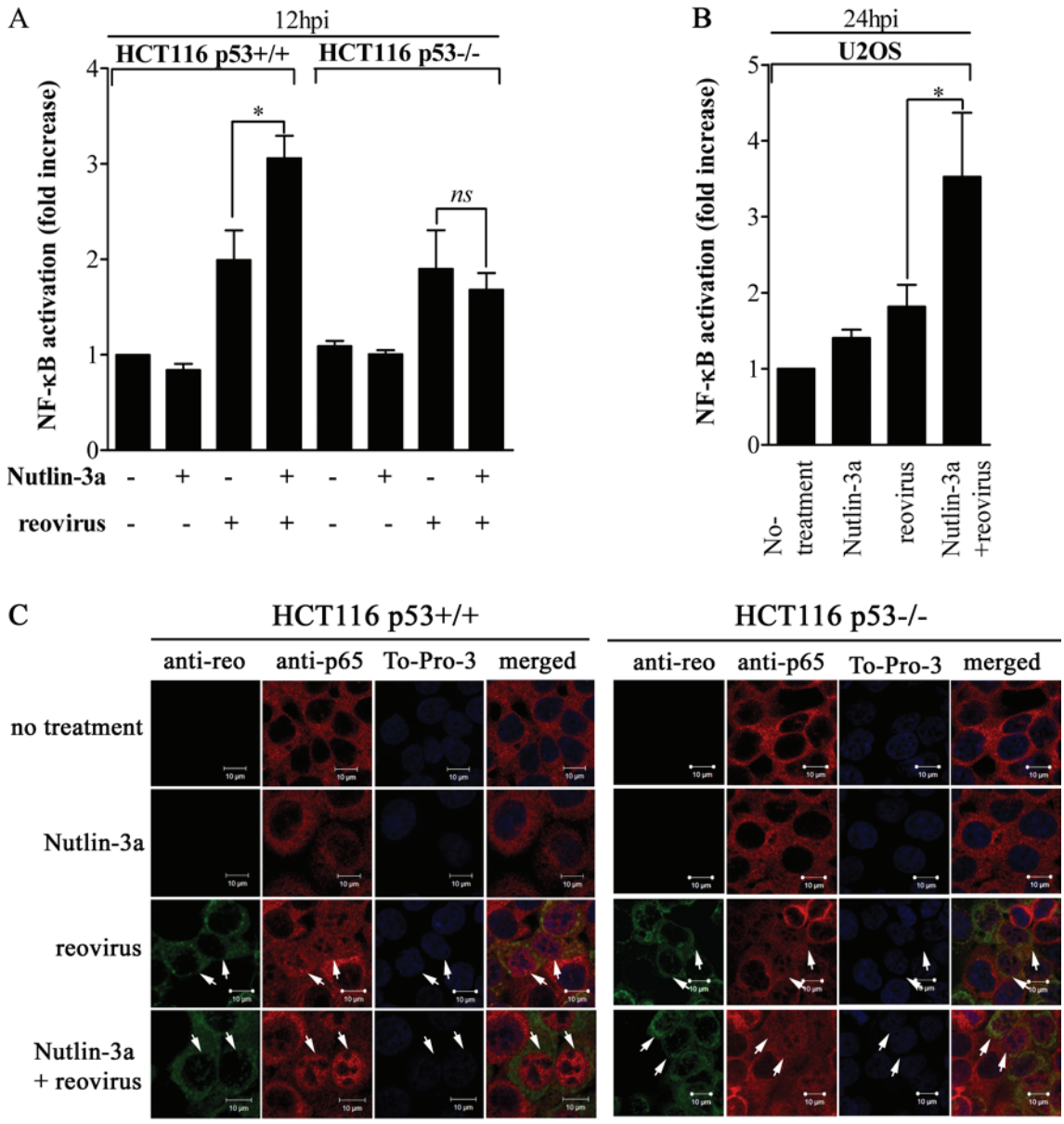
A
12hpi
HCT116 p53+/+
HCT116 p53-/-
NF-κB activation (fold increase)
0
1
2
3
4
*
ns
Nutlin-3a - + - + - + - +
reovirus - - + + - - + +
B
24hpi
U2OS
NF-κB activation (fold increase)
0
1
2
3
4
5
*
No-treatment
Nutlin-3a
reovirus
Nutlin-3a +reovirus
C
HCT116 p53+/+
HCT116 p53-/-
anti-reo
anti-p65
To-Pro-3
merged
no treatment
Nutlin-3a
reovirus
Nutlin-3a + reovirus

Fig. 3.9. Inhibition of NF-κB activation reduces cell death caused by the combination of reovirus and Nultin-3a. (A) NF-κB inhibitors (N and B) blocked NF-κB p65 translocation from the cytoplasm to nucleus. (B) NF-κB inhibitor N (±*s.e.m.*, n=5) and (C) NF-κB inhibitor B significantly reduced the level of cell death induced by the combined reovirus and Nutlin-3a treatment (±*s.e.m.*, n=3). Cell death was determined by quantifying the sub-G1 populations of the PI-stained cells. Student's *t*-test was used to compare two groups of data; NS: not significant, ***P*<0.001 and ****P*<0.0001.

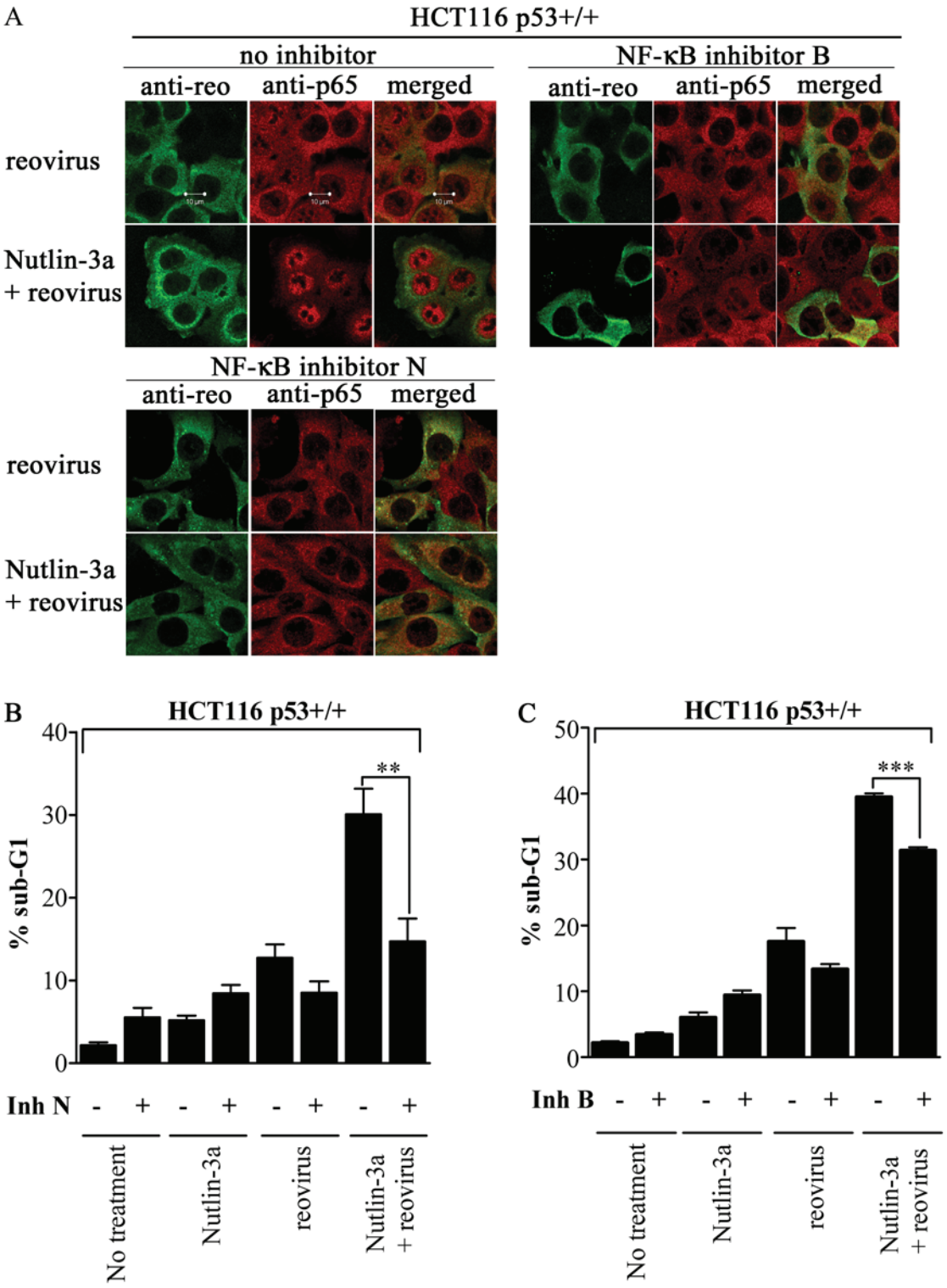
A
HCT116 p53+/+
no inhibitor
NF-κB inhibitor B
NF-κB inhibitor N
anti-reo
anti-p65
merged
reovirus
Nutlin-3a
+ reovirus
B
HCT116 p53+/+
% sub-G1
Inh N
No treatment
Nutlin-3a
reovirus
Nutlin-3a
+ reovirus
C
HCT116 p53+/+
% sub-G1
Inh B
No treatment
Nutlin-3a
reovirus
Nutlin-3a
+ reovirus

Fig. 3.10. Upregulation of p53-target genes (A) *noxa*, (B) *puma*, (C) *bax* and (D) *p21* induced by Nutlin-3a and reovirus was inhibited by NF-κB inhibitor N. HCT116 p53+/+ cells were pretreated with NF-κB inhibitor N for 1 hour before Nutlin-3a treatment. At 6 h post Nutlin-3a treatment, cells were infected by reovirus at an MOI of 1. RNA samples were collected at 24 hpi and subjected to RNA purification, cDNA synthesis and real-time PCR (representative of two independent experiments, ±*s.e.m.*).

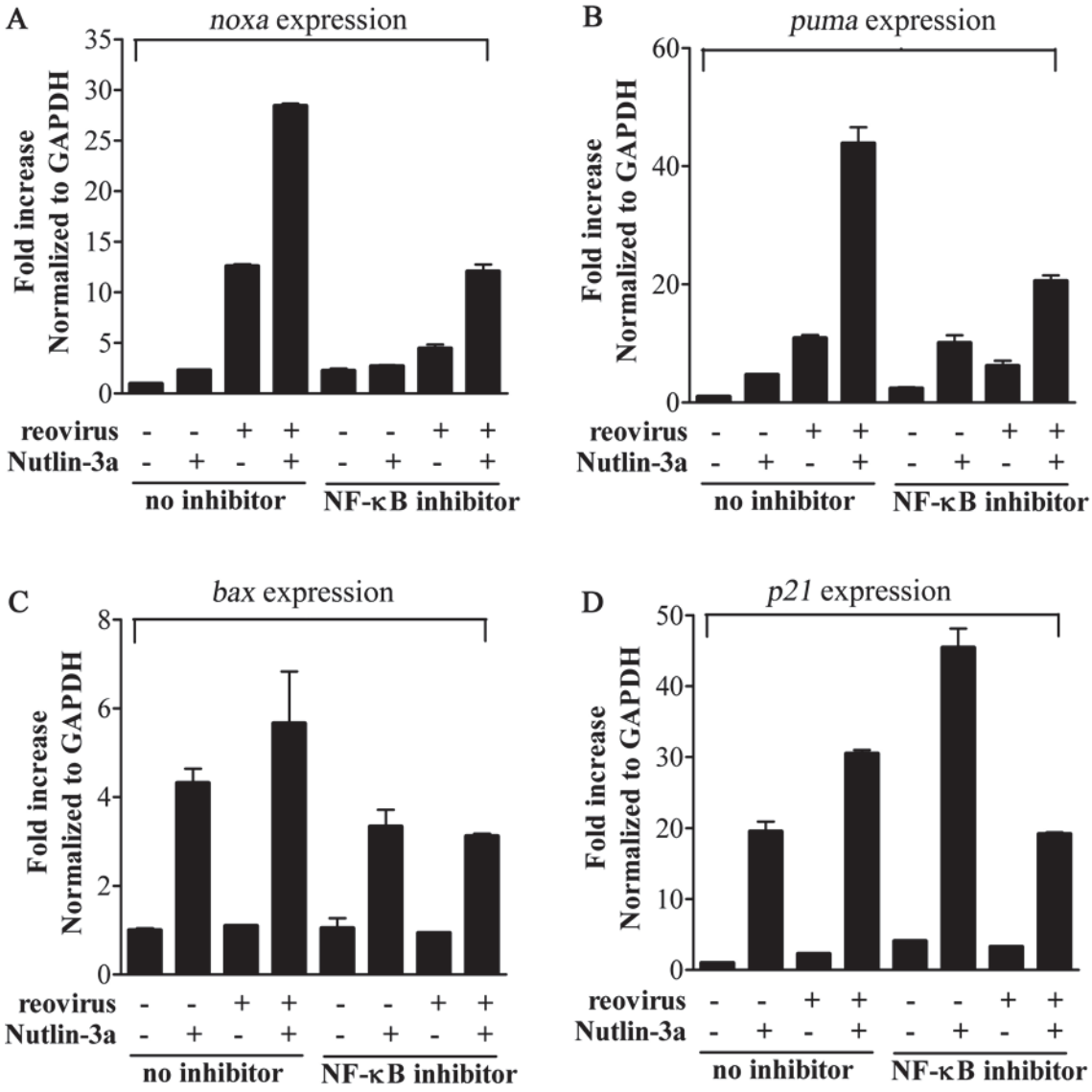
A
noxa expression
Fold increase
Normalized to GAPDH
35
30
25
20
15
10
5
0
reovirus - - + + - - + +
Nutlin-3a - + - + - + - +
no inhibitor
NF-κB inhibitor
B
puma expression
Fold increase
Normalized to GAPDH
60
40
20
0
reovirus - - + + - - + +
Nutlin-3a - + - + - + - +
no inhibitor
NF-κB inhibitor
C
bax expression
Fold increase
Normalized to GAPDH
8
6
4
2
0
reovirus - - + + - - + +
Nutlin-3a - + - + - + - +
no inhibitor
NF-κB inhibitor
D
p21 expression
Fold increase
Normalized to GAPDH
50
40
30
20
10
0
reovirus - - + + - - + +
Nutlin-3a - + - + - + - +
no inhibitor
NF-κB inhibitor

Fig. 3.11. Apoptosis induced by Nutlin-3a and reovirus is not due to the activation of the TRAIL signaling pathway. (A) Effects of soluble DR4 (100 ng/mL), DR5 (100 ng/mL) and anti-TRAIL (30 μg/mL) antibody towards TRAIL-induced cell cytotoxicity (TRAIL: 20 ng/mL) at 24 hours post treatment. (B) Soluble DR4, DR5 and anti-TRAIL antibody did not reduce levels of apoptosis induced by the combination of Nutlin-3a and reovirus. Competitive soluble DR4 or DR5 ligands (500 μg/mL) or anti-TRAIL antibody (300 μg/mL) were used to treat HCT116 p53+/+ cells one hour before Nutlin-3a treatment. Apoptosis was determined at 24 hpi by Annexin V and 7-AAD staining (±*s.e.m.*, n=3). Student's *t*-test was used to compare two groups of data; NS: not significant, ***P*<0.001 and ****P*<0.0001.

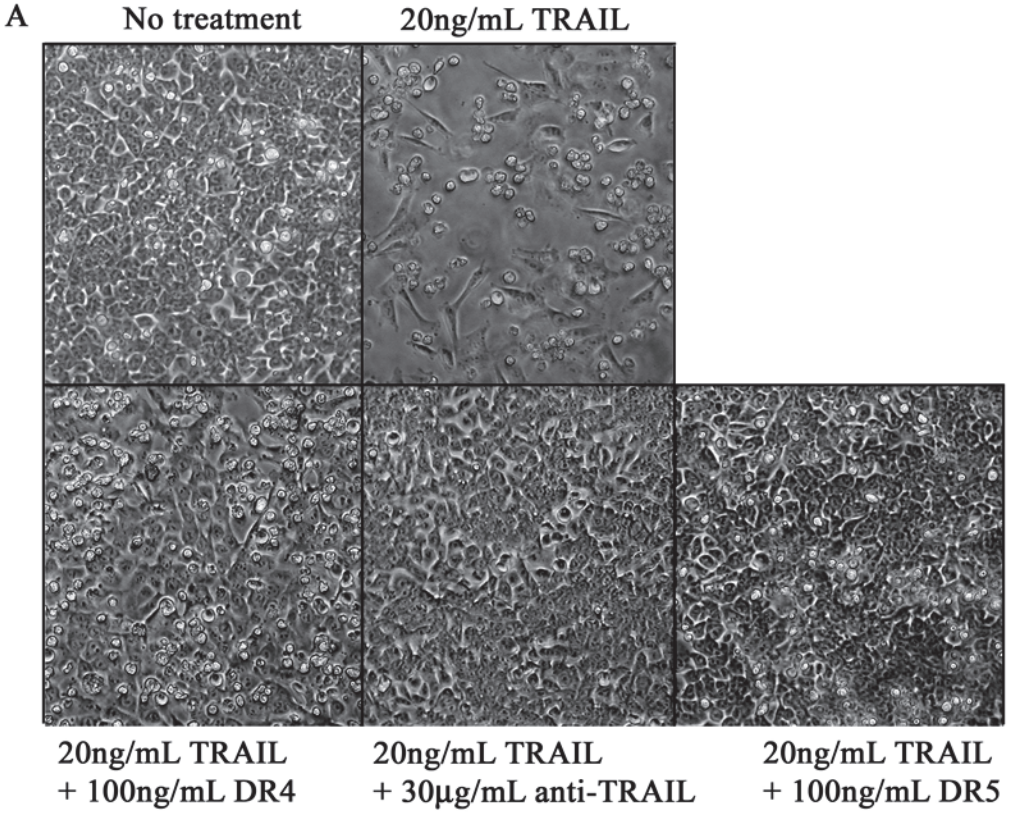
A
No treatment
20ng/mL TRAIL
20ng/mL TRAIL
+ 100ng/mL DR4
20ng/mL TRAIL
+ 30µg/mL anti-TRAIL
20ng/mL TRAIL
+ 100ng/mL DR5

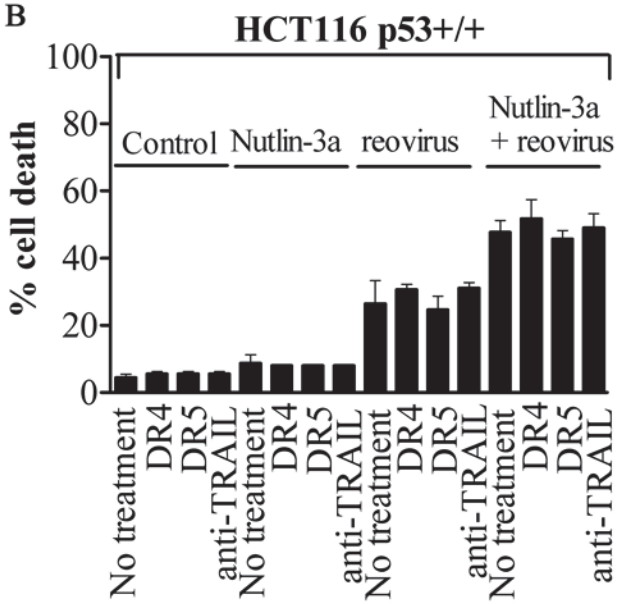
B
HCT116 p53+/+
% cell death
100
80
60
40
20
0
Control
Nutlin-3a
reovirus
Nutlin-3a
+ reovirus
No treatment
DR4
DR5
anti-TRAIL

Fig. 3.12. Nutlin-3a significantly enhances both reovirus-induced cytotoxicity and reovirus dissemination in HCT116 p53+/+ cells. (A) IC_{50} values for reovirus in HCT116 p53+/+ or p53-/- cells in the presence or absence of 5 μM Nutlin-3a at 48 hpi (±*s.e.m.,* n=3). Immunohistochemical staining of reovirus-infected (B) HCT116 cells and (C) U2OS cells in the presence or absence of Nutlin-3a treatment. Lower panel of (B), quantification of plaque size on reovirus infected HCT116 cells (±*s.e.m.,* plaque number n=14). Cells were fixed at 7 days post infection and stained using anti-reovirus antibody. Shown as the representative of three respective experiments.

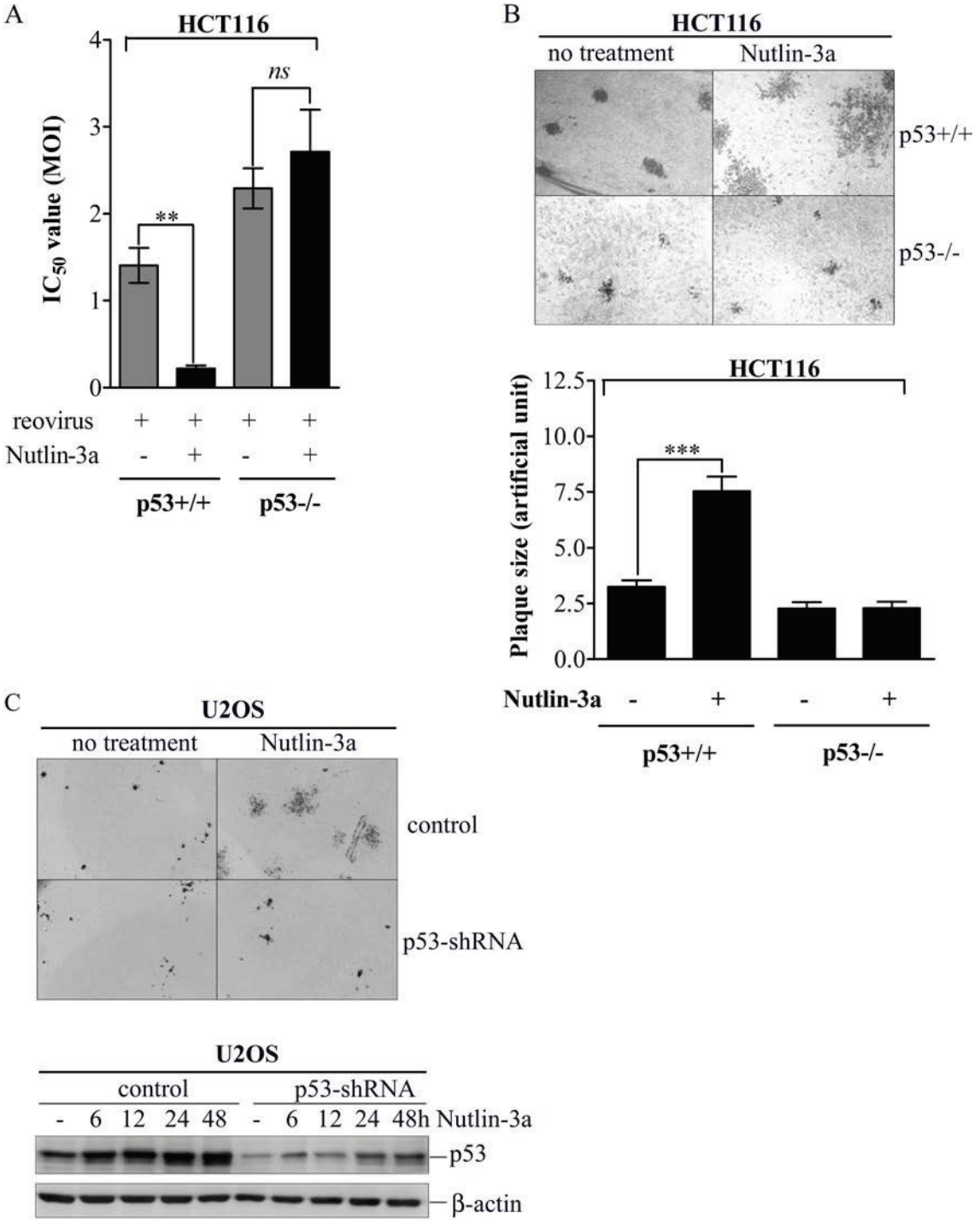
A
HCT116
ns
**
IC50 value (MOI)
4
3
2
1
0
reovirus + + + +
Nutlin-3a - + - +
p53+/+
p53-/-
B
HCT116
no treatment
Nutlin-3a
p53+/+
p53-/-
HCT116
Plaque size (artificial unit)
12.5
10.0
7.5
5.0
2.5
0.0
***
Nutlin-3a - + - +
p53+/+
p53-/-
C
U2OS
no treatment
Nutlin-3a
control
p53-shRNA
U2OS
control
p53-shRNA
- 6 12 24 48 - 6 12 24 48h Nutlin-3a
p53
β-actin

Chapter 4 Sub-lethal Concentrations of Traditional Chemotherapy Agents Induce Accumulation of p53 and Enhance Reovirus-induced Apoptosis

4.1. Introduction

The majority of traditional chemotherapy agents target fast-growing tumor cells based on the rationale that cancer cells are rapidly dividing and more sensitive to damage during DNA synthesis. Ideally, most normal cells are quiescent and rest in the G_0/G_1 phase of the cell cycle. Therefore, chemotherapy drugs that damage dividing cells in S or M phase would have a selective bias towards tumor cells. Drug-induced DNA damage (such as single- or double-strand breaks) activates the cellular response for DNA repair. Prolonged exposure to these chemotherapy drugs will induce apoptosis in fast dividing cells and lead to tumor cell death and tumor mass reduction. However, these chemotherapy drugs also damage fast growing normal cells, causing side effects to patients. Since the first chemotherapy drug was applied clinically in the 1940's (GILMAN and PHILIPS 1946), traditional chemotherapeutics have been widely used and save patients' lives every day. However, emerging clinical trials have proved that traditional chemotherapy drugs have reached their plateau of efficacy as primary treatments, and combination therapies coupling traditional chemotherapy drugs with specific inhibitors or alternative therapies have become important in cancer treatment (Bagnyukova et al. 2010).

Since Nutlin-3a triggered accumulation of p53 significantly enhances reovirus-induced apoptosis (Chapter 3), I attempted to use sub-lethal concentrations of certain traditional chemotherapy drugs to stabilize p53 and then determine whether these drugs could enhance reovirus-induced apoptosis. This was to test the possibility of tailoring

patients' treatment based on the p53 status in their cancer and treating accordingly with a combination of low concentrations of chemotherapy drugs and reovirus. Four common traditional chemotherapy agents were chosen as test drugs and they were etoposide (Etp), actinomycin D (ActD), 5-fluorouracil (5-FU) and doxorubicin (Dox). Etoposide (also known as VP16) as well as doxorubicin (Adriamycin®) are topoisomerase II inhibitors that introduce single- or double-strand breaks in the DNA. Actinomycin D forms a stable complex with DNA to block the movement of RNA polymerase (Sobell 1985). 5-Fluorouricial, a pyrimidine analog, acts primarily as a thymidylate synthase inhibitor and incorporates its metabolites into DNA and RNA to interrupt DNA replication and RNA processing (Longley et al. 2003). All these drugs can trigger a DNA damage response in cells and inevitably activate wild-type p53.

4.2. Results

4.2.1. Sub-lethal Concentrations of Traditional Chemotherapy Agents Stabilize p53

In order to determine a concentration of each drug that both induces p53 accumulation yet does not cause extensive cell death by itself, an MTS cell proliferation assay was carried out on HCT116 p53+/+ cells in the presence of serial dilutions of each drug. As shown in Fig. 4.1A-D, the four drugs tested induced accumulation of p53 in a relatively dose-dependent manner. I therefore chose a low concentration of each drug, at which p53 was obviously accumulated while at the same time did not cause extensive cell death, for further study.

4.2.2. A Low Concentration of ActD or Etp Enhances Reovirus-induced Cell Death in a p53-dependent Manner

To determine whether the low concentration of these chemotherapy agents could enhance reovirus-induced cell death and whether the enhancement is p53-dependent, low concentrations of Etp (1.6 μM), ActD (0.63 nM), 5-FU (0.39 μg/mL) or Dox (60 ng/mL) were added to the culture media of either HCT116 p53+/+ or HCT116 p53-/- cells right after reovirus infection. At 24 hpi, cells were harvested and stained for the percentage of cell death using Annexin V and 7-AAD staining followed by FACS analysis. As shown in Fig. 4.2A, other than 5-FU, none of the other three drugs at the indicated concentrations induced a significant level of cell death by itself. When any of the four drugs was combined with reovirus, levels of apoptosis were significantly enhanced in HCT116 p53+/+ cells. However, compared to reovirus infection alone, the level of cell death was not significantly enhanced in HCT116 p53-/- cells when ActD, Etp or 5-FU were supplemented to the media after reovirus infection. The levels of cell death induced by the combination of reovirus and Dox were similar between p53+/+ and p53-/- cells, indicating that p53-independent apoptosis pathways were induced in the presence of reovirus and Dox combination.

At 24 hpi, cells were also collected and analysed for the percentage of cells that were infected by reovirus by FACS using an antibody specific against reovirus. As shown in Fig. 4.2B, the percentages of reovirus-infected cells (percentage of infection) were similar between HCT116 p53+/+ and p53-/- cells treated with the four drugs. Furthermore, except for Etp treatment, the percentage of infection was not higher in drug-treated cells than in cells infected by reovirus alone. Therefore, the enhancement of cell death (as shown in Fig. 4.2A) was not due to the number of cells being infected by reovirus. Hence,

specific chemotherapy agents (such as ActD and Etp) enhance reovirus-mediated cell death in a p53-dependent manner. This enhancement of cell death was reovirus-dependent since UV-inactivated reovirus (UV-reovirus) did not cause significant augmentation of cell death (Fig. 4.2C). Therefore, low concentrations of ActD (0.63 nM) and Etp (1.6 μM) were chosen for further study due to the p53-dependent induction of enhanced cell death when combined with reovirus.

4.2.3. The Enhancement of Cell Death induced by a Low Concentration of ActD or Etp is Caspase-dependent

To determine whether cell death induced by the addition of low dose of chemotherapy drugs was apoptosis-dependent, a caspase inhibitor, ZVAD, was used to block apoptosis. As shown in Fig. 4.3, addition of ZVAD to the medium significantly reduced the level of cell death induced by reovirus alone and by the combination of reovirus and ActD or Etp (ActD/Etp) at indicated concentrations. Therefore, the higher level of cell death induced by the combination of ActD/Etp (at the indicated concentrations) and reovirus is due to caspase-dependent apoptosis.

4.2.4. p53-target Genes are Upregulated by the Combination of Reovirus and a Low Concentration of ActD/Etp

As mentioned in Chapter 3, a combination of reovirus and Nutlin-3a significantly enhances the expression of certain p53-target genes such as *puma* and *bax* compared to reovirus infection or Nutlin-3a treatment alone. I therefore determined whether the combination of reovirus and ActD/Etp also elevated the expression levels of p53-target genes. As shown in Fig. 4.4A and B, reovirus infection alone induced expression of *noxa*

and *puma* in a relatively p53-independent manner, consistent with previous observations (Fig. 3.5A, B). However, in HCT116 p53+/+ cells, the chosen concentrations of ActD or Etp alone did not induce significant upregulation of *noxa* or *puma* (Fig. 4.4A and B). *p21*, on the other hand, was upregulated by either ActD or Etp at the chosen concentrations in HCT116 p53+/+ cells. Furthermore, the combination of reovirus and ActD/Etp significantly enhanced the up-regulation of *p21* in HCT116 p53+/+ cells compared to single drug treatment (Fig. 4.4D). Expression of *bax* in HCT116 p53+/+ cells was not affected by ActD treatment but was enhanced by Etp treatment; the combination of ActD/Etp and reovirus significantly augmented the expression of *bax* (Fig. 4.4C). On the other hand, in HCT116 p53-/- cells, *bax* and *p21* expressions were not affected by Etp or a combination of reovirus and Etp/ActD. Interestingly, expression levels of *bax* and *p21* were slightly downregulated in the presence of ActD compared to the no-treatment control. Since ActD can block RNA synthesis (Goldberg et al. 1963; Goldberg and REICH 1964; Goldberg 1971), the chosen concentration (0.63 nM) of ActD could have blocked RNA synthesis of p53-target genes in HCT116 p53-/- cells. Meanwhile, in HCT116 p53+/+ cells, the major effect of this very low concentration of ActD might be to activate p53, which directly resulted in the upregulation of these p53-target genes.

Therefore, the combination treatment of reovirus and ActD/Etp on p53+/+ cells significantly upregulates p53-target genes compared to drug treatment or reovirus-infection alone.

4.2.5. Apoptosis Induced by the Combination of Reovirus and a Low Concentration of ActD/Etp Requires *p21* and *bax*

Since various p53-target genes were upregulated by the combination of reovirus and ActD/Etp, I wanted to further determine which gene(s) are important for the enhancement of apoptosis by the combinations. Therefore, HCT116 p53+/+ cells and its isogenic knockout cells (described in Chapter 3) were infected by reovirus or treated with a combination of reovirus and ActD/Etp. The levels of apoptosis were determined. As shown in Fig. 4.5, reovirus-induced apoptosis was not significantly affected by loss of the p53-target genes such as *puma*, *bax*, *p21* and *noxa*. However, the enhancement of apoptosis induced by the combination of Etp and reovirus was significantly reduced by the lack of *bax* or *bax* and *p21* combined. Furthermore, levels of cell death caused by the combination of ActD and reovirus were significantly decreased when *bax*, *p21* or both *bax* and *p21* genes were missing from HCT116 cells. In contrast, the status of *puma* or *noxa* did not play a major role in enhancing the apoptosis induced by the combination of reovirus and either of these two chemotherapy drugs.

4.2.6. A Combination of Reovirus and ActD Elevates NF-κB Activation

As p53 accumulation caused by Nutlin-3a treatment enhances reovirus-induced activation of NF-κB (Fig. 3.8), I wanted to further determine whether stabilization of p53 by a low concentration of ActD/Etp also induces higher levels of NF-κB activation. Nuclear translocation of p65 was used as an indicator for NF-κB activation. As shown in Fig. 4.6, treatment with ActD or Etp of either HCT116 p53+/+ cells or p53-/- cells did not induce noticeable nuclear translocation of p65. Reovirus induced NF-κB activation in both HCT116 p53+/+ and p53-/- cells. NF-κB activation was further enhanced by the ActD treatment in HCT116 p53+/+ cells, as p65 distribution was further shifted to the

nucleus in HCT116 p53+/+ cells but not in p53-/- cells. However, Etp treatment did not affect the activation of NF-κB induced by reovirus (Fig. 4.6).

To determine whether the augmentation of NF-κB activation was required for the enhancement of apoptosis induced by the combination of reovirus and ActD/Etp, the NF-κB inhibitor N was used to block NF-κB activation. As shown in Fig. 4.7, the level of cell death induced by either reovirus alone or reovirus and ActD/Etp was significantly reduced when NF-κB activation was blocked by the treatment with the NF-κB inhibitor N. Hence, NF-κB activation is required for the enhancement of cell death induced by the combination of reovirus and low concentrations of ActD or Etp.

4.2.7. Treatment of ActD or Etp Significantly Enhances Reovirus Dissemination

Increased levels of cytotoxicity caused by the addition of ActD or Etp to reovirus infected cells may be due to improved reovirus release and spread. Therefore, the levels of reovirus spread in the presence of ActD or Etp treatment was determined using a plaque size assay.

As shown in Fig. 4.8, in p53+/+ cells reovirus spread much better in the presence of low concentrations of ActD or Etp than in cells that were not treated. The sizes of the plaques were not affected by treatment with ActD or Etp in p53-/- HCT116 cells, indicating that the enhancement of reovirus dissemination in the presence of these drugs is p53-dependent.

4.2.8. Establishment of HCT116 Xenografts in NOD-SCID Mice and Pilot Experiments to Determine the Dosages of ActD/Etp and Duration of Injections

As shown above, using HCT116 p53+/+ and p53-/- cells, a combination of reovirus and ActD/Etp induces significantly higher levels of cell death in p53 wild-type cells compared to reovirus or individual drug treatment alone. I next wanted to determine whether a combination of a low dose of ActD/Etp and oncolytic reovirus administration could provide a more efficient way of eliminating tumors in mice that contain wild-type p53.

Both ActD and Etp have been used as chemotherapy drugs for treating various types of cancer. *In vivo* mouse xenografts studies have been carried out as well. In general, for mouse studies, ActD was used at concentrations ranging from 45 to 225 μg/kg and up to 5 μg/mouse as therapeutic concentrations (Weissbach et al. 1966; Yamamoto et al. 2009), while Etp was used at concentrations ranging from 2 to 90 mg/kg with 2 mg/kg defined as a low dose (Bouvet et al. 1998; Shieh et al. 2006; Rezai et al. 2007). Since the objective of my study was to determine whether stabilization of p53 enhances reovirus-induced apoptosis and virus dissemination, a low concentration of ActD or Etp that induces p53 accumulation in tumors *in vivo* was used first.

Eight NOD-SCID mice were *s.c.* injected at the right flank with HCT116 p53+/+ cells (5×10^6 cells per mouse) to establish tumor xenografts. Once palpable tumors were established, vehicle fluid (40% DMSO), low concentrations of ActD (45 μg/kg) or Etp (10 mg/kg) were injected into the NOD-SCID mice *via* intraperitoneal injection (*i.p.*). As shown in Table 4.1, mice were sacrificed and tumors were excised at different days post-injection. To determine whether p53 was activated/accumulated in tumors after the respective injections, the excised tumors were homogenized and subjected to RNA extraction, cDNA synthesis and qRT-PCR using primers specific for *p21* and *puma*. As shown in Fig. 4.9A and B, mice in group A were sacrificed one day after the first

injection. *Puma* and *p21* were slightly upregulated after one injection of 10 mg/kg Etp but not by ActD injection of 45 μg/kg. Mice in group B were injected with either drug twice in two days and sacrificed 2 days after the initial injection. Expression levels of *p21* and *puma* in the tumors from Etp-injected mice were increased compared to group-A mice, indicating that multiple injections of Etp were needed. However, two injections of ActD at 45 μg/kg did not affect the expression levels of either *p21* or *puma*, indicating that a higher dosage of ActD was needed. Mice in group C were injected twice with either drug but left alone without any injection for an extra day. As shown in Fig. 4.9A and B, *p21* and *puma* expression in tumors from Etp-injected mice failed to be upregulated after one drug-free day, indicating that multiple injections of Etp were needed to activate p53 in the tumor. ActD failed to affect either *p21* or *puma* expression when the drug was metabolized one day after two injections.

Therefore, multiple injections of 10 mg/kg Etp and either more injections or higher concentrations of ActD are required to achieve p53 activation in the tumor xenografts in NOD-SCID mice.

Five injections of each different concentrations of ActD or Etp, as described in Table 4.2, were then *i.p.* injected to mice that were bearing palpable tumors (Etp at 5, 10 or 20 mg/kg; ActD at 45 or 180 μg/kg). Real-time qRT-PCR using specific primers for *p21*, *puma* or *noxa* was carried out to determine whether p53 was activated after injections. As shown in Fig. 4.10A, B and C, neither ActD nor Etp could induce upregulation of *p21*, *puma* or *noxa* in HCT116 p53-/- cells (groups G-L). Five injections of 5 mg/kg Etp could induce upregulation of p53-target genes but the fold increase was rather small. Among the ActD concentrations tested here, five injections of 180 μg/kg ActD in NOD-SCID mice induced obvious upregulation of *p21*, *puma* and *noxa* as shown

in Fig. 4.10A, B and C (group F). Western blotting analysis also indicated that five injections of 180 μg/kg ActD stimulated drastic p53 accumulation (Fig. 4.10D). Therefore, a schedule of 5 injections of 180 μg/kg ActD was used to accumulate/activate p53 in the *in vivo* experiments that were next performed.

4.2.9. A Combination of Reovirus and a Low Dosage of ActD Significantly Reduces Tumor Growth in NOD-SCID Mice

To determine whether the combination of a low concentration of ActD plus reovirus infection enhances tumor regression, male NOD-SCID mice bearing HCT116 p53+/+ tumors were grouped and treated according to the schedule described in Table 4.3. Since chemotherapy drugs were added right after reovirus infection and remained present throughout the *in vitro* experiment, reovirus injection was accompanied by ActD injection followed by four extra injections in the *in vivo* experiment. Mice were monitored for health and tumor growth daily after reovirus injection.

After five injections of vehicle or ActD with or without the injection of reovirus, mice were allowed to recover for one day, since the combination group lost significant weight and had an ill appearance. Unfortunately, at 6 days after the initial injection, mice that were treated with the combination of reovirus and ActD (group D) were moribund, although all the other groups (A, B and C) stayed healthy. Therefore, mice in group D together with three mice of each A, B or C group were sacrificed at 6 days post injection. Tumors were excised and weights measured, followed by single-cell suspension processed for western blot analysis and reovirus plaque titration.

As shown in Fig. 4.11, the combination of reovirus and ActD (Group D) significantly reduced the weight of tumors compared to individual treatment alone.

Tumors injected with ActD (Group B) showed clearly accumulated p53, as shown in Fig. 4.12A using western blot analysis. However, the levels of p53 in tumors in the combination group were slightly lower than those in the ActD-alone group. T3D reovirus has not been considered to be particularly effective at inhibiting protein translation of the host cell (Smith et al. 2005), blockage of protein synthesis could still be observed in reovirus infected cells at a late stage of infection (data not shown). Therefore, the lower levels of p53 in the combination group might be due to reovirus-induced mRNA-translation inhibition.

Reovirus production in the combination group (Group D), on the other hand, was higher than the group with reovirus injection alone (Group C) (Fig. 4.12A). Reovirus production by the tumors was further analysed by reovirus plaque titration. As shown in Fig. 4.12B, the total reovirus production per cell (normalized by tumor weight) was significantly higher in tumors from mice that were treated with the combination of ActD and reovirus compared to tumors from mice treated with reovirus injection alone. Hence, the combination of reovirus and ActD significantly enhanced the tumor regression ability of reovirus *in vivo* as well as increased reovirus production levels in the tumor. Since accumulation of p53 did not affect reovirus production within the first round of reovirus life cycle *in vitro* (Fig. 3.1A), it was unlikely that the reduction in tumor weight was due to increased reovirus replication in a single cell. Instead, a higher rate of reovirus spread due to p53 accumulation likely resulted in more tumor cells being infected by reovirus. Thus, the tumors produced more reovirus in the course of 6 days before the mice were sacrificed. These results indicate that the combination of ActD and reovirus very likely enhances reovirus spread in tumor cells. On the other hand, mice in groups A, B and C

stayed healthy until 21 days post initial injection (Fig. 4.13A) and both reovirus and ActD reduced tumor mass significantly (Fig. 4.13B).

The combination of reovirus and ActD may have caused unforeseen side effects in NOD-SCID mice, which resulted in lethal reactions. However, since reovirus does not cause disease in wild-type mice, it remains untested whether the combination of ActD and reovirus would induce lethal reactions in an immunocompetent model.

4.3. Discussion

Results from this study showed that the p53 status of tumor cells affects the efficiency of reovirus oncolysis when reovirus is combined with certain chemotherapy drugs such as ActD and Etp *in vitro*. The accumulation of p53 induced by the low dosage of ActD or Etp significantly enhances reovirus-induced apoptosis (Fig. 4.2), which is caspase-dependent and requires *p21* and *bax* (Fig. 4.3 and Fig. 4.5). ActD, but not Etp, enhances reovirus-induced NF-κB activation at the time point tested, but the level of the activation is not as high as that in the presence of Nutlin-3a (Fig. 3.8). However, blocking NF-κB activation significantly reduces the level of cell death caused by not only the combination of reovirus and ActD, but also by the combined treatment of reovirus and Etp (Fig. 4.7). It is possible that the combination of reovirus with different p53-activators/accumulators could induce NF-κB activation with different kinetics, and hence the highest level of NF-κB activation would be detected at a different time-point. This result (Fig. 4.7) and what was observed in reovirus-infected cells in the presence of Nutlin-3a (Fig. 3.9), indicate that drugs that activate p53 can enhance the level of NF-κB activation in the presence of reovirus infection.

It is noteworthy that the combination of reovirus and Nutlin-3a does not significantly enhance the *p21* upregulation compared to Nutlin-3a treatment alone (Fig. 3.5D), possibly because at a later stage of apoptosis the pro-arrest gene *p21* is not required for cell death. However, the results shown above indicate that the upregulation of *p21* by ActD/Etp is further enhanced by reovirus infection (Fig. 4.4D). Since Nutlin-3a was added to the cell medium 6 hours before reovirus infection but ActD/Etp was added at the same time as reovirus infection, the combination of reovirus and Nutlin-3a likely induced apoptosis earlier than the combination of reovirus and ActD/Etp. Upregulation of *p21* in reovirus and ActD/Etp-treated HCT116 p53+/+ cells may therefore be blocked at a later time-point to allow apoptosis to proceed.

Among the p53-target genes, *bax* and *p21* are more important than othere for the enhancement of apoptosis induced by the combination of ActD/Etp and reovirus (Fig. 4.5). This result is similar to what was observed in the Nutlin-3a and reovirus combination study as described in Chapter 3 (Fig. 3.6B), where the augmentation of apoptosis induced by the combination of reovirus and Nutlin-3a requires *p21* and *bax*. Since reovirus infection caused similar levels of cell death in all the cells tested (Fig. 4.5B), it is less likely that HCT116 Bax-/-, p21-/- or Bax-/-p21-/- cells were inherently resistant to reovirus-induced apoptosis. Therefore, the sensitivity of p53 wild-type cancer cells to the combination of reovirus and p53-stabilizing drugs/small molecules very likely depends on the status of *p21* and *bax* in the cells.

It has been reported that higher concentrations of Etp (10 or 20 μM) alone could induce NF-κB activation (Strozyk et al. 2006; Chang and Miyamoto 2006; Meley et al. 2010). Moreover, p53-mediated NF-κB activation could enhance Etp-induced cell death

in medulloblastoma in both caspase-dependent and –independent manners (Meley et al. 2010). In my experiments, Etp did not affect p65 translocation (activation). It is possible that the low concentration of Etp used in this study (1.6 μM) was not to the threshold required to assist reovirus-induced NF-κB activation. Alternatively, NF-κB activation occurs in a time-dependent manner and in most cases happens quickly after reovirus stimulation (Connolly et al. 2000). Further, Meley *et al.* reported that 20 μM of Etp could induce NF-κB activation within 2 h post treatment while 10 ng/mL TNFα stimulated NF-κB activation within 1 h (Meley et al. 2010). Therefore, it is possible that activation of NF-κB in the presence of the combination of reovirus and Etp occurred earlier (or later) than 12 hpi, when levels of NF-κB activation were determined using immunostaining in this study.

Results from my *in vivo* experiments showed that the combination of ActD and reovirus significantly reduces the tumor burden in mice (Fig. 4.11). Moreover, the level of reovirus production in mice treated with the combination of reovirus and ActD is significantly higher than that in reovirus-treated mice (Fig. 4.12B). Since the addition of ActD does not affect productive reovirus infection *in vitro* (Fig. 4.2B), reovirus spreads better in response to ActD treatment, where p53 accumulates in the tumor. Unfortunately, the combination of reovirus and ActD caused lethal reactions in the NOD-SCID mice. It was reported earlier that high doses of reovirus cause pathological reactions in NOD-SCID mice, while leaving wild-type mice non-symptomatic (Loken et al. 2004). Reovirus infects cardiac myocytes and venous endothelial cells in NOD-SCID mice, and these mice over time show “black-foot” lesion as well as lesions in the heart. It is likely that reovirus infection in normal tissues could be enhanced with the treatment of ActD where

p53 was activated in our *in vivo* experimental model, causing the unexpected death of the animals. Although it was reported previously that in immunocompetent models reovirus did not infect normal tissues and therefore should not risk the host with enhanced reovirus infection due to the ActD treatment, it is still important to determine whether the combination of reovirus and ActD could worsen the symptoms reovirus might cause *in vivo*.

Previous studies that combined reovirus with chemotherapeutics did not address the role of p53 (Pandha et al. 2009; Sei et al. 2009). My results here raise the possibility that the status of p53 in cancer cells might have an impact on the effects of a combination of chemotherapy drugs with reovirus. Determining whether a combination of chemotherapy drugs with reovirus has differential effects on p53+/+ cells and p53-/- cells would be important to direct personalized cancer therapy in the future.

Fig. 4.1 Cell-viability assay for HCT116 p53+/+ cells using various concentrations of chemotherapy drugs. Serial dilutions of (A) ActD, (B) Dox, (C) Etp and (D) 5-FU were used to treat HCT116 p53+/+ cells and MTS reagents were added at 48 h post treatment. Accumulation of p53 was determined by western blot analysis using p53-specific antibody. Representative of two independent experiments (triplicate wells, ±*s.e.m.*).

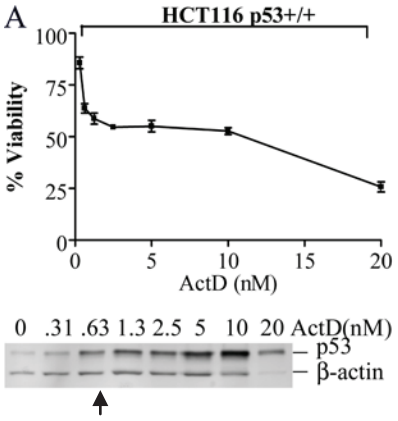
A
HCT116 p53+/+
% Viability
100
75
50
25
0
0 5 10 15 20
ActD (nM)
0 .31 .63 1.3 2.5 5 10 20 ActD(nM)
p53
β-actin

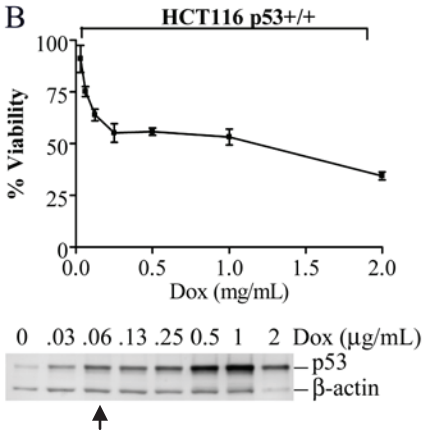
B
HCT116 p53+/+
% Viability
100
75
50
25
0
0.0 0.5 1.0 1.5 2.0
Dox (mg/mL)
0 .03 .06 .13 .25 0.5 1 2 Dox (μg/mL)
p53
β-actin

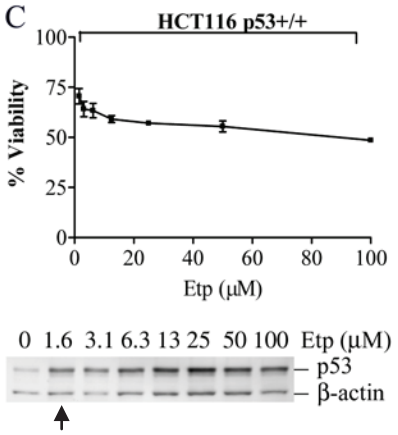
C
HCT116 p53+/+
% Viability
100
75
50
25
0
0 20 40 60 80 100
Etp (μM)
0 1.6 3.1 6.3 13 25 50 100 Etp (μM)
p53
β-actin

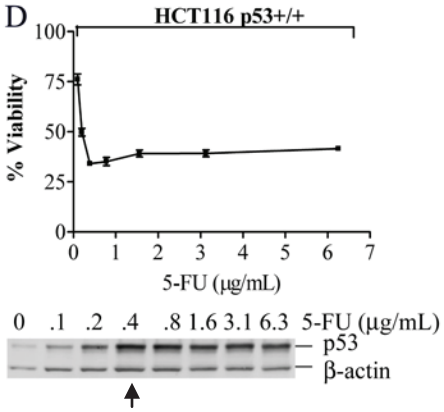
D
HCT116 p53+/+
% Viability
100
75
50
25
0
0 1 2 3 4 5 6 7
5-FU (μg/mL)
0 .1 .2 .4 .8 1.6 3.1 6.3 5-FU (μg/mL)
p53
β-actin

Fig. 4.2. A low concentration of ActD or Etp combined with reovirus induces enhanced levels of p53-dependent cell death. HCT116 p53+/+ and p53-/- cells were infected by reovirus at an MOI of 1 for an hour and then supplemented with or without low concentrations of Dox, Etp, ActD or 5-FU. (A) Cell death induced by reovirus or the combination of reovirus and low concentrations of Dox, Etp, ActD or 5-FU. Cell death was analysed by Annexin V and 7-AAD staining at 24 hpi. (B) Percentage of cells that were infected by reovirus with or without the treatment of Dox, Etp, ActD or 5-FU at 24 hpi, determined by FACS analysis using anti-reovirus antibody. (C) Cytotoxicity on HCT116 p53+/+ cells and p53-/- cells induced by reovirus, UV-inactivated reovirus (UV-reovirus) or the combination of reovirus and low concentrations of chemotherapy drugs. Significantly higher level of cell death compared to reovirus infection alone.

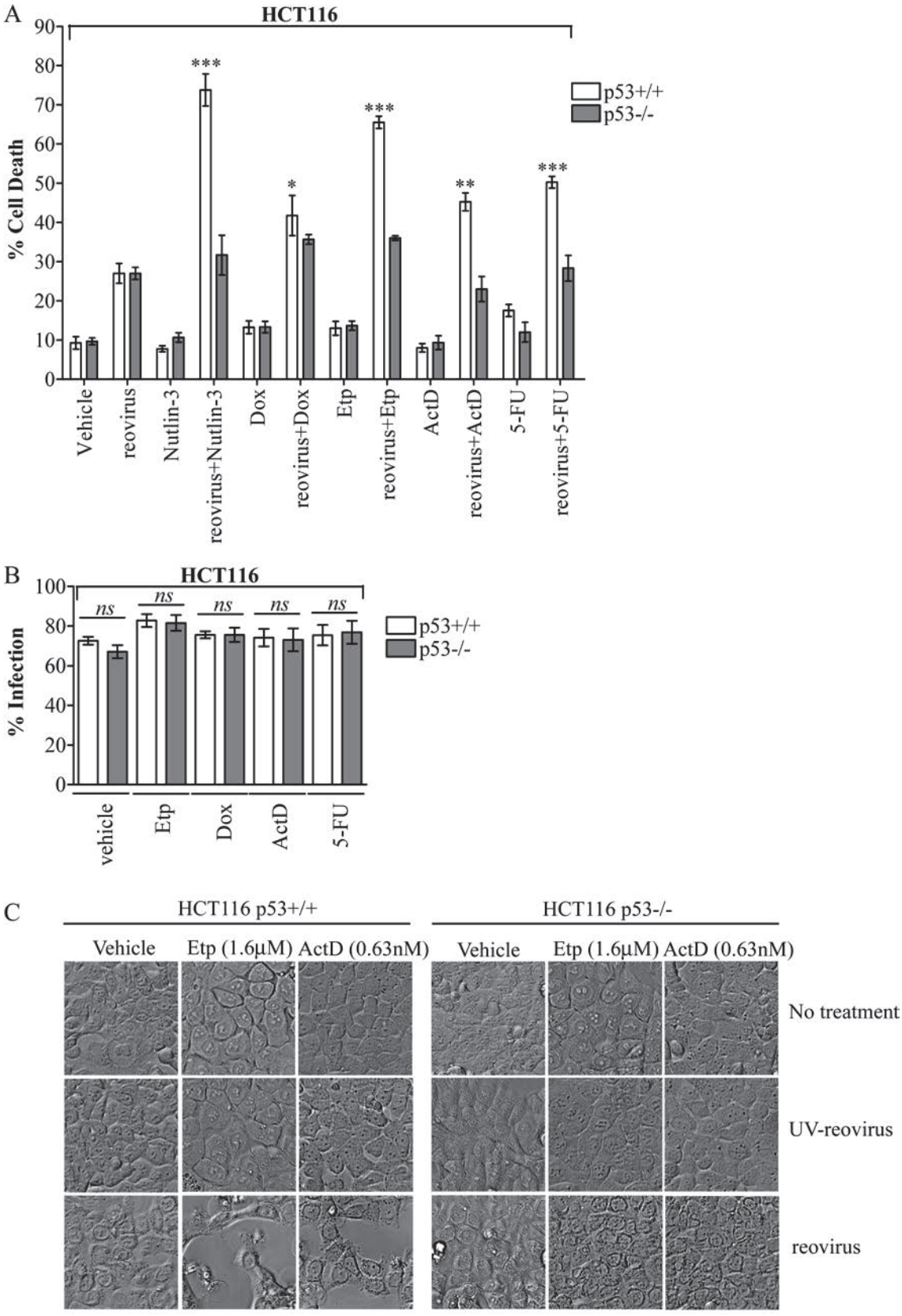
A
HCT116
% Cell Death
p53+/+
p53-/-
Vehicle
reovirus
Nutlin-3
reovirus+Nutlin-3
Dox
reovirus+Dox
Etp
reovirus+Etp
ActD
reovirus+ActD
5-FU
reovirus+5-FU
B
HCT116
% Infection
ns
p53+/+
p53-/-
vehicle
Etp
Dox
ActD
5-FU
C
HCT116 p53+/+
HCT116 p53-/-
Vehicle
Etp (1.6μM)
ActD (0.63nM)
No treatment
UV-reovirus
reovirus

Fig. 4.3. Caspase inhibitor ZVAD blocks the enhancement of cell death induced by the combination of reovirus and a low concentration of ActD or Etp. HCT116 p53+/+ cells and p53-/- cells were treated with ZVAD for 1 hour before reovirus infection. Following reovirus infection, ZVAD and a low concentration of ActD or Etp were added to culture media of reovirus infected cells. Cell death was determined by Annexin V and 7-AAD staining at 24 hpi. Student's *t*-test was used to compare two groups of data; NS: not significant, **P*<0.05 and ****P*<0.0001.

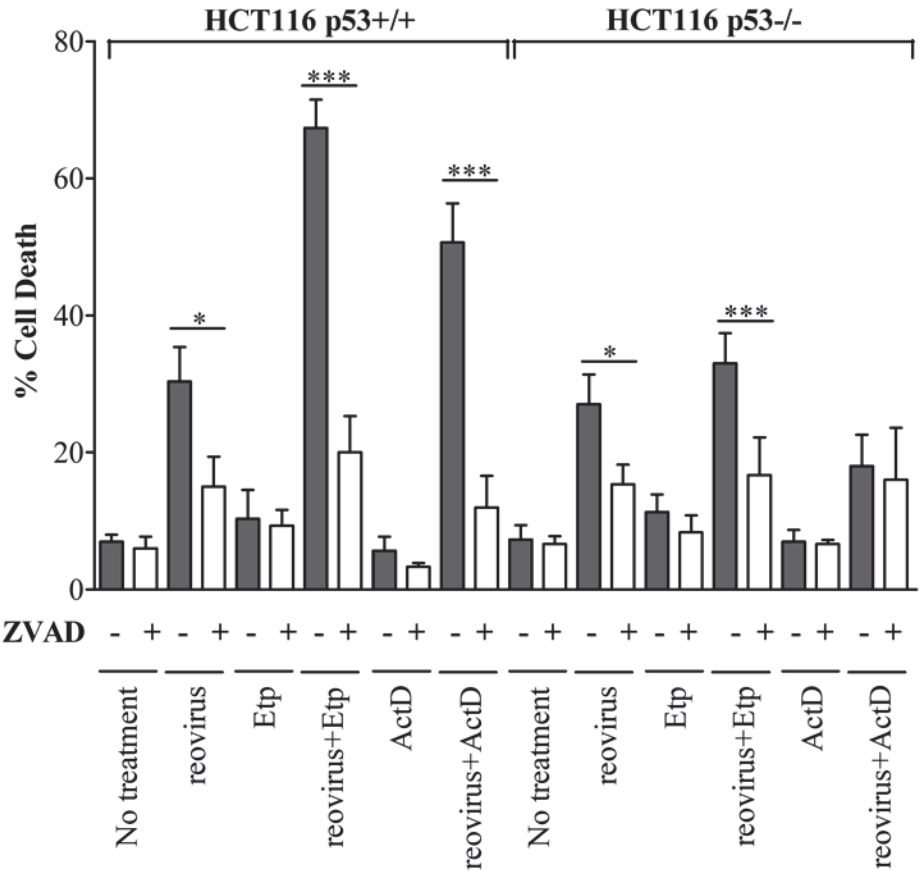
HCT116 p53+/+
HCT116 p53-/-
% Cell Death
80
60
40
20
0
***
***
*
*
***
ZVAD - + - + - + - + - + - + - + - + - + - + - + - +
No treatment
reovirus
Etp
reovirus+Etp
ActD
reovirus+ActD
No treatment
reovirus
Etp
reovirus+Etp
ActD
reovirus+ActD

Fig. 4.4. A combination of Etp/ActD with reovirus significantly enhances expression levels of p53-target genes (*noxa*, *puma*, *bax* and *p21*) compared to single treatment alone. (A) *noxa*, (B) *puma*, (C) *bax* and (D) *p21* expression levels in HCT116 p53+/+ and p53-/- cells treated with reovirus (reo), Etp/ActD or the combination of Etp/ActD and reovirus. RNA samples were collected at 24 hpi and processed for real-time q-PCR analysis using gene-specific primers (±*s.e.m.*, n=3). Student's *t*-test was used to compare two groups of data; NS: not significant, **P*<0.05, ***P*<0.001 and ****P*<0.0001.

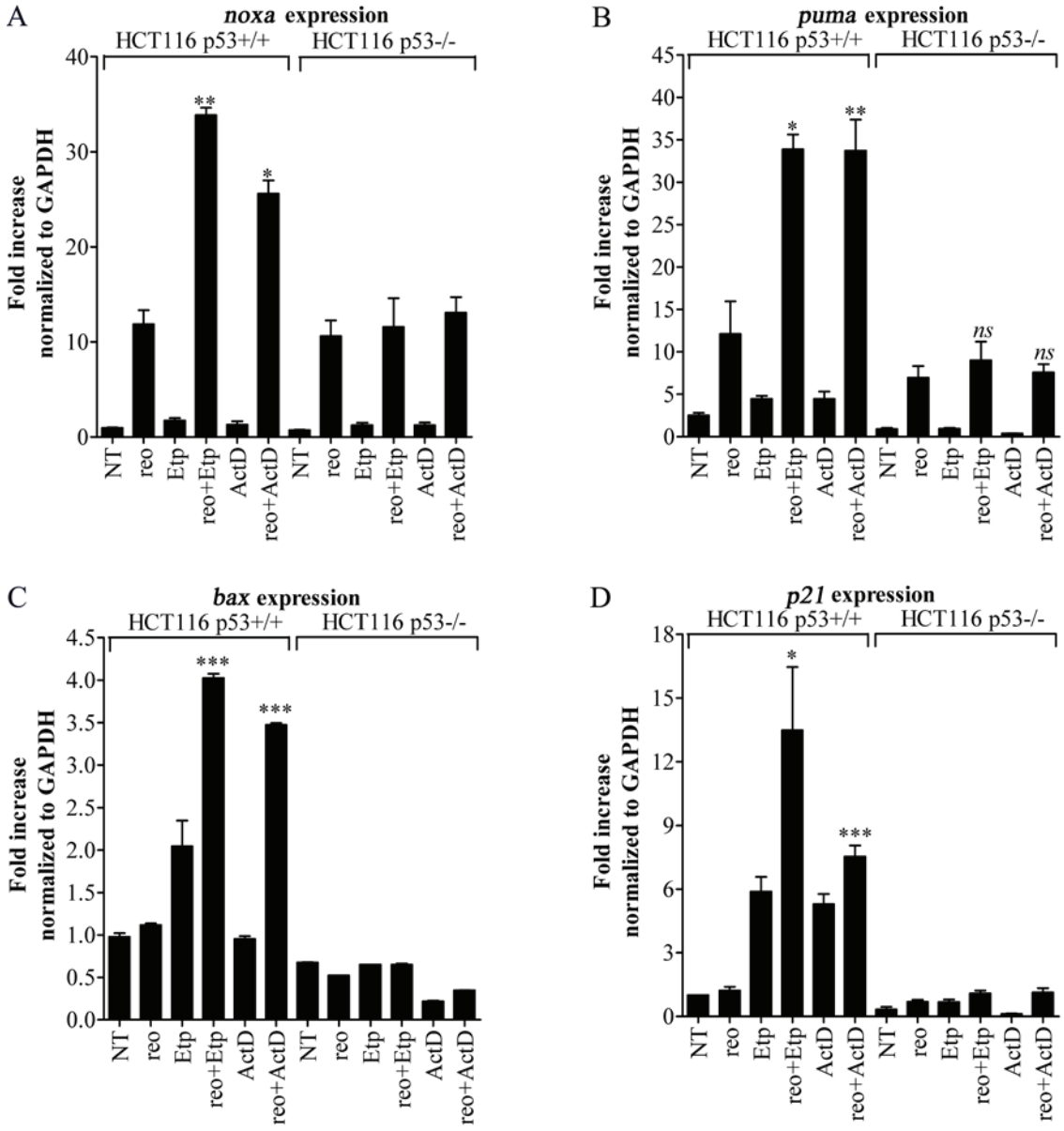
A
noxa expression
HCT116 p53+/+
HCT116 p53-/-
Fold increase normalized to GAPDH
NT
reo
Etp
reo+Etp
ActD
reo+ActD
B
puma expression
ns
C
bax expression
D
p21 expression

Fig. 4.5. The enhancement of apoptosis induced by the combination of reovirus and ActD/Etp requires *bax* and *p21*. HCT116 p53+/+ and its isogenic knockout (p53-/-, PUMA-/-, Bax-/-, p21-/-, PUMA-/-p21-/- and Bax-/-p21-/-) cells, as well as HCT116 p53+/+ cells infected with lentivirus containing shRNAs control (shRNA control) or sequences against Noxa (Noxa-kd1, Noxa-kd2), were infected with reovirus at an MOI of 1 in the presence or absence of ActD or Etp treatment. Cells were collected at 24 hpi and subjected to Annexin V and 7-AAD staining to determine the percentage of cell death (±*s.e.m.*, n=3). Student's *t*-test was used to compare two groups of data; NS: not significant, **P*<0.05, ***P*<0.001 and ****P*<0.0001.

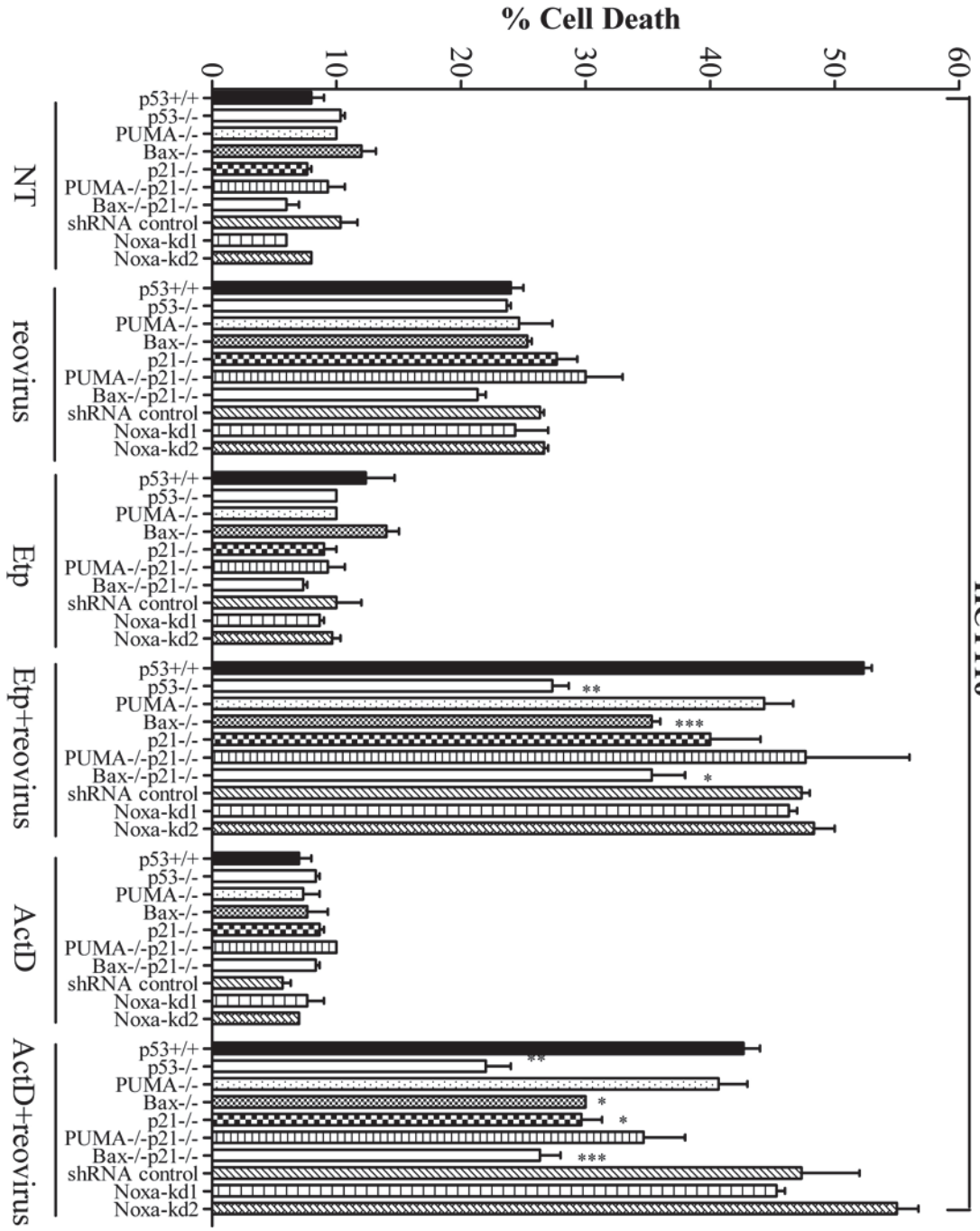
% Cell Death
0
10
20
30
40
50
60
HCT116
NT
reovirus
Etp
Etp+reovirus
ActD
ActD+reovirus
p53+/+
p53-/-
PUMA-/-
Bax-/-
p21-/-
PUMA-/-p21-/-
Bax-/-p21-/-
shRNA control
Noxa-kd1
Noxa-kd2
**
***
*
*
*
***

Fig. 4.6. NF-κB activation determined by NF-κB p65 subunit translocation. HCT116 p53+/+ and p53-/- cells were infected with reovirus at an MOI of 1 in the presence or absence of Act (0.63 nM) or Etp (1.6 μM) treatment. Cells were fixed at 12-h post ActD/Etp treatment and cells were stained with anti-p65, anti-reo antibody and To-pro-3 for nucleus staining. NT: no treatment.

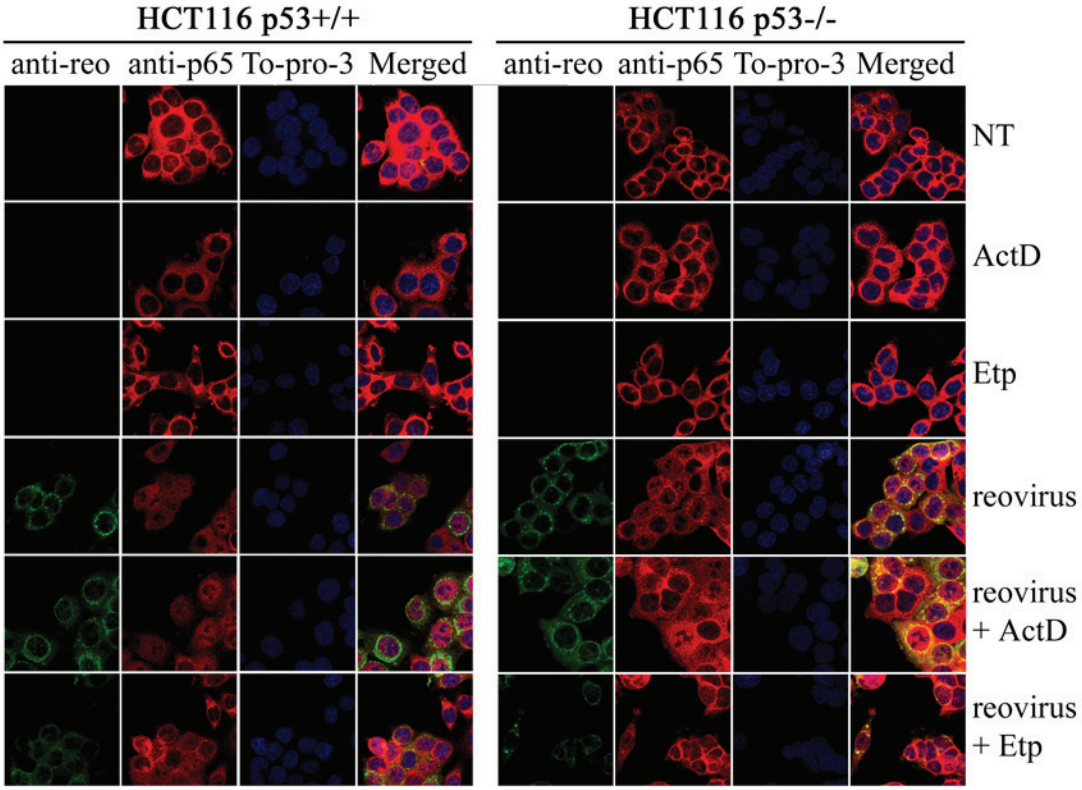
HCT116 p53+/+
HCT116 p53-/-
anti-reo
anti-p65
To-pro-3
Merged
anti-reo
anti-p65
To-pro-3
Merged
NT
ActD
Etp
reovirus
reovirus + ActD
reovirus + Etp

Fig. 4.7. NF-κB inhibitor N significantly reduces cell death induced by the combination of reovirus and ActD/Etp. HC116 p53+/+ cells were treated with NF-κB inhibitor N for 1 hour before reovirus infection in the absence or presence of either ActD (0.63 nM) or Etp (1.6 μM) treatment. Cells were collected at 24 hpi for PI staining and the percentage of sub-G1 for each sample was normalized to reovirus infection alone (±*s.e.m.*, n=3). Student's *t*-test was used to compare two groups of data; **P*<0.05.

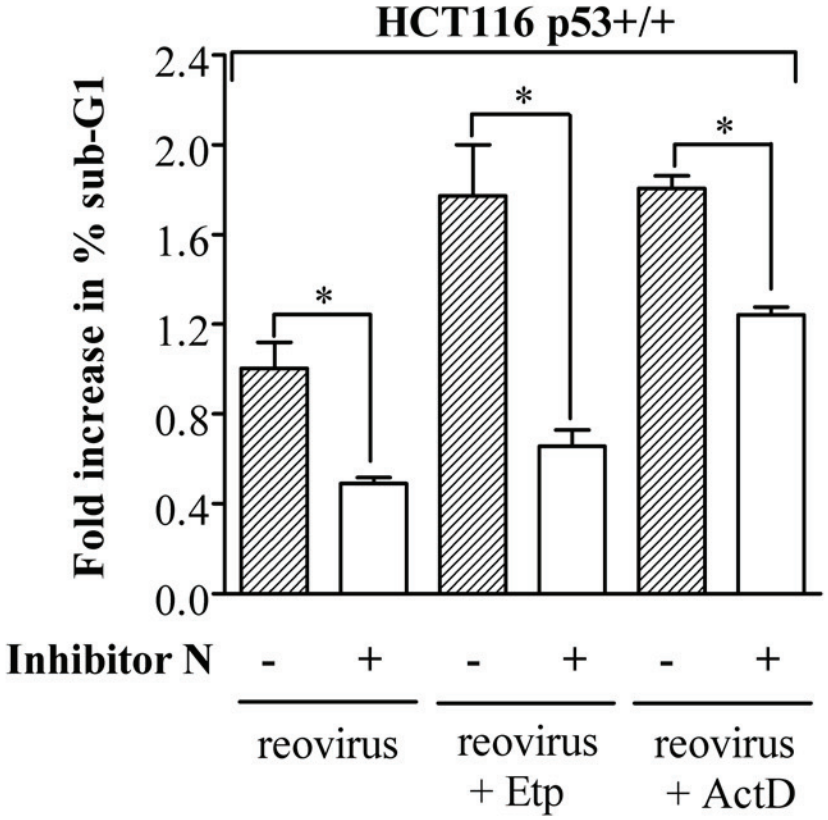
HCT116 p53+/+
Fold increase in % sub-G1
2.4
2.0
1.6
1.2
0.8
0.4
0.0
*
*
*
Inhibitor N
-
+
-
+
-
+
reovirus
reovirus + Etp
reovirus + ActD

Fig. 4.8. Treatment with ActD or Etp significantly enhances reovirus dissemination. Immunohistochemical staining of the plaques formed on reovirus-infected HCT116 cells in the presence or absence of ActD (0.63 nM) or Etp (1.6 μM) treatment.

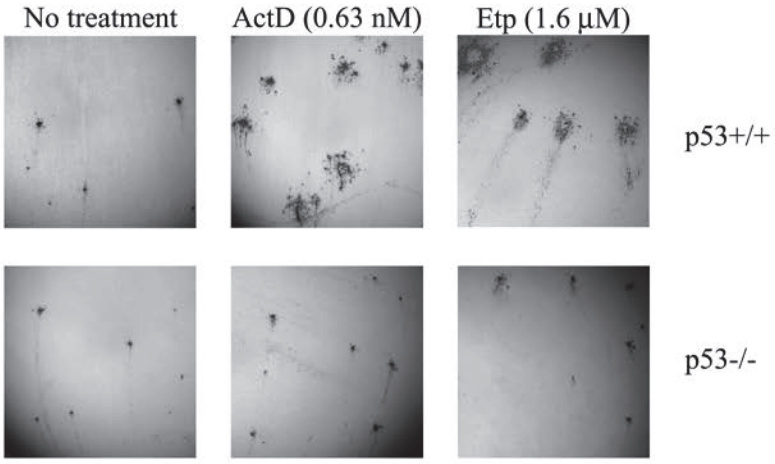
No treatment
ActD (0.63 nM)
Etp (1.6 μM)
p53+/+
p53-/-

Fig. 4.9. RNA levels for *p21* and *puma* in tumors after *i.p.* injection of 10 mg/kg Etp or 45 μg/kg ActD in NOD-SCID mice in pilot experiment 1. HCT116 p53+/+ cells were allowed to establish a tumors and mice were *i.p.* injected with either 10 mg/kg Etp or 45 μg/kg ActD according to the schedule shown in Table 4.1. A, B and C indicate the group as described by Table 4.1. Tumors were excised and the expression levels of *p21* and *puma* were analysed to determine whether p53 was activated by the injections. NT: no treatment.

A

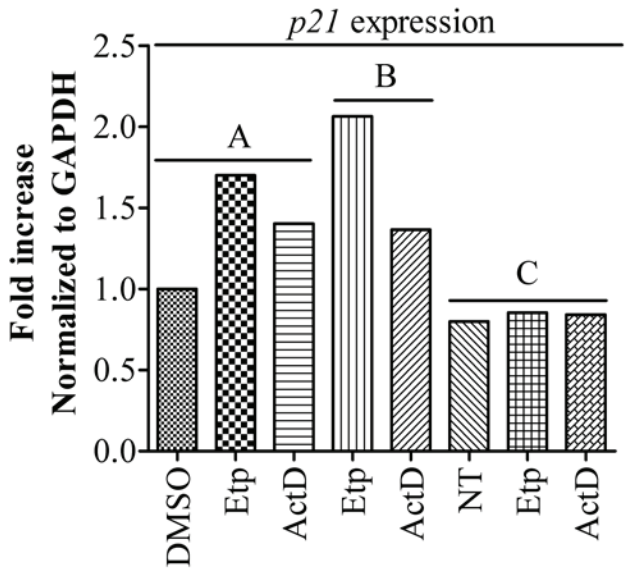
p21 expression
Fold increase
Normalized to GAPDH
2.5
2.0
1.5
1.0
0.5
0.0
A
B
C
DMSO
Etp
ActD
Etp
ActD
NT
Etp
ActD

B

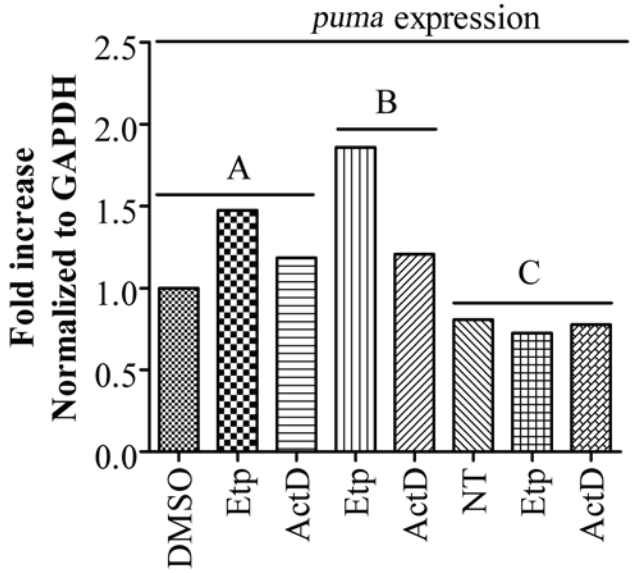
puma expression
Fold increase
Normalized to GAPDH
2.5
2.0
1.5
1.0
0.5
0.0
A
B
C
DMSO
Etp
ActD
Etp
ActD
NT
Etp
ActD

Fig. 4.10. Effects of multiple injections of various concentrations of ActD or Etp on p53 activation in tumors. A-C, expression of *p21*, *puma* or *noxa* in tumors that were established from HCT116 (p53+/+ and p53-/-) cells on NOD-SCID mice. Mice were *i.p.* injected with ActD or Etp according to the schedule shown in Table 4.2. D. Western blot analysis of p53 protein levels in tumors. Two mice per group, except one in group J (20 mg/kg Etp injected on a mouse bearing an HCT116 p53-/- tumor).

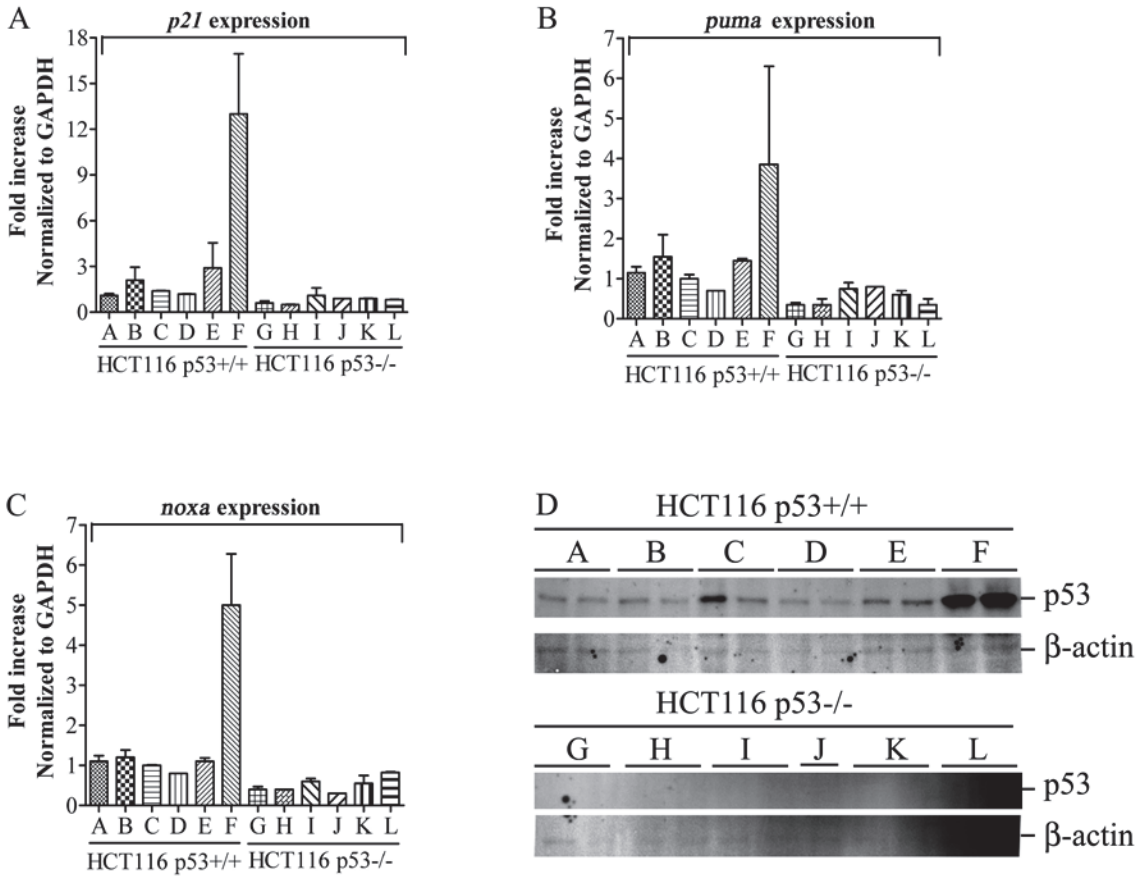
A
p21 expression
Fold increase
Normalized to GAPDH
18
15
12
9
6
3
0
A B C D E F G H I J K L
HCT116 p53+/+ HCT116 p53-/-
B
puma expression
Fold increase
Normalized to GAPDH
7
6
5
4
3
2
1
0
A B C D E F G H I J K L
HCT116 p53+/+ HCT116 p53-/-
C
noxa expression
Fold increase
Normalized to GAPDH
7
6
5
4
3
2
1
0
A B C D E F G H I J K L
HCT116 p53+/+ HCT116 p53-/-
D
HCT116 p53+/+
A B C D E F
p53
β-actin
HCT116 p53-/-
G H I J K L
p53
β-actin

Fig. 4.11. Weight of the tumors established in NOD-SCID mice treated with ActD, reovirus or a combination of reovirus and ActD. Tumor xenografts established from HCT116 p53+/+ cells were injected with vehicle or ActD with or without a concurrent injection of 1 x 10^7 pfu of reovirus (as described in Table 4.3). At 6 days post initial injection, mice were sacrified, tumors were excised and weight measured (±*s.e.m.*, n=3 except n=4 for the reovirus + ActD group). Student's *t*-test was used to compare two groups of data; **P*<0.05 and ****P*<0.0001.

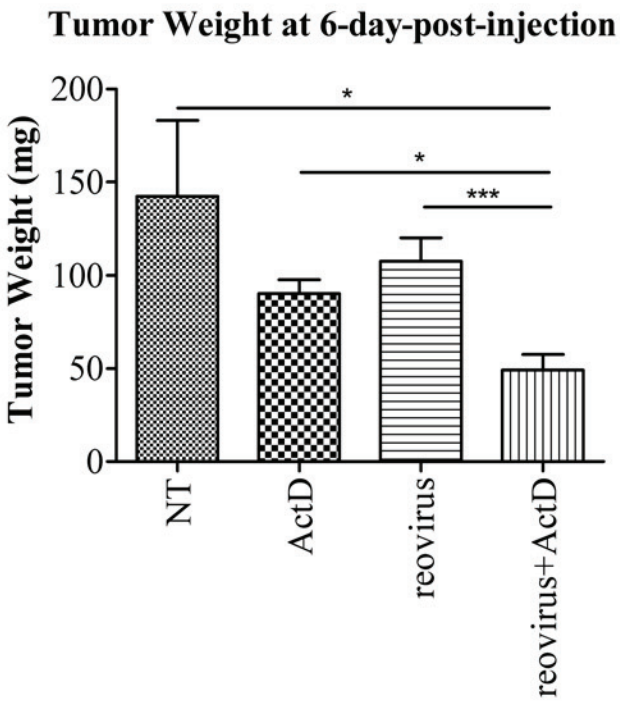
Tumor Weight at 6-day-post-injection
Tumor Weight (mg)
200
150
100
50
0
*
*
***
NT
ActD
reovirus
reovirus+ActD

Fig. 4.12. ActD injections cause accumulation of p53 in tumor xenografts established from HCT116 p53+/+ cells, and a higher level of reovirus production. Tumor xenografts established from HCT116 p53+/+ cells were injected with vehicle or ActD with or without concurrent injection of 1 x 10^7 pfu of reovirus. Mice were sacrified, tumors were excised and single-cell suspensions were processed for either (A) western blot or (B) virus plaque analysis. Different lanes represent individual mouse. Total reovirus production was determined by combining the titration of each fraction of the process. (±*s.e.m.*, reovirus n=3; ActD + Reovirus n=4).

A

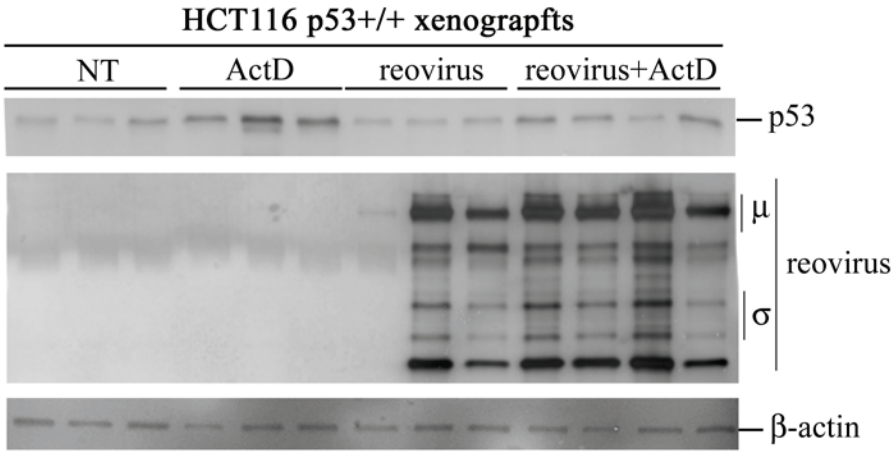
HCT116 p53+/+ xenograpfts
NT
ActD
reovirus
reovirus+ActD
p53
μ
σ
reovirus
β-actin

B

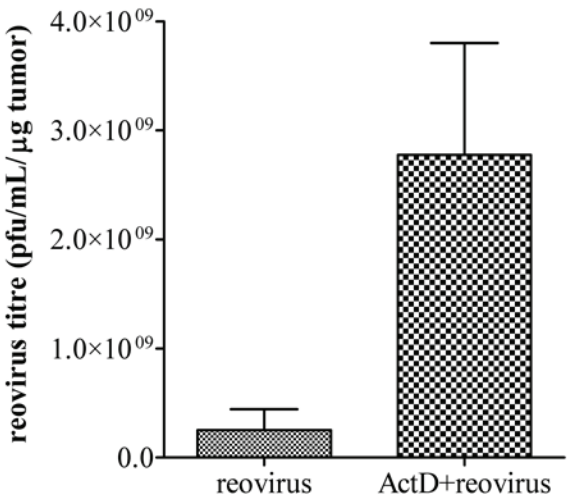
reovirus production in HCT116 p53+/+ xenograph
reovirus titre (pfu/mL/μg tumor)
4.0×10 09
3.0×10 09
2.0×10 09
1.0×10 09
0.0
reovirus
ActD+reovirus

Fig. 4.13. Tumor weight and growth after treatment with ActD or reovirus. NOD-SCID mice bearing HCT116 p53+/+ tumors were injected with vehicle, ActD (180 μg/kg) or one injection of 1 x 10^7 pfu of reovirus. Healthy mice were kept until 21 days post initial injections. (A) Growth of tumors established from HCT116 p53+/+ cells. (B) Weight of tumors at 21 days post injection. Mice were sacrified to excise tumors and tumor weights were measured (±*s.e.m.*, n=4 for no treatment group, n=5 for reovirus group and n=6 for ActD group). Student's *t*-test was used to compare two groups of data, **P*<0.05.

A

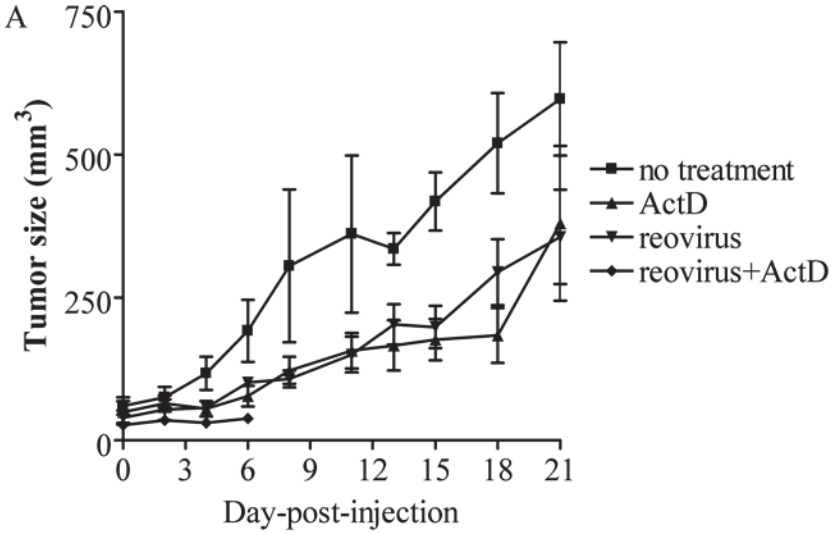

B **Tumor weight at 21-day-post-injection**

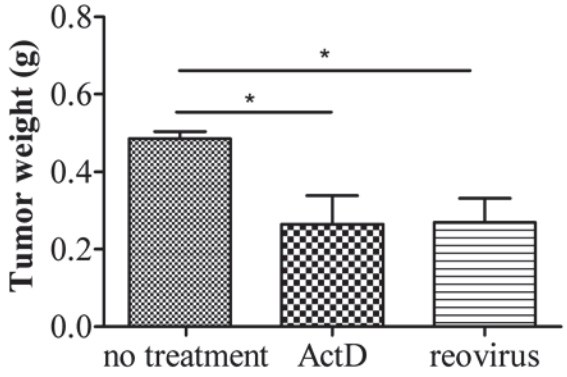

Table 4.1. Pilot Experiment Testing ActD/Etp Concentrations and Duration of Injections in NOD-SCID mice.

		Treatment schedule			
group	**mice**	Day 0	Day 1	Day 2	Day 3
	#1	Vehicle	Sacrificed		
	#2	Etp (10 mg/kg)	Sacrificed		
A	**#3**	ActD (45 μg/kg)	Sacrificed		
	#4	Etp (10 mg/kg)	Etp (10 mg/kg)	Sacrificed	
B	**#5**	ActD (45 μg/kg)	ActD (45 μg/kg)	Sacrificed	
	#6	NT	NT	NT	Sacrificed
	#7	Etp (10 mg/kg)	Etp (10 mg/kg)	NT	Sacrificed
C	**#8**	ActD (45 μg/kg)	ActD (45 μg/kg)	NT	Sacrificed

NT: No treatment

Table. 4.2. Groups of Mice Treated with Multiple Injections of Various Concentrations of Etp or ActD.

Tumor	group	mice	5 x injection
HCT116 p53+/+	A	#1	Vehicle
		#2	Vehicle
	B	#3	5 mg/kg Etp
		#4	5 mg/kg Etp
	C	#5	10 mg/kg Etp
		#6	10 mg/kg Etp
	D	#7	20 mg/kg Etp
		#8	20 mg/kg Etp
	E	#9	45 μg/kg ActD
		#10	45 μg/kg ActD
	F	#11	180 μg/kg ActD
		#12	180 μg/kg ActD
HCT116 p53-/-	G	#13	Vehicle
		#14	Vehicle
	H	#15	5 mg/kg Etp
		#16	5 mg/kg Etp
	I	#17	10 mg/kg Etp
		#18	10 mg/kg Etp
	J	#19	20 mg/kg Etp
	K	#20	45 μg/kg ActD
		#21	45 μg/kg ActD
	L	#22	180 μg/kg ActD
		#23	180 μg/kg ActD

Table 4.3. Schedule of Treatment with ActD and/or reovirus.

		Treatment schedule						
group	**mice**	Day 0	Day 1	Day 2	Day 3	Day 4	Day 5	Day 6
	#1	Vehicle	Vehicle	Vehicle	Vehicle	Vehicle	NT	Sacrificed
	#2	Vehicle	Vehicle	Vehicle	Vehicle	Vehicle	NT	Sacrificed
A	**#3**	Vehicle	Vehicle	Vehicle	Vehicle	Vehicle	NT	Sacrificed
	#4	ActD	ActD	ActD	ActD	ActD	NT	Sacrificed
	#5	ActD	ActD	ActD	ActD	ActD	NT	Sacrificed
B	**#6**	ActD	ActD	ActD	ActD	ActD	NT	Sacrificed
	#7	Vehicle + reovirus	Vehicle	Vehicle	Vehicle	Vehicle	NT	Sacrificed
	#8	Vehicle + reovirus	Vehicle	Vehicle	Vehicle	Vehicle	NT	Sacrificed
C	**#9**	Vehicle + reovirus	Vehicle	Vehicle	Vehicle	Vehicle	NT	Sacrificed
	#10	ActD + reovirus	ActD	ActD	ActD	ActD	NT	Died
	#11	ActD + reovirus	ActD	ActD	ActD	ActD	NT	Died
	#12	ActD + reovirus	ActD	ActD	ActD	ActD	NT	Died
D	**#13**	ActD + reovirus	ActD	ActD	ActD	ActD	NT	Died

A: No treatment/NT

B: ActD

C: reovirus

D: reovirus+ActD

Chapter 5 Activated Sub-Ras Signaling Pathways Promote Various Steps of Reovirus Replication

5.1. Introduction

Since it was discovered that reovirus preferentially infects Ras-transformed cells and promoted cell death in cancer cells, the possibility of using reovirus as a therapeutic option has been widely investigated. Inhibition of viral protein synthesis in non-transformed cells was indicated to be the reason behind the preferential replication of reovirus in Ras-transformed cells (Strong et al. 1998). However, the underlying mechanism of reovirus selectively killing Ras-transformed cells is still not completely understood.

Ras is at the hub of a plethora of signaling pathways that control critical cellular processes. These pathways can potentially contribute to reovirus preferential replication in Ras-transformed cells, individually or cooperatively. To investigate which sub-Ras pathway(s) cause reovirus preferential replication in Ras-transformed cells, it is important to first determine which steps of reovirus replication require activated Ras. Every step of the first round of reovirus replication (within 24 hours post infection, hpi) was compared for murine fibroblast NIH 3T3 cells with or without stable transformation by Ras.

As discussed in Chapter 1, *ras* mutation is one of the most prevalent mutations in human cancer. Many mutations in the effector regions of Ras (residues 32-40) are known to inhibit the biological function of Ras and to block the interaction between Ras and its target proteins. In particular, subtle changes in this region can lead to partial loss-of-function mutations in which Ras interaction with some of its effectors is lost but interactions with the others are maintained. These mutant versions of Ras along with the

G12V GTPase-deficient mutant version (RasV12) can constitutively activate different sub-Ras effector pathways (Rodriguez-Viciana et al. 1997; Fiordalisi et al. 2001). These effector mutants of Ras are important tools to study the roles of individual sub-Ras effector pathways in Ras tumorigenesis. Therefore, NIH 3T3 cells stably transformed by the Ras effector mutants were used to determine the effect of sub-Ras signaling pathways on reovirus replication in Ras-transformed cells.

5.2. Results

5.2.1. Reovirus Preferentially Replicates in Ras-transformed NIH 3T3 Cells

To confirm that reovirus preferentially infects Ras-transformed cells, NIH 3T3 cells were freshly transformed by activated Ras (V12) retrovirus or the vector control retrovirus (pBABEpuro). Ras-transformed and non-transformed cells were then infected with reovirus at an MOI of 10. Consistent with previous reports (Strong et al. 1998), reovirus induced higher levels of cytotoxicity in Ras-transformed cells by 48 hpi (Fig. 5.1A) and total reovirus production determined by plaque titration was dramatically higher in Ras-transformed cells than in non-transformed cells (Fig. 5.1B). When protein synthesis was monitored at 48 hpi using [^{35}S]-methionine pulse labelling (1 h), reoviral protein synthesis was more pronounced in Ras-transformed cells than in non-transformed cells (Fig. 5.1C). These results confirmed that reovirus preferentially replicates in Ras-transformed cells.

The progression of reovirus infection was then followed using fluorescence-activated cell sorting (FACS). As shown in Fig. 5.2, close to three times more Ras-transformed cells were positive for reovirus-protein staining by 6 hpi, and consistently more positive staining for viral proteins was detected at each timepoints in Ras-

transformed cells. Since cells that were stained positive for reovirus proteins by 6 hpi should be the result of *de novo* infection, it is possible that Ras-transformation might provide advantages for reovirus replication at steps prior to protein synthesis.

5.2.2. Ras-transformation does not Affect Reovirus Binding or Internalization

A successful reovirus infection initiates with receptor-mediated virus binding followed by endocytosis-mediated reovirus internalization (Fig. 1.1). Reovirus then undergoes partial proteolysis, which results in cleavage of outer capsid protein μ1/μ1C into δ protein (reovirus uncoating) and loss of σ3 protein. The so-formed ISVP particle is able to penetrate the endosomal membrane and enters the cytoplasm where RNA and protein synthesis occur. To determine which step(s) preceding viral protein synthesis are enhanced by Ras-transformation, reovirus binding efficiency and the rate of internalization were compared between non-transformed and Ras-transformed NIH 3T3 cells. As shown in Fig. 5.3, after reovirus was allowed to bind to cells on ice for one hour, the cell surface biotinylated viral protein (μ1C) was similar between the non-transformed and Ras-transformed cells, indicating that the binding efficiency is not affected by Ras-transformation. While reovirus was allowed to internalize into cells, the percentage of reovirus that was outside the cell membrane decreased at a similar rate for non-transformed and Ras-transformed cells. Therefore, reovirus binding and internalization steps are not affected by Ras-transformation in NIH 3T3 cells.

Following reovirus internalization, an uncoating process is essential for successful reovirus infection, since protease-inhibitors or raising the endosomal pH with NH_4Cl inhibits reovirus infection in permissive cells (Sturzenbecker et al. 1987; Baer and Dermody 1997). The rate of reovirus uncoating in both non-transformed and Ras-

transformed cells was determined (Marcato et al. 2007). It was shown that when cell-associated reovirus particles were allowed to enter the cells and undergo partial digestion (μ1/μ1C cleavage into δ protein), at any given time the ratio of δ to μ1C was lower in non-transformed cells, indicating that the rate of the cleavage of μ1C to δ was more efficient in Ras-transformed cells than in non-transformed cells. Therefore, reovirus binding and internalization by non-transformed and Ras-transformed cells are comparable, while the increased uncoating in Ras-transformed cells causes more Ras-transformed cells to be infected efficiently.

5.2.3. The Rate of Reovirus Protein Synthesis is not Affected by Ras-transformation

Previously, based ^{35}S-pulse labelling protein synthesis from 12 to 48 hpi, it was reported that the rate of reovirus protein synthesis in Ras-transformed cells was higher than in non-transformed cells during this period of time. Moreover, no significant difference in reovirus transcripts between non-transformed and Ras-transformed cells were detected using end-point reverse transcriptase polymerase chain reaction (PCR) (Strong et al. 1998). However, the results presented by Marcato *et al.* showed that reovirus uncoating is more efficient in Ras-transformed cells (Marcato et al., 2007). Moreover, using a quantitative real-time PCR method (qRT-PCR), consistently higher levels of reovirus RNA synthesis was detected in Ras-transformed cells compared to non-transformed cells, while the rate of the viral RNA synthesis was not affected (Marcato et al. 2007). Further, the fold increase in viral RNA synthesis between Ras-transformed cells and non-transformed cells correlated well with the fold increase in the percentage of infected cells for Ras-transformed and non-transformed cells. Therefore, the efficiency of

viral protein synthesis is likely similar between non-transformed and Ras-transformed cells.

To further assess whether the efficiency of viral protein synthesis is siilar in non-transformed and Ras-transformed cells, *in vitro* translation lysates were prepared from non-transformed and Ras-transformed cells, and *in vitro* transcribed control and viral RNAs were translated in a cell-free system. The majority of mature mRNAs in eukaryotes that are synthesized by RNA polymerase II have a 5' structure containing a 5'-5' triphosphate-linked guanine which is modified with a 5' 7-methyl group (m^7G) (capped mRNAs). This cap structure is added to the RNA molecules by guanylyl transferase and methyltransferase (Shuman 1995). The m^7G cap structure affects stabilization of nuclear and cytoplasmic mRNAs as well as transport of mRNAs (Furuichi et al. 1977; Izaurralde and Mattaj 1995; O'Mullane and Eperon 1998). More importantly, the m^7G cap is essential for cap-dependent translation, although various mechanisms of cap-independent translation initiation have been discovered (Malys and McCarthy 2011). Reovirus RNAs are naturally capped, although at late infection uncapped RNAs are produced (Zarbl et al. 1980). We therefore *in vitro* transcribed mRNAs with or without the addition of a cap-analog to produce either capped or uncapped mRNAs (Fig. 5.4A). As shown in Fig. 5.4B, when the same amounts of uncapped and capped RNAs were added to the *in vitro* translation lysates, capped RNAs were significantly more efficiently translated by non-transformed and Ras-transformed cell lysates, although both lysates could translate the uncapped RNAs. Furthermore, the amounts of protein that were synthesized within 90 min were comparable for lysates prepared from non-transformed cells and from Ras-transformed cells. Therefore, in a cell-free translation system, the efficiencies of both control eGFP and reoviral RNA S4 translation were similar for non-transformed and Ras-

transformed cell lysates, indicating that reovirus protein synthesis is not enhanced by Ras-transformation.

5.2.4. Apoptosis-mediated Reovirus Release is Enhanced in Ras-transformed NIH 3T3 Cells

More detailed titre experiments showed that significantly higher levels of reovirus were released from Ras-transformed cells than from non-transformed cells (Fig. 5.5A): by 24 hpi, titres of reovirus that were released to the medium (Released reovirus) from Ras-transformed cells were about 200 times higher than those from non-transformed cells, while the total production of infectious reovirus was about 23 times higher from Ras-transformed cells than that from non-transformed cells. Western blot analysis comparing total *versus* released reovirus from non-transformed and Ras-transformed cells also confirmed that significantly higher levels of reovirus were released from Ras-transformed cells (Fig. 5.5B). Enhanced reovirus release might be the result of increased levels of reovirus-induced apoptosis.

Indeed, Marcato *et al.* showed that significantly higher levels of cell death were induced in Ras-transformed cells than in non-transformed cells by 24 hpi (Marcato et al. 2007). When background cell death was subtracted, the percentage of cell death in Ras-transformed cells was about 9-time higher than in non-transformed cells. Furthermore, caspase inhibitor I Z-VAD(OMe)-FMK (ZVAD) significantly blocked the majority of cell death as well as the release of the reovirus. The presence of ZVAD also blocked the productive infection of reovirus by 48 hpi, indicating that the enhancement of apoptosis-mediated reovirus release in Ras-transformed cells is important for reovirus preferential replication in Ras-transformed cells. Therefore, significantly more reovirus were released

into the medium from Ras-transformed cells than from non-transformed cells, causing a more efficient second round of reovirus infection to be initiated more efficiently in Ras-transformed cells.

5.2.5. Reovirus Replication in Cells Transformed by Ras Effector Mutants

It was observed that the reovirus particles recovered from Ras-transformed cells were about four times more infectious than those from non-transformed cells, but the rate of reovirus assembly in non-transformed and Ras-transformed cells was similar (Marcato et al. 2007). Three steps of reovirus replication are enhanced in Ras-transformed cells: 1) three folds increase in reovirus uncoating; 2) nine-folds increase in reovirus-induced apoptosis and 3) reovirus particles assembled in Ras-transformed cells are four times more infectious than those from non-transformed cells. The combined effects of Ras-mediated enhancement of reovirus uncoating, infectivity and reovirus-mediated apoptosis therefore account for the more than two-$\log_{10}$ increase in reovirus titre.

As discussed in Chapter 1, Ras is at the hub of numerous signaling pathways in cells, mediating vital cellular processes such as survival, mRNA translation, endocytosis and apoptosis. Using Ras-effector mutants which preferentially interact with one of the downstream effectors of Ras, it has been shown that the Ras/RalGEF/p38 pathway is important for reovirus oncolysis (Norman et al. 2004). Since Ras-transformation enhances various steps of reovirus replication, it is important to determine which sub-Ras pathway(s) can affect the multiple steps of reovirus replication.

NIH 3T3 cells were transformed by either constitutively activated Ras (V12), or specific effector mutants (V12S35, V12G37 and V12C40) (Fig. 5.6A, B). The V12S35 mutant Ras interacts with Raf and activates the Raf/MEK pathway; the V12G37 mutant

Ras interacts with RalGEF and activates the RalGEF/Ral pathway; the V12C40 mutant Ras interacts with PI3K and activates the PI3K/Akt pathway (Fiordalisi et al. 2001). Cells transformed with all these Ras mutants and non-transformed cells, were infected by reovirus at an MOI of 10 and reovirus titre was determined by plaque titration. As shown in Fig. 5.6C, reovirus production varied among the different Ras mutant cells. For the three effector-mutant cells, levels of reovirus production from V12S35 cells resembled those from the constitutively activated RasV12 the most. However, although reovirus production was not significantly different at 24 hpi, all three effector-loop mutant transformed cells produced more reovirus than did non-transformed cells by 72 hpi. Therefore, it is likely that the Ras-activated Raf pathway contributes to the enhancement of reovirus replication in Ras-transformed cells better than do the other two effector pathways. However, Ras-activated RalGEF and PI3K pathways might also provide advantages for reovirus replication in Ras-transformed cells after several rounds of the reovirus replication.

5.2.6. Differential Uncoating Efficiency in Ras Effector-Mutant Cells

The rates of reovirus uncoating in the Ras effector-mutant cells were first investigated. Cells were pre-cooled for an hour before reovirus was applied at an MOI of 100. After 1 hour of binding at 4 ^{o}C, reovirus was allowed to internalize and uncoat at 37 ^{o}C. The extent of reovirus uncoating was indicated by the level of μ1C converted to δ. As shown in Fig. 5.7A, the rate of uncoating was higher in V12S35 and V12G37 mutant cells than in V12C40 mutant cells. The uncoating process is believed to be mediated by pancreatic serine proteases such as chymotrypsin and trypsin in natural infection conditions (Bodkin et al. 1989; Bass et al. 1990). Lysosomal cysteine proteases (such as

cathepsin L) were also shown to be important for conversion of virions to ISVP for virus entry into cells intracellularly (Baer et al. 1999; Ebert et al. 2002). Hence, in a cancer environment, reovirus would more likely be uncoated by cysteine proteases. Therefore, levels of matured cathepsin L were determined in the Ras effector-mutant cells. As shown in Fig. 5.7B, compared to that in non-transformed cells, the level of cathepsin L was significantly higher in Ras-transformed cells. Among the Ras effector-mutant cells, the V12S35 (activated Raf pathway) transformed cells contained the highest levels of cathepsin L while the V12C40 (activated PI3K pathway) transformed cells contained the lowest level. The expression level of cathepsin L was consistent with the rate of reovirus uncoating in these cells, indicating that the different sub-Ras pathways affect the uncoating step of reovirus likely through regulating this cysteine protease.

5.2.7. Reovirus-mediated Apoptosis in Ras Effector-Mutant Cells

Reovirus-induced apoptosis was then measured in Ras effector-mutant cells. In these experiments, the percentage apoptosis induced by reovirus was normalized to the percentage of infection for each effector mutant. As shown in Fig. 5.8, the levels of reovirus-induced apoptosis, although not significantly enhanced in all Ras effector-mutants cells, varied among the mutant cells, with V12G37 (RalGEF) mutant cells consistently more apoptotic than the other mutant cells. Therefore, the RalGEF signaling pathway might render cells more sensitive to reovirus-induced apoptosis, which would result in higher level of reovirus release and therefore better spread of the virus.

5.2.8. Reovirus Dissemination in Ras Effector-Mutant Cells

Reovirus spread and dissemination determined using a plaque-size assay, varied drastically among Ras effector-mutant cells. As shown in Fig. 5.9, non-Ras NIH 3T3 cells failed to support the spread of reovirus infection and therefore produced very small reovirus plaques. Ras-transformed cells, however, produced significantly larger plaques than did non-transformed cells, confirming again that reovirus dissemination is significantly enhanced in Ras-transformed cells. Interestingly, V12S35 mutant cells produced very large plaques which were only slightly smaller than those produced by Ras-transformed cells. On the other hand, V12C40 mutant cells supported very limited level of reovirus spread and produced the smallest reovirus plaques among the three Ras loop-mutant transformed cells. These data suggest that sub-Ras pathways (distinguished by Ras loop mutants) can affect reovirus dissemination differently.

5.3. Discussion

To effectively apply reovirus as a cancer therapy agent, we need to fully understand the mechanisms of its preferential replication in Ras-transformed cells. Translation deregulation has been associated with the preferential replication of reovirus in Ras-transformed cells in previous studies (Strong et al. 1998; Coffey et al. 1998). Using quantitative analysis of individual steps within the reovirus life cycle, our group showed that Ras-transformation affects three steps of reovirus replication (Marcato et al. 2007): Firstly, uncoating of reovirus particles occurs with greater efficiency in Ras-transformed cells. At the same time, reovirus binding and internalization are not affected by Ras-transformation (Fig. 5.3). As mentioned above, the activities of lysosomal cysteine proteases such as cathepsins are required for reovirus uncoating. Ras transformation of murine fibroblast cells can enhance production and activity of

cathepsins through activation of the Raf pathway (Collette et al. 2004). In this case, the Raf/MEK pathway might upregulate cathepsins and cause higher levels of reovirus uncoating. Indeed, based on Ras mutants that activate certain sub-Ras pathway individually, data presented above showed that the V12S35 (Raf pathway activated) mutant transformed cells had a higher level of matured cathepsin L, and reovirus uncoating was more efficient in these mutant cells (Fig. 5.7A and B). Interestingly, V12G37 (RalGEF pathway activated) mutant cells also uncoated reovirus efficiently while containing higher levels of matured cathepsin L than the non-transformed cells (Fig. 5.7A and B). It was reported that the cathepsin L expression is controlled by different sub-Ras pathways and is cell-type dependent. For example, Raf-signaling pathways were sufficient for transforming rat fibroblast cells while rat epithelial cells require all of the three major sub-Ras pathways (Raf, PI3K and RalGEF cascades) (Collette et al. 2004). On the other hand, constitutively activated Ras increases the level of cathepsin L in human fibroblast cells which is mediated through activation of Raf and PI3K sub-pathways (Urbanelli et al. 2010). Therefore, the Raf-signaling pathway seems to be essential for cathepsin L overexpression in tumorigenesis and therefore is important for reovirus oncolysis.

A direct result of the enhancement of uncoating is more viral RNA synthesis, which leads to higher levels of viral protein being synthesized (Marcato et al. 2007). Therefore, it was proved that reovirus protein synthesis is not affected by Ras-transformation. This result was further confirmed by protein translation in a cell-free system. Lysates prepared from non-transformed and Ras-transformed cells translate either eGFP RNA or reovirus S4 RNA with similar efficiencies within 90 minutes (Fig. 5.4),

indicating that the viral protein synthesis rate is similar in non-transformed and Ras-transformed cells.

Secondly, progeny virus particles produced by Ras-transformed cells have a four-fold higher pfu-to-particle ratio than found for those from non-transformed cells (Marcato et al. 2007). Reovirus particles from Ras-transformed and non-transformed cells, however, are identical based on transmission electron microscopy and the virus particles show similar protein profiles following gel electrophoresis. This suggests that subtle modifications of virus structural proteins may be responsible for the enhanced infectivity of reovirus generated from Ras-transformed cells. Notably, reovirus is the first oncolytic virus shown to be regulated at the level of infectivity by host cells. Reovirus proteins have been shown to undergo extensive modifications (Ewing et al. 1985). For instance, the reovirus outer capsid protein μ1 is modified by a myristoyl group and this modification is implicated in the process of penetration through the membrane (Liemann et al. 2002). Other proposed modifications on μ1 have included phosphorylation and polyadenylation (Nibert et al. 2001). It is possible that Ras activation in transformed cells promotes modifications or conformational changes of certain reovirus proteins which can positively affect virion infectivity, more likely at the early stages of virus infection (i.e. binding, entry, and/or uncoating). Identification of the enzymes that are responsible for modifications on viral proteins in Ras-transformed cells as well as the sub-Ras pathway(s) that contribute to the modifications may provide important information on potential targets for anti-cancer drugs.

Thirdly, reovirus-mediated apoptosis is enhanced in Ras-transformed cells compared to non-transformed cells (Marcato et al. 2007). The enhancement of reovirus-mediated apoptosis directly results in significantly higher levels of reovirus released from

the infected cells (Fig. 5.5). As a result, more surrounding Ras-transformed cells are infected. My data also showed that reovirus induces higher levels of apoptosis in RalGEF effector-mutant transformed NIH 3T3 cells compared to the other two effector-mutant (Ral and PI3K) transformed cells (Fig. 5.8). Activation of NF-κB and JNK are indicated to be important in mediating reovirus-induced apoptosis. Interestingly, RalGEF has been indicated to mediate the activation of NF-κB as well as c-jun phosphorylation (mediated by JNK activation) (Henry et al. 2000; de Ruiter et al. 2000; Chien et al. 2006). Therefore, Ras-activation in transformed cells might provide reovirus with an environment with higher levels of activation of NF-κB and/or JNK, and therefore makes the Ras-transformed cells more prone to reovirus-induced apoptosis.

Our lab showed that Ras transformation averts antiviral response upon reovirus infection and inhibits interferon-β (IFN-β) expression within the infected Ras-transformed cells (Shmulevitz et al. 2010). Diminished IFN-β production is caused by inhibition of retinoic acid-inducible gene I (RIG-I) signaling. Furthermore, V12S35 (Raf) mutant cells showed diminished IFN-β expression. Therefore, reovirus may take advantage of Ras-transformation to enhance several steps of the reovirus life cycle, with the Raf signaling pathway rendering cells insensitive to reovirus infection by diminishing antiviral responses as well as reducing IFN-β production. Furthermore, results from my study showed that the Raf and RalGEF signaling pathways are able to enhance uncoating, while the RalGEF sub-Ras pathway contributes to reovirus-induced apoptosis. Consistent with these data, V12S35 (Raf) mutant cells produced the biggest plaques upon reovirus infection, followed by V12G37 (RalGEF) cells while V12C40 (PI3K) mutant cells were only able to slightly increase the size of the reovirus plaque (Fig. 5.9) and (Shmulevitz et

al. 2010). Overall, these data suggest that the preferential replication of reovirus in Ras-transformed cells is affected by various sub-Ras pathways.

Fig. 5.1. Reovirus preferentially replicates in Ras-transformed NIH 3T3 cells. Non-transformed and Ras-transformed NIH 3T3 cells were infected with reovirus at an MOI of 10. (A) Cytotoxicity caused by reovirus in NIH 3T3 cells. Images of cells were taken at 48 hpi. (B) Total reovirus titre from reovirus-infected NIH 3T3 cells at 24, 48 and 72 hpi (representative of two independent experiments; ±*s.e.m.*). (C) Reoviral protein synthesis at 48 hpi in reovirus infected NIH 3T3 cells. Reovirus infected NIH 3T3 (non- and Ras-transformed) cells were pulse-labelled using [^{35}S]-methionine at 48 hpi for one hour. Proteins were separated using SDS-PAGE (10% w/v) and detected by autoradiography using a Typhoon 9400 imager. Shown as a representative experiment with duplicate wells.

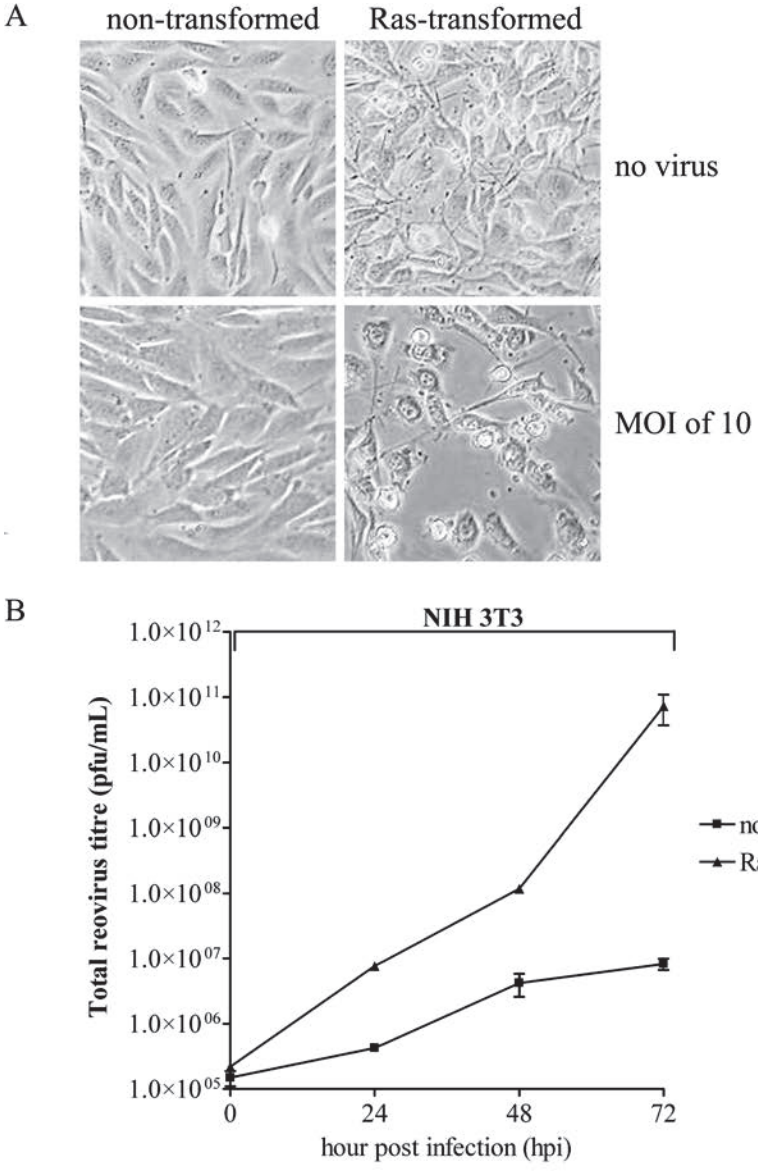
A
non-transformed
Ras-transformed
no virus
MOI of 10
B
NIH 3T3
Total reovirus titre (pfu/mL)
1.0×10 12
1.0×10 11
1.0×10 10
1.0×10 09
1.0×10 08
1.0×10 07
1.0×10 06
1.0×10 05
0
24
48
72
hour post infection (hpi)
non-transformed
Ras-transformed
C
Ras - - - - + + + +
reovirus - - + + - - + +
reoviral protein
λ
μ
σ

Fig. 5.2. Percentage of reovirus-infected non-transformed or Ras-transformed NIH 3T3 cells determined by FACS analysis. At various time-points, reovirus-infected NIH 3T3 cells were collected, fixed, blocked and stained with anti-reovirus antibody and sorted. The percentage of cells positive for reovirus protein expression is depicted in each panel. Figure taken from Marcato *et al.* 2007. I helped collect and process the time-course samples.

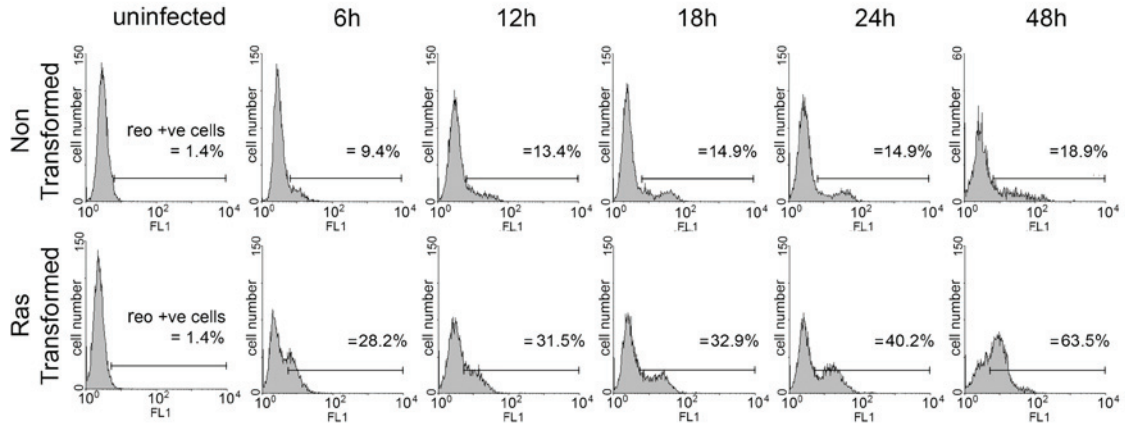
uninfected
6h
12h
18h
24h
48h
Non Transformed
Ras Transformed
cell number
FL1
reo +ve cells = 1.4%
= 9.4%
=13.4%
=14.9%
=14.9%
=18.9%
reo +ve cells = 1.4%
=28.2%
=31.5%
=32.9%
=40.2%
=63.5%

Fig. 5.3. Reovirus binding and internalization in non-transformed and Ras-transformed cells. Efficiency of reovirus binding and internalization was determined by biotinylation of the cell surface-bound reovirus using a cell-membrane-impermeable biotin reagent. Reovirus was allowed to bind to cells at 4 ^{o}C for 1 hour. Cells were then either lysed for biotin pull-down assay or incubated at 37 ^{o}C for 20, 40 or 60 min before biotinylation and lysis. Cell surface-bound reovirus was pulled-down by biotin-conjugated agarose and μ1C protein was detected by western blotting using an anti-reovirus antibody. Numbers under the upper blot indicate the ratio of the residual μ1C protein to the initially bound μ1C protein.

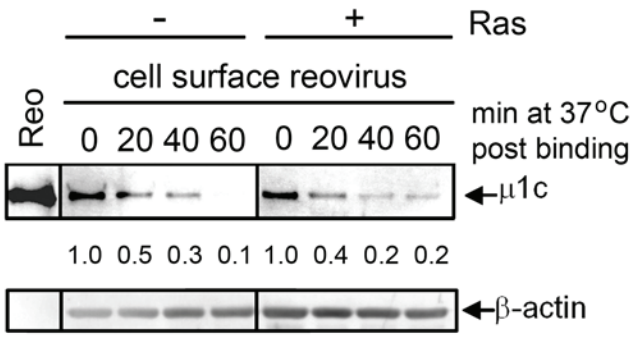
-
+
Ras
cell surface reovirus
Reo
0 20 40 60 0 20 40 60
min at 37°C
post binding
μ1c
1.0 0.5 0.3 0.1 1.0 0.4 0.2 0.2
β-actin

Fig. 5.4. The efficiency of viral protein synthesis is smilar for non-transformed and Ras-transformed NIH 3T3 cells. (A) *In vitro* transcribed control eGFP mRNA and reovirus S4 mRNA (uncapped or capped) were separated on a 1% agarose gel. (B) *In vitro* translation of eGFP and S4 transcripts (uncapped or capped) in lysates prepared from non-transformed and Ras-transformed NIH 3T3 cells.

A

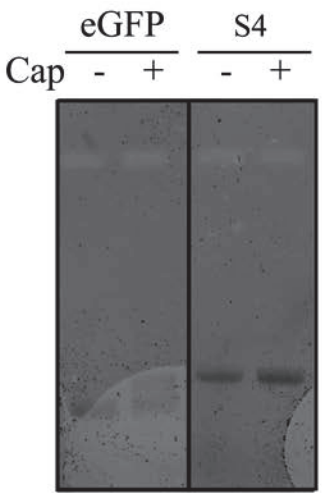

B

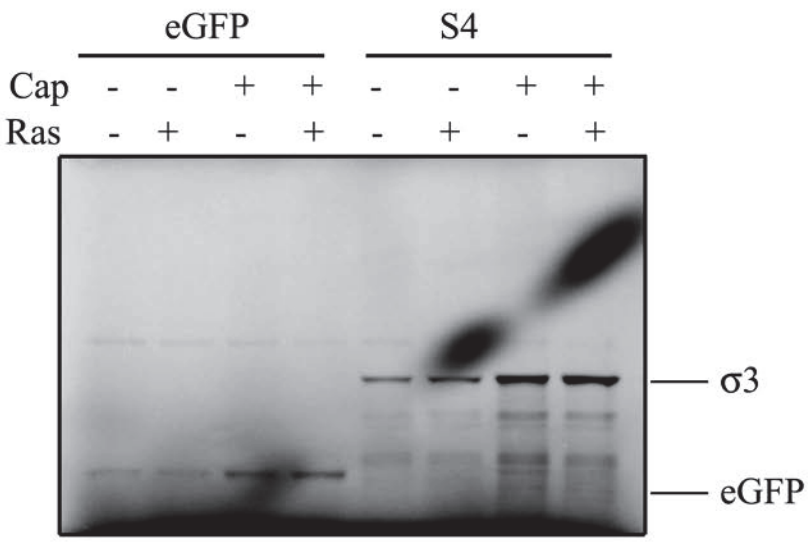

Fig. 5.5. Reovirus release is significantly enhanced in Ras-transformed cells. (A) Plaque titration analysis of total (left panel) and released (right) reovirus at different time-points. Non-transformed and Ras-transformed NIH 3T3 cells were infected by reovirus at an MOI of 10. (B) Detection of total and released reovirus at various time-points using western blotting with anti-reovirus antibody. Figure from Marcato *et al.* 2007. I helped collect samples and perform the plaque titration for the time-course samples.

A

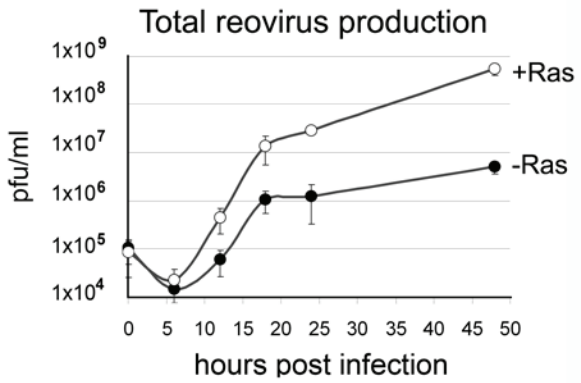
Total reovirus production
1x10^9
1x10^8
1x10^7
1x10^6
1x10^5
1x10^4
pfu/ml
+Ras
-Ras
0 5 10 15 20 25 30 35 40 45 50
hours post infection

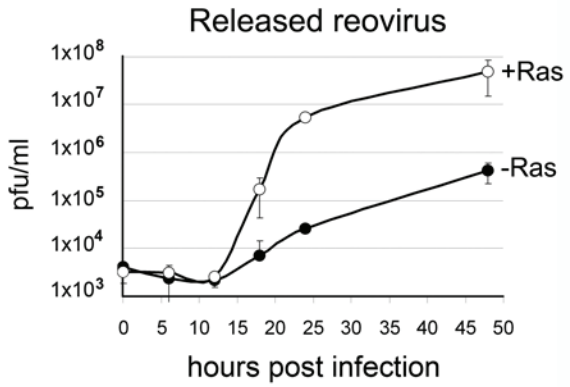
Released reovirus
1x10^8
1x10^7
1x10^6
1x10^5
1x10^4
1x10^3
pfu/ml
+Ras
-Ras
0 5 10 15 20 25 30 35 40 45 50
hours post infection

B

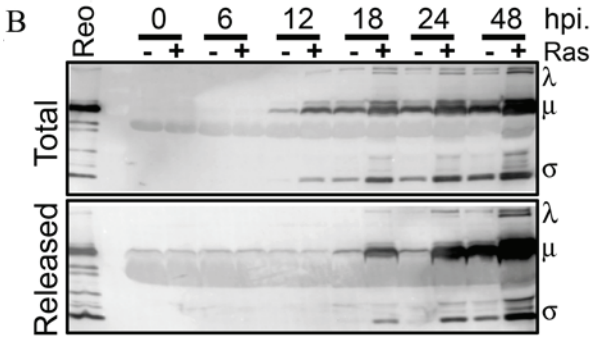
Reo
0
6
12
18
24
48
hpi.
- + - + - + - + - + - +
Ras
Total
Released
λ
μ
σ
λ
μ
σ

Fig. 5.6. Reovirus replication in NIH 3T3 cells transformed by Ras effector-loop mutants. Retrovirus containing Ras effector-loop mutant (V12S35, V12G37 and V12C40) sequences, control vector and the constitutively activated RasV12 mutant were used to transform NIH 3T3 cells. (A) Images of control and Ras transformed cells. (B) Ras-activation assay of the Ras-mutant cells. Activated Ras (GTP-bound) was pulled-down by an agarose-conjugated GST-RBD fusion protein as described in Materials and Methods. Levels of RBD-binding activated Ras were determined by western blotting using antibody against Ras (upper panel). (C) Reovirus titre of control and Ras-mutant cells at various time-points (±*s.e.m.*, n=3).

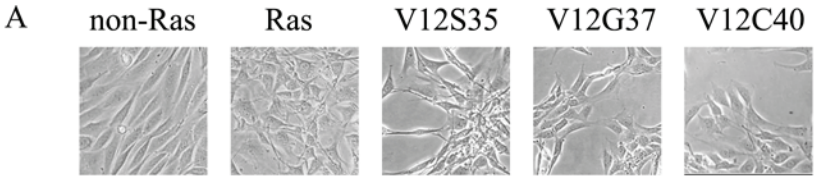
A
non-Ras
Ras
V12S35
V12G37
V12C40

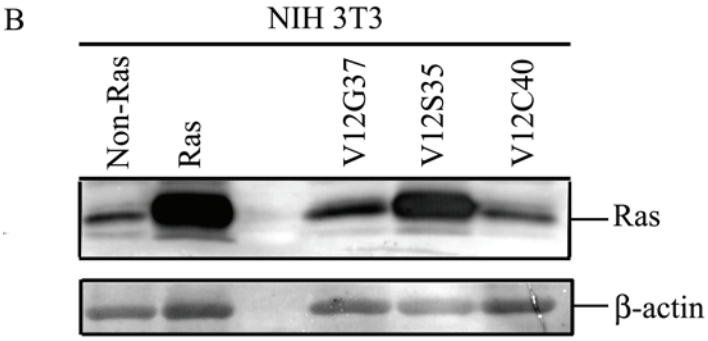
B
NIH 3T3
Non-Ras
Ras
V12G37
V12S35
V12C40
Ras
β-actin

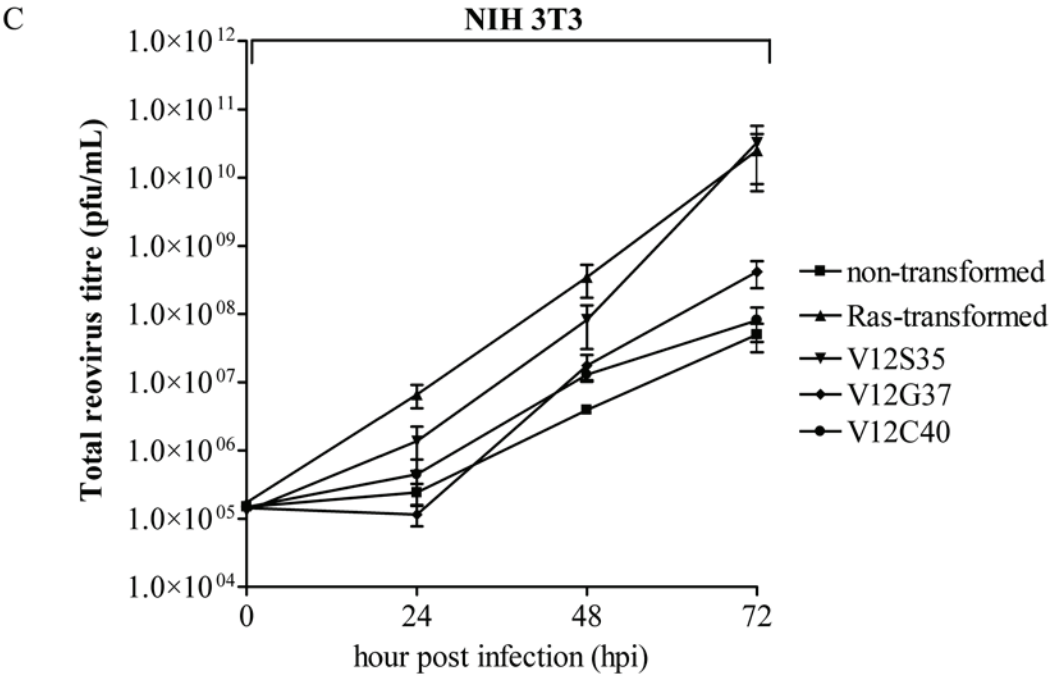
C
NIH 3T3
Total reovirus titre (pfu/mL)
1.0×10 12
1.0×10 11
1.0×10 10
1.0×10 09
1.0×10 08
1.0×10 07
1.0×10 06
1.0×10 05
1.0×10 04
0
24
48
72
hour post infection (hpi)
non-transformed
Ras-transformed
V12S35
V12G37
V12C40

Fig. 5.7. Reovirus uncoats with different efficiencies in Ras effector-mutant cells. (A) Uncoating of reovirus is indicated by the conversion of μ1C into δ. Ras effector-mutant cells were infected at an MOI of 100 at 4 ^{o}C for 1 h before the virus was internalized and uncoated at 37 ^{o}C. (B) Levels of cathepsin L and phosphorylated Erk in control, RasV12 and Ras effector-mutant cells determined by western blotting analysis. Total Erk expression was used as an internal loading control.

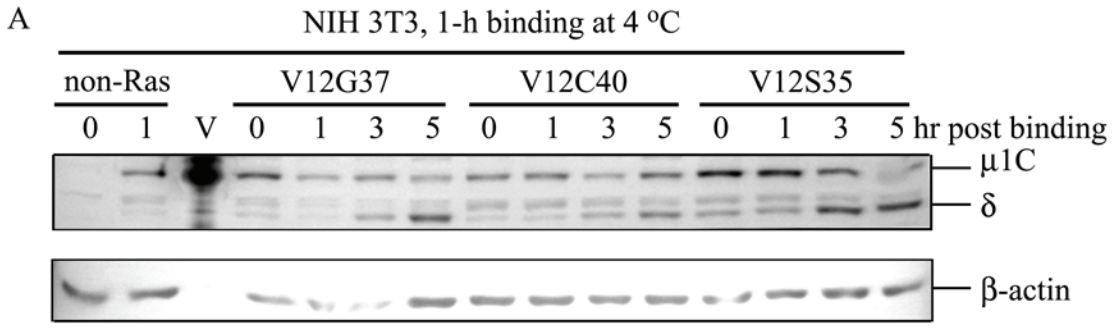
A
NIH 3T3, 1-h binding at 4 °C
non-Ras
V12G37
V12C40
V12S35
0 1 V 0 1 3 5 0 1 3 5 0 1 3 5 hr post binding
μ1C
δ
β-actin

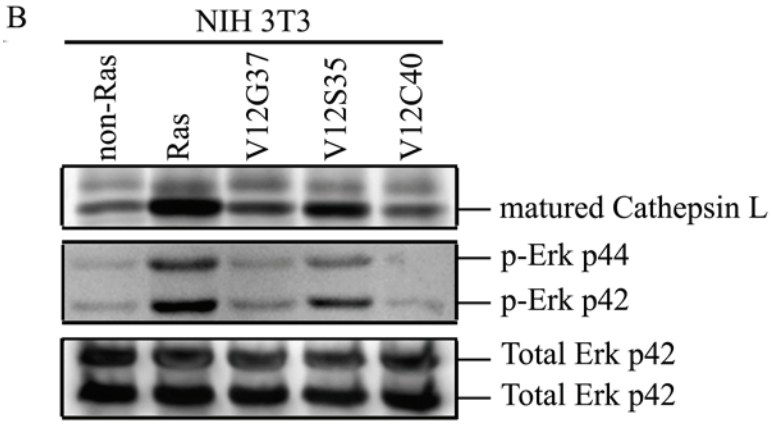
B
NIH 3T3
non-Ras
Ras
V12G37
V12S35
V12C40
matured Cathepsin L
p-Erk p44
p-Erk p42
Total Erk p42
Total Erk p42

Fig. 5.8. Reovirus-induced apoptosis in Ras effector mutant cells. NIH 3T3 cells transformed by RasV12, V12S35, V12G37 and V12C40 expression construacts, together with non-transformed cells, were infected with reovirus and apoptosis was determined by Annexin V and PI staining. The extent of apoptosis was then normalized to the percentage of infection to represent the apoptosis level of infected cells (±*s.e.m.*, n=3).

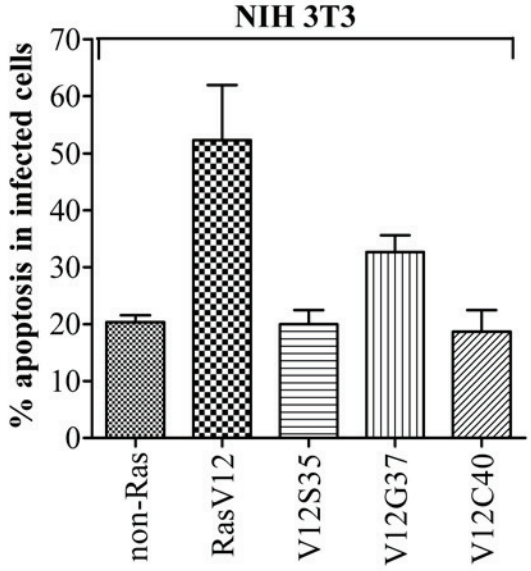
NIH 3T3
% apoptosis in infected cells
70
60
50
40
30
20
10
0
non-Ras
RasV12
V12S35
V12G37
V12C40

Fig. 5.9. Reovirus dissemination in Ras loop-mutant transformed cells reflected by plaque size. Immunohistostaining of plaques formed on reovirus-infected NIH 3T3 cells that were transformed by either RasV12 or the Ras loop mutants V12S35, V12G37 and V12C40 in a course of 5 days.

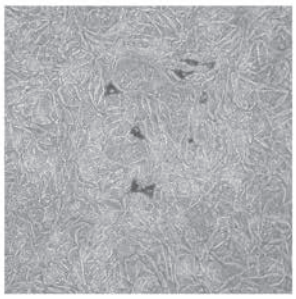

Non-Ras

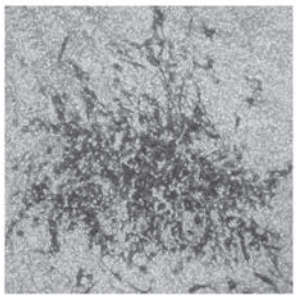

Ras

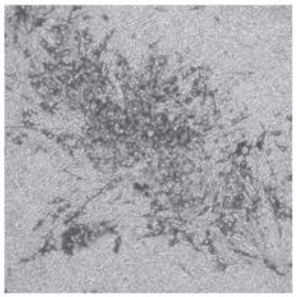

V12S35

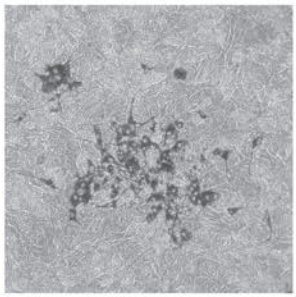

V12G37

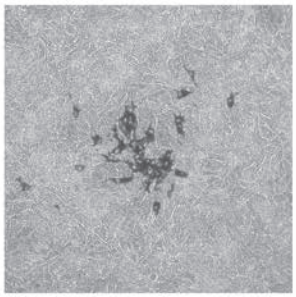

V12C40

Chapter 6 Conclusions

The studies presented in this dissertation investigated 1) the mechanism of enhanced apoptosis induced by the combination of reovirus and p53 activators/accumulators as well as potential clinical applications of the combination; 2) the molecular mechanisms of reovirus preferential replication in Ras-transformed cells. I showed for the first time that enhanced reovirus-mediated apoptosis is possible through the combination of reovirus with either an MDM2 antagonist (Nutlin-3a) or low concentrations of traditional chemotherapy drugs that cause p53 accumulation. I was also able to characterize certain steps in the reovirus life cycle that are enhanced by Ras-transformation, and explored the sub-Ras signaling pathways that contribute to the enhancement.

6.1. Boosting Reovirus Cancer-Killing Activities by Combining Reovirus with p53 Activators/Accumulators

My study of the combination effects of reovirus and Nutlin-3a is the first to investigate the possibility of a combination therapy of a p53 stabilizer and reovirus. My data demonstrate that reovirus production by HCT116 p53+/+ cells and p53-/- cells are comparable. However, addition of Nutlin-3a, an MDM2 antagonizer and p53 stabilizer, significantly enhances reovirus-induced cytotoxicity in a p53-dependent manner. This higher level of cell death is due to the significant augmentation of reovirus-induced apoptosis and is caspase-dependent. Furthermore, the enhancement of apoptosis caused by the combination of reovirus and Nutlin-3a requires the upregulation of p53-target

genes (*p21* and *bax*) and NF-κB activation, and the combination results in significantly improved virus dissemination/spread. Therefore, this study presents the proof of principle for using a p53 stabilizer to enhance reovirus oncolysis.

The combination of reovirus and other chemotherapeutics at sub-lethal dosages *in vitro* was tested as well. Low concentrations of ActD or Etp enhanced reovirus-induced apoptosis in HCT116 p53+/+ cells but not in p53-/- cells, while the drugs themselves did not trigger significant levels of apoptosis. Other chemotherapy drugs such as Dox, at the concentrations tested, enhanced reovirus-induced cell death in both p53+/+ cells and p53-/- cells, indicating that different chemotherapy drugs trigger death pathways with various dependence on p53. Therefore, obtaining information on whether a chemotherapy drug can enhance reovirus-induced apoptosis coupled with p53 status of the tumor might help to decrease the administration dosage and choose the proper drug as a combination partner. Since ActD and Etp each enhance reovirus-induced apoptosis in a p53-dependent manner, the mechanism was investigated. Interestingly, these drugs have similar mechanisms for enhancing reovirus-induced apoptosis similar to that found for Nutlin-3a: activation of NF-κB, as well as expression of *p21* and *bax*, are required for the enhancement of apoptosis induced by the combination of reovirus and ActD/Etp, although the dependence on NF-κB is not as obvious as seen for the combination of reovirus and Nutlin-3a.

NF-κB is an important transcription factor that is involved in inflammation and innate immunity. NF-κB also induces cellular alterations that promote tumor formation (Karin et al. 2002) and is constitutively activated in a wide range of human cancers

(Chaturvedi et al. 2011). Since reovirus-induced apoptosis requires activation of NF-κB, it would be interesting to determine whether a constitutively activated NF-κB can provide an advantage for reovirus replication in tumor cells. Ras-transformation downregulates RIG-I signaling through the Raf/MEK pathway and inhibits the production of IFN-β (Shmulevitz et al. 2010). Since HCT116 cells contain a K-ras activation mutation (Fearon et al. 1990), IFN-β production in these cells might be reduced. However, proapoptotic signaling in melanoma cells induced by RIG-I was reported to be IFN-β independent and RIG-I induced p53-independent upregulation of proapoptotic genes such as *noxa* and *puma* (Besch et al. 2009). Since RIG-I and its adaptor protein IFN-β promoter stimulator 1 (IPS-1) were recently implicated to be important to reovirus-induced apoptosis through activation of IRF-3 (Holm et al. 2007), it will be interesting to determine whether activation of IRF-3 is required for the enhancement of apoptosis induced by the combination of reovirus and a p53 accumulator/activator.

NF-κB has been identified as one of the critical mediators for cancer cell chemo- or radiotherapy resistance (Baldwin 2001). The chemoresistance of CEM human T leukemic cells has been attributed to the induction of *p21* by NF-κB (Wuerzberger-Davis et al. 2005). Addition of Etp to these cells induces higher levels of *p21* and lead to increased chemoresistance (Chang and Miyamoto 2006). In my study, addition of Nutlin-3a did not significantly enhance *p21* expression. However, the combination of reovirus and ActD or Etp significantly augmented the level of *p21* expression compared to ActD or Etp alone. On the other hand, the combination of reovirus and ActD or Etp induced significantly higher levels of cell death compared to each single treatment alone. It seems that reovirus takes advantage of the induction of *p21* caused by the addition of the

chemotherapy drugs to induce cell death. Therefore, reovirus might convert a disadvantaged situation (where *p21* upregulation contributes to resistance) into a beneficial condition (where cell death is enhanced). It would be useful to determine whether the combination of reovirus and chemotherapy drugs could be applied to chemoresistant cancer cells.

To develop tumor xenografts from human HCT116 p53+/+ cells and p53-/- cells, effects of the combination of ActD/Etp and reovirus were tested *in vivo* in an immunocompromised mouse model (NOD-SCID mice). It was shown that *i.p.* injections of ActD, but not Etp, significantly accumulated p53 in p53+/+ tumors that were established in NOD-SCID mice. Furthermore, compared to reovirus or ActD treatment alone, co-administeration of reovirus and ActD to p53+/+ tumors significantly enhanced tumor regression. Unfortunately, NOD-SCID mice treated with the combination of reovirus and ActD died prematurely. The immune system of NOD-SCID mice is severely compromised and thus susceptible to reovirus-related pathologic lesions (Loken et al. 2004). ActD is also immunosuppressive (Rasmussen and Arvin 1982). Therefore, treatment with ActD likely abrogated the residual immune activity in NOD-SCID mice (Imada 2003) and resulted in the rapid spread of reovirus without protection of normal tissue or organs by the immune system. Ideally, immunocompetent animal models should be developed to test the efficacy of the combination of this chemotherapy drug and reovirus. In my animal model, to decrease the size of the experimental groups, only the p53+/+ tumor xenografts were tested for the combination therapy. In an immunocompetent model, p53-/- tumor xenografts will also need to be tested for tumor regression with the combination therapy.

It is worth mentioning that both Nutlin-3a and the chemotherapy drugs (such as ActD and Etp) stimulate p53 accumulation in cells containing the wild-type p53. However, over 50% of human cancers contain p53 mutations (Dey et al. 2008). Activating p53 pathways in these cells would need small molecules that can re-activate the p53 mutants. Since stabilization of p53 has been shown to enhance reovirus-induced apoptosis (Chapters 3 and 4), the combination of reovirus and the drugs that re-activate p53 mutants theoretically should also induce augmented levels of cell death. Therefore, it will be interesting in the future to test a combination of reovirus and a p53 re-activator in tumors containing p53 mutations.

6.2. Molecular Mechanisms of Reovirus Preferential Replication in Ras-transformed Cells

The detailed comparison of reovirus replication in non-transformed cells and Ras-transformed NIH 3T3 cells enabled us to further decipher the underlying mechanisms of reovirus preferential killing of Ras-transformed cancer cells. There are three steps in the reovirus replication cycle that are enhanced by Ras-transformation (Marcato et al. 2007). Originally, it was believed that reovirus protein synthesis is enhanced in Ras-transformed cells and that this is the fundamental mechanism for reovirus preferential replication in Ras-transformed cells (Strong et al. 1998). One of the discrepancies between the two studies noted here are the different quantitative methodologies used to detect reovirus transcripts. As discussed in Chapter 5, Strong *et al.* used traditional end-point reverse-transcriptase PCR (RT-PCR) while Marcato *et al.* used quantitative real-time PCR (qRT-

PCR). The limitation of end-point RT-PCR and the low resolution of agarose-gel resolvation of the PCR products amplified from cDNA (Heid et al. 1996) made it difficult to detect a 4-fold difference on RNA levels between Ras-transformed and non-transformed cells, which is readily detectable by real-time PCR. Since levels of both reoviral transcripts and protein are about 3-4 fold higher in Ras-transformed cells, it is unlikely that protein synthesis is enhanced in Ras-transformed cells compared to non-transformed cells (Marcato et al. 2007). Moreover, my *in vitro* translation data further confirm that the rate of translation of control and reoviral mRNA is not affected by Ras-transformation. One shortcoming of the *in vitro* translation method used here, however, is that cell lysates from non-infected cells were used. It was reported previously that reovirus infection in L cells could cause a transition of translating capped RNA into discriminately synthesizing uncapped RNA (Skup and Millward 1980; Lemieux et al. 1984). Therefore, it is not clear whether protein synthesis efficiency is affected by virus infection and if a transition of capped to uncapped protein synthesis at a later time of reovirus infection plays a role in reovirus replication in Ras-transformed cells. *In vitro* translation lysates from infected cells might give a better indication on whether 1) in cell types other than L cells, the transition from capped to uncapped protein synthesis exists at a late stage of reovirus infection, and 2) Ras-transformation has any effects on capped or uncapped translation of reoviral transcripts.

The double-stranded RNA activated protein kinase (PKR) has been found to be activated in reovirus infected non-transformed cells but not in Ras-transformed cells and inactivation of PKR could enhance reovirus replication in non-transformed cells (Strong et al. 1998). PKR, along with other pattern recognition receptors such as RIG-I,

melanoma differentiation-associated protein 5 (MDA5) and Toll-like receptors (TLRs), play important roles in detecting foreign pathogens such as RNA viruses and initiates immune responses such as activating IFN-β production (Meylan and Tschopp 2006). Recently, our lab investigated the IFN response in Ras-transformed and non-transformed cells (Shmulevitz et al. 2010) and showed that high levels of RIG-I and PKR are indeed expressed in non-transformed cells after reovirus infection. Furthermore, inhibition of RIG-I could block IFN-β expression while blockage of PKR activation could partially inhibit it. Additionally, the inhibition of RIG-I or PKR renders non-transformed cells more susceptible to reovirus infection. Therefore, PKR does not inhibit reovirus protein synthesis in non-transformed cells as hypothesized before (Strong et al. 1998), but rather mediates IFN-β production in non-transformed cells to prevent reovirus spreading and secondary infection.

Our data also suggest that the uncoating process for reovirus partially determines the susceptibility of cells to reovirus infection. The importance of reovirus uncoating was also confirmed in another study (Alain et al. 2007a). Based on the use of Ras effector-mutant cells, my data suggest that, Raf effector-mutant cells contain the highest levels of cathepsin L, and the uncoating efficiency of reovirus is the highest in cells transformed by different Ras-effector mutants cells. It would be interesting to determine whether inhibition of the Raf pathway (using either siRNA or MEK inhibitors) would block the uncoating process of reovirus. At the same time, cathepsins are not the only proteases that can affect reovirus uncoating. Therefore, blocking one protease might not be sufficient to block reovirus uncoating and subsequent replication. Nonetheless, in cancers, cathepsins that are membrane bound or secreted contribute to the invasion of tumor cells and are

thus suggested to be prognostic markers for cancers such as brain and ovarian cancer (Levicar et al. 2003; Kolwijck et al. 2010). Hence, reovirus might benefit from increased level of cathepsins in aggressive tumor cells and preferentially replicate and kill these tumor cells.

As introduced in Chapter 1, reovirus-induced apoptosis is correlated with the activation of JNK and NF-κB (Connolly et al. 2000; Clarke et al. 2001b; Clarke et al. 2003). Since Ras-transformation itself is associated with the activation of JNK and NF-κB (Cox and Der 2003; Kennedy and Davis 2003), it is not surprising that Ras-transformation enhances reovirus-induced apoptosis (Marcato et al. 2007), and increases the percentage of reovirus release. When Ras-effector mutant cells were infected by reovirus, there was no statistically significant difference in terms of reovirus-induced apoptosis among these mutant cells. However, RalGEF mutant cells consistently undergo higher level of apoptosis (Fig. 5.8). The Ras-mediated RalGEF pathway can activate NF-κB through activation of TBK1 (Henry et al. 2000; Chien et al. 2006) and is likely mediating reovirus-induced apoptosis. On the other hand, it is also possible that Ras-effector pathways other than Raf, PI3K and RalGEF might mediate reovirus-induced apoptosis. For example, Ras effectors RASSFs potentially can promote apoptosis upon Ras-activation (Cox and Der 2003; Gordon and Baksh 2011).

Results obtained from Ras effector-mutant cells need to be confirmed by inhibition of individual pathways using specific RNAi methods. Nonetheless, our results show that reovirus preferential replication does not rely on one single effector pathway but rather on cooperation of different pathways, as evidenced by the wide range of plaque

sizes shown with these cells (Fig. 5.9). Therefore, for future directions, confirmation of individual sub-Ras pathways that are responsible for the enhancement of a particular step of reovirus replication would be important. Identifying these pathways may present novel targets for cancer therapy as well as better designs in administrating reovirus as single-agent treatment or combination therapies.

6.3. Perspective Clinical Application of Oncolytic Viruses

Historically, viral oncolytic activity was observed in various occasions in the early 1990s (Cattaneo et al. 2008). The thorough examinations of the molecular mechanisms of various oncolytic viruses have significantly pushed the field forward (listed in Table 6.1), and many of these viruses are being tested in clinical trials as alternative cancer therapeutics. For example, one of the most studied replication-conditional oncolytic adenoviruses Onyx 015, although proved not to be dependent on status of p53 for its tropism *in vivo* (Goodrum and Ornelles 1998), has been shown to be well tolerated by patients and induce partial to complete response. Other oncolytic viruses such as Newcastle Disease virus, Herpes simplex virus, Seneca valley virus and Vaccinia virus can also been engineered or "armed" to replicate specifically in tumor cells and are being tested in clinical trials as reviewed in (Eager and Nemunaitis 2011). Compared to these engineered viruses, T3D reovirus is not associated with pathological symptoms and therefore does not need any genetic modifications. In fact, reovirus is well tolerated by patients in clinical trials and show promises as a safe cancer therapeutic option. Despite our increased understanding of the oncolytic virus, more and more evidence indicates that

using an oncolytic virus as a single treatment is unlikely to achieve complete tumor regression in patients. This is due to either limited virus release within the tumor tissues, or clearance of the virus by the acquired antiviral immune responses. Strategies to overcome these obstacles must be tested to improve the applicability of oncolytic viruses. Reovirus and other oncolytic viruses are being tested in conjunction with radiotherapy or various chemotherapy drugs as reviewed in (Eager and Nemunaitis 2011; Pesonen et al. 2011; Wennier et al. 2011). However, these studies did not demonstrate either reduced virus clearance or improved virus spread in tumor cells. Results from my project reported in this dissertation indicate that the combination of a p53 activator/accumulator and reovirus may improve reovirus efficacy by increasing the reovirus release in tumor tissue through the enhancement of reovirus-induced tumor cell death. Single application of traditional chemotherapy drugs has also shown limited efficacies due to their adverse side effects in patients. The combination of reovirus and a p53 activator/accumulator might help to decrease the dosage of traditional chemotherapy drugs such as ActD to decrease the side effects. On the other hand, certain chemotherapy drugs such as ActD not only cause p53 accumulation, but also have immunosuppressive effects. Combining a low dosage of a chemotherapy drug with reovirus may temporally reduce the immune response against reovirus and assist reovirus to reach the tumor site.

Meanwhile, oncolytic viruses have been shown to not only eliminate tumor through direct lysis of the tumor cells but also trigger immune responses to assist the clearance of the tumor (Eager and Nemunaitis 2011; Melcher et al. 2011). Administration of reovirus, however, both augments the immune response to clear the tumor but also enhances the processing and presentation of tumor antigens (Gujar et al., 2010; Gujar et

al., 2011). Furthermore, application of the reovirus-stimulated DC cells into healthy mice prevents further tumor challenge. Whether the combination of reovirus and a p53 activator/accumulator can enhance the ability of reovirus to induce tumor antigen presentation is still not clear and will be important to determine. It will also be interesting to determine whether a p53 activator/accumulator can assist other oncolytic viruses to spread in tumors and improve the efficacy of oncolysis of these viruses.

My results also show that various steps of the reovirus replication cycle are enhanced by Ras-transformation and that the steps that are enhanced by Ras-activation may be affected by different sub-Ras pathways. Elucidating the signaling pathways necessary for reovirus oncolysis will not only contribute to the understanding of reovirus, but can also be instrumental for reovirus to be applied as a cancer therapy. For example, reovirus can only synergize with anti-cancer drugs that do not block its replication cycle. Co-administration of protease inhibitors and reovirus may not achieve synergistic effect since reovirus uncoating will be blocked and results in inefficient reovirus replication. Apoptosis promoting drugs, on the other hand, will benefit reovirus oncolysis. Hence, our understanding on the molecular mechanism of reovirus oncolysis can provide insights to design personalized cancer therapy for patients. Reovirus is not the only oncolytic virus that exploits the activation of Ras-signaling pathways in cancer cells. Newcastle disease virus and vesicular stomatitis virus have been shown to replicate preferentially in Ras-transformed cells (Reichard et al. 1992; Lech and Russell 2010). The methodology used in this study can therefore also be applied to determine molecular mechanisms of these viruses, which will help to enhance our understanding and guide therapeutic administration of these oncolytic viruses.

Table 6.1. Selectivity of representative oncolytic viruses.

Family	virus	Molecular Basis of the Cancer Selectivity	References
Reovirus	T3D	Constitutively activated Ras signaling pathway	Strong et al. 1998; Coffey et al. 1998
Adenoviruses	ΔE1B (55 kDa)	Loss of p53 function or altered nuclear mRNA transport	Bischoff et al. 1996; O'Shea et al. 2004
	ΔE1A (24 kDa)	Aberrant pRB pathway	Heise et al. 2000; Fueyo et al. 2000
	ΔE1B (19 kDa)	Aberrant apoptotic pathways	Leitner et al. 2009
Parvoviruses	H-1PV	Activation of Raf signaling pathway; SMAD4 mutations and IFN signaling	Riolobos et al. 2010; Rommelaere et al. 2010; Dempe et al. 2010
Poxviruses	Vaccinia virus	Engineered to target upregulated receptors on cancer cells	reviewed in Guse et al. (2011)
	Myxoma virus	Disruption of IFN production through Erk; activated Akt pathway	Wang et al. 2004; Wang et al. 2006
Paramyxoviruses	Measles virus	Attenuated and engineered to target upregulated receptors on cancer cells	Galanis 2010; Lech and Russell 2010
	Newcastle disease virus	Lack of IFN response; activation of Ras, Rac-1 or N-myc signaling pathways	Reichard et al. 1992; Lech and Russell 2010
Rhabdovirus	Vesicular stomatitis virus	Attenuated and target defective IFN signaling; activation of Ras/Raf/MEK/ERK	Noser et al. 2007; Le Boeuf and Bell 2010
Herpes viruses	Herpes simplex viruses	Engineered to target upregulated ribonucleotide reductase; activated MAP2K to inhibit PKR-eIF2α; Activation of Ras signaling pathway	Yoon et al. 1998; Smith et al. 2000; Smith et al. 2006; Sarinella et al. 2006

References

Al-Hajj M, Wicha MS, ito-Hernandez A, Morrison SJ, and Clarke MF. Prospective identification of tumorigenic breast cancer cells. (2003) *Proc.Natl.Acad.Sci.U.S.A* **100**, 3983-3988.

Alain T, Hirasawa K, Pon KJ, Nishikawa SG, Urbanski SJ, Auer Y *et al.* Reovirus therapy of lymphoid malignancies. (2002) *Blood* **100**, 4146-4153.

Alain T, Kim M, Johnston RN, Urbanski S, Kossakowska AE, Forsyth PA *et al.* The oncolytic effect in vivo of reovirus on tumour cells that have survived reovirus cell killing in vitro. (2006) *Br.J.Cancer* **95**, 1020-1027.

Alain T, Kim TS, Lun X, Liacini A, Schiff LA, Senger DL *et al.* Proteolytic disassembly is a critical determinant for reovirus oncolysis. (2007a) *Mol.Ther.* **15**, 1512-1521.

Alain T, Wong JF, Endersby R, Urbanski SJ, Lee PW, Muruve DA *et al.* Reovirus decreases azoxymethane-induced aberrant crypt foci and colon cancer in a rodent model. (2007b) *Cancer Gene Ther.* **14**, 867-872.

Baer GS and Dermody TS. Mutations in reovirus outer-capsid protein sigma3 selected during persistent infections of L cells confer resistance to protease inhibitor E64. (1997) *J.Virol.* **71**, 4921-4928.

Baer GS, Ebert DH, Chung CJ, Erickson AH, and Dermody TS. Mutant cells selected during persistent reovirus infection do not express mature cathepsin L and do not support reovirus disassembly. (1999) *J.Virol.* **73**, 9532-9543.

Baeuerle PA and Baltimore D. NF-kappa B: ten years after. (1996) *Cell* **87**, 13-20.

Bagnyukova TV, Serebriiskii IG, Zhou Y, Hopper-Borge EA, Golemis EA, and Astsaturov I. Chemotherapy and signaling: How can targeted therapies supercharge cytotoxic agents? (2010) *Cancer Biol.Ther.* **10**, 839-853.

Baldwin AS, Jr. The NF-kappa B and I kappa B proteins: new discoveries and insights. (1996) *Annu.Rev.Immunol.* **14**, 649-683.

Baldwin AS. Control of oncogenesis and cancer therapy resistance by the transcription factor NF-kappaB. (2001) *J.Clin.Invest* **107**, 241-246.

Barton ES, Forrest JC, Connolly JL, Chappell JD, Liu Y, Schnell FJ *et al.* Junction adhesion molecule is a receptor for reovirus. (2001) *Cell* **104**, 441-451.

Bass DM, Bodkin D, Dambrauskas R, Trier JS, Fields BN, and Wolf JL. Intraluminal proteolytic activation plays an important role in replication of type 1 reovirus in the intestines of neonatal mice. (1990) *J.Virol.* **64**, 1830-1833.

Bell J. Oncolytic viruses: an approved product on the horizon? (2010) *Mol.Ther.* **18**, 233-234.

Berard A and Coombs KM. Mammalian reoviruses: propagation, quantification, and storage. (2009) *Curr.Protoc.Microbiol.* **Chapter 15**, Unit15C-

Besch R, Poeck H, Hohenauer T, Senft D, Hacker G, Berking C *et al.* Proapoptotic signaling induced by RIG-I and MDA-5 results in type I interferon-independent apoptosis in human melanoma cells. (2009) *J.Clin.Invest* **119**, 2399-2411.

Bischoff JR, Kirn DH, Williams A, Heise C, Horn S, Muna M *et al.* An adenovirus mutant that replicates selectively in p53-deficient human tumor cells. (1996) *Science* **274**, 373-376.

Bodkin DK, Nibert ML, and Fields BN. Proteolytic digestion of reovirus in the intestinal lumens of neonatal mice. (1989) *J.Virol.* **63**, 4676-4681.

Borsa J, Copps TP, Sargent MD, Long DG, and Chapman JD. New intermediate subviral particles in the in vitro uncoating of reovirus virions by chymotrypsin. (1973) *J.Virol.* **11**, 552-564.

Borsa J, Morash BD, Sargent MD, Copps TP, Lievaart PA, and Szekely JG. Two modes of entry of reovirus particles into L cells. (1979) *J.Gen.Virol.* **45**, 161-170.

Bos JL. ras oncogenes in human cancer: a review. (1989) *Cancer Res.* **49**, 4682-4689.

Bouvet M, Fang B, Ekmekcioglu S, Ji L, Bucana CD, Hamada K *et al.* Suppression of the immune response to an adenovirus vector and enhancement of intratumoral transgene expression by low-dose etoposide. (1998) *Gene Ther.* **5**, 189-195.

Brown CJ, Cheok CF, Verma CS, and Lane DP. Reactivation of p53: from peptides to small molecules. (2011) *Trends Pharmacol.Sci.* **32**, 53-62.

Bullock AN and Fersht AR. Rescuing the function of mutant p53. (2001) *Nat.Rev.Cancer*, 68-76.

Bykov VJ, Issaeva N, Shilov A, Hultcrantz M, Pugacheva E, Chumakov P *et al.* Restoration of the tumor suppressor function to mutant p53 by a low-molecular-weight compound. (2002) *Nat.Med.* **8**, 282-288.

Camonis JH and White MA. Ral GTPases: corrupting the exocyst in cancer cells. (2005) *Trends Cell Biol.* **15**, 327-332.

Cattaneo R, Miest T, Shashkova EV, and Barry MA. Reprogrammed viruses as cancer therapeutics: targeted, armed and shielded. (2008) *Nat.Rev.Microbiol.* **6**, 529-540.

Chandran K, Farsetta DL, and Nibert ML. Strategy for nonenveloped virus entry: a hydrophobic conformer of the reovirus membrane penetration protein micro 1 mediates membrane disruption. (2002) *J.Virol.* **76**, 9920-9933.

Chang PY and Miyamoto S. Nuclear factor-kappaB dimer exchange promotes a p21(waf1/cip1) superinduction response in human T leukemic cells. (2006) *Mol.Cancer Res.* **4**, 101-112.

Chaturvedi MM, Sung B, Yadav VR, Kannappan R, and Aggarwal BB. NF-kappaB addiction and its role in cancer: 'one size does not fit all'. (2011) *Oncogene* **30**, 1615-1630.

Chen Z, Hagler J, Palombella VJ, Melandri F, Scherer D, Ballard D *et al.* Signal-induced site-specific phosphorylation targets I kappa B alpha to the ubiquitin-proteasome pathway. (1995) *Genes Dev.* **9**, 1586-1597.

Chien Y, Kim S, Bumeister R, Loo YM, Kwon SW, Johnson CL *et al.* RalB GTPase-mediated activation of the IkappaB family kinase TBK1 couples innate immune signaling to tumor cell survival. (2006) *Cell* **127**, 157-170.

Chien Y and White MA. RAL GTPases are linchpin modulators of human tumour-cell proliferation and survival. (2003) *EMBO Rep.* **4**, 800-806.

Chua KB, Crameri G, Hyatt A, Yu M, Tompang MR, Rosli J *et al.* A previously unknown reovirus of bat origin is associated with an acute respiratory disease in humans. (2007) *Proc.Natl.Acad.Sci.U.S.A* **104**, 11424-11429.

Clarke P, Meintzer SM, Gibson S, Widmann C, Garrington TP, Johnson GL *et al.* Reovirus-induced apoptosis is mediated by TRAIL. (2000) *J.Virol.* **74**, 8135-8139.

Clarke P, Meintzer SM, Moffitt LA, and Tyler KL. Two distinct phases of virus-induced nuclear factor kappa B regulation enhance tumor necrosis factor-related apoptosis-inducing ligand-mediated apoptosis in virus-infected cells. (2003) *J.Biol.Chem.* **278**, 18092-18100.

Clarke P, Meintzer SM, Spalding AC, Johnson GL, and Tyler KL. Caspase 8-dependent sensitization of cancer cells to TRAIL-induced apoptosis following reovirus-infection. (2001a) *Oncogene* **20**, 6910-6919.

Clarke P, Meintzer SM, Wang Y, Moffitt LA, Richardson-Burns SM, Johnson GL *et al.* JNK regulates the release of proapoptotic mitochondrial factors in reovirus-infected cells. (2004) *J.Virol.* **78**, 13132-13138.

Clarke P, Meintzer SM, Widmann C, Johnson GL, and Tyler KL. Reovirus infection activates JNK and the JNK-dependent transcription factor c-Jun. (2001b) *J.Virol.* **75**, 11275-11283.

Clarke P and Tyler KL. Down-regulation of cFLIP following reovirus infection sensitizes human ovarian cancer cells to TRAIL-induced apoptosis. (2007) *Apoptosis.* **12**, 211-223.

Coffey CM, Sheh A, Kim IS, Chandran K, Nibert ML, and Parker JS. Reovirus outer capsid protein micro1 induces apoptosis and associates with lipid droplets, endoplasmic reticulum, and mitochondria. (2006) *J.Virol.* **80**, 8422-8438.

Coffey MC, Strong JE, Forsyth PA, and Lee PW. Reovirus therapy of tumors with activated Ras pathway. (1998) *Science* **282**, 1332-1334.

Cohen JJ, Duke RC, Fadok VA, and Sellins KS. Apoptosis and programmed cell death in immunity. (1992) *Annu.Rev.Immunol.* **10**, 267-293.

Collette J, Ulku AS, Der CJ, Jones A, and Erickson AH. Enhanced cathepsin L expression is mediated by different Ras effector pathways in fibroblasts and epithelial cells. (2004) *Int.J.Cancer* **112**, 190-199.

Connolly JL and Dermody TS. Virion disassembly is required for apoptosis induced by reovirus. (2002) *J.Virol.* **76**, 1632-1641.

Connolly JL, Rodgers SE, Clarke P, Ballard DW, Kerr LD, Tyler KL *et al.* Reovirus-induced apoptosis requires activation of transcription factor NF-kappaB. (2000) *J.Virol.* **74**, 2981-2989.

Cox AD and Der CJ. The dark side of Ras: regulation of apoptosis. (2003) *Oncogene* **22**, 8999-9006.

Dalerba P, Cho RW, and Clarke MF. Cancer stem cells: models and concepts. (2007) *Annu.Rev.Med.* **58**, 267-284.

Danthi P, Coffey CM, Parker JS, Abel TW, and Dermody TS. Independent regulation of reovirus membrane penetration and apoptosis by the mu1 phi domain. (2008a) *PLoS.Pathog.* **4**, e1000248-

Danthi P, Kobayashi T, Holm GH, Hansberger MW, Abel TW, and Dermody TS. Reovirus apoptosis and virulence are regulated by host cell membrane penetration efficiency. (2008b) *J.Virol.* **82**, 161-172.

Datta SR, Dudek H, Tao X, Masters S, Fu H, Gotoh Y *et al.* Akt phosphorylation of BAD couples survival signals to the cell-intrinsic death machinery. (1997) *Cell* **91**, 231-241.

de Ruiter ND, Wolthuis RM, van DH, Burgering BM, and Bos JL. Ras-dependent regulation of c-Jun phosphorylation is mediated by the Ral guanine nucleotide exchange factor-Ral pathway. (2000) *Mol.Cell Biol.* **20**, 8480-8488.

Dean M, Fojo T, and Bates S. Tumour stem cells and drug resistance. (2005) *Nat.Rev.Cancer* **5**, 275-284.

DeBiasi RL, Clarke P, Meintzer S, Jotte R, Kleinschmidt-Demasters BK, Johnson GL *et al.* Reovirus-induced alteration in expression of apoptosis and DNA repair genes with potential roles in viral pathogenesis. (2003) *J.Virol.* **77**, 8934-8947.

Dempe S, Stroh-Dege AY, Schwarz E, Rommelaere J, and Dinsart C. SMAD4: a predictive marker of PDAC cell permissiveness for oncolytic infection with parvovirus H-1PV. (2010) *Int.J.Cancer* **126**, 2914-2927.

Dey A, Verma CS, and Lane DP. Updates on p53: modulation of p53 degradation as a therapeutic approach. (2008) *Br.J.Cancer* **98**, 4-8.

Diehn M, Cho RW, Lobo NA, Kalisky T, Dorie MJ, Kulp AN *et al.* Association of reactive oxygen species levels and radioresistance in cancer stem cells. (2009) *Nature* **458**, 780-783.

Ding K, Lu Y, Nikolovska-Coleska Z, Wang G, Qiu S, Shangary S *et al.* Structure-based design of spiro-oxindoles as potent, specific small-molecule inhibitors of the MDM2-p53 interaction. (2006) *J.Med.Chem.* **49**, 3432-3435.

Ducut Sigala JL, Bottero V, Young DB, Shevchenko A, Mercurio F, and Verma IM. Activation of transcription factor NF-kappaB requires ELKS, an IkappaB kinase regulatory subunit. (2004) *Science* **304**, 1963-1967.

Duncan MR, Stanish SM, and Cox DC. Differential sensitivity of normal and transformed human cells to reovirus infection. (1978) *J.Virol.* **28**, 444-449.

Eager RM and Nemunaitis J. Clinical development directions in oncolytic viral therapy. (2011) *Cancer Gene Ther.* **18**, 305-317.

Ebert DH, Deussing J, Peters C, and Dermody TS. Cathepsin L and cathepsin B mediate reovirus disassembly in murine fibroblast cells. (2002) *J.Biol.Chem.* **277**, 24609-24617.

Errington F, Steele L, Prestwich R, Harrington KJ, Pandha HS, Vidal L *et al.* Reovirus activates human dendritic cells to promote innate antitumor immunity. (2008) *J.Immunol.* **180**, 6018-6026.

Etoh T, Himeno Y, Matsumoto T, Aramaki M, Kawano K, Nishizono A *et al.* Oncolytic viral therapy for human pancreatic cancer cells by reovirus. (2003) *Clin.Cancer Res.* **9**, 1218-1223.

Ewing DD, Sargent MD, and Borsa J. Switch-on of transcriptase function in reovirus: analysis of polypeptide changes using 2-D gels. (1985) *Virology* **144**, 448-456.

Favre D and Trepo C. Translational extracts active biologically in vitro obtained from eukaryotic monolayer cells: a versatile method for viral RNA studies. (2001) *J.Virol.Methods* **92**, 177-181.

Fearon ER, Cho KR, Nigro JM, Kern SE, Simons JW, Ruppert JM *et al.* Identification of a chromosome 18q gene that is altered in colorectal cancers. (1990) *Science* **247**, 49-56.

Feig LA. Ral-GTPases: approaching their 15 minutes of fame. (2003) *Trends Cell Biol.* **13**, 419-425.

Fiordalisi JJ, Johnson RL, Ulku AS, Der CJ, and Cox AD. Mammalian expression vectors for Ras family proteins: generation and use of expression constructs to analyze Ras family function. (2001) *Methods Enzymol.* **332**, 3-36.

Forsyth P, Roldan G, George D, Wallace C, Palmer CA, Morris D *et al.* A phase I trial of intratumoral administration of reovirus in patients with histologically confirmed recurrent malignant gliomas. (2008) *Mol.Ther.* **16**, 627-632.

Foster BA, Coffey HA, Morin MJ, and Rastinejad F. Pharmacological rescue of mutant p53 conformation and function. (1999) *Science* **286**, 2507-2510.

Freedman DA, Wu L, and Levine AJ. Functions of the MDM2 oncoprotein. (1999) *Cell Mol.Life Sci.* **55**, 96-107.

Friedler A, Hansson LO, Veprintsev DB, Freund SM, Rippin TM, Nikolova PV *et al.* A peptide that binds and stabilizes p53 core domain: chaperone strategy for rescue of oncogenic mutants. (2002) *Proc.Natl.Acad.Sci.U.S.A* **99**, 937-942.

Fueyo J, Gomez-Manzano C, Alemany R, Lee PS, McDonnell TJ, Mitlianga P *et al.* A mutant oncolytic adenovirus targeting the Rb pathway produces anti-glioma effect in vivo. (2000) *Oncogene* **19**, 2-12.

Furuichi Y, LaFiandra A, and Shatkin AJ. 5'-Terminal structure and mRNA stability. (1977) *Nature* **266**, 235-239.

Galanis E. Therapeutic potential of oncolytic measles virus: promises and challenges. (2010) *Clin.Pharmacol.Ther.* **88**, 620-625.

Ghosh S and Karin M. Missing pieces in the NF-kappaB puzzle. (2002) *Cell* **109 Suppl**, S81-S96.

GILMAN A and PHILIPS FS. The Biological Actions and Therapeutic Applications of the B-Chloroethyl Amines and Sulfides. (1946) *Science* **103**, 409-436.

Goldberg IH. The interaction of actinomycin with DNA. (1971) *Antibiot.Chemother.* **17**, 67-86.

Goldberg IH, Rabinowitzk M, and REICH E. Basis of actinomycin action. II. Effect of actinomycin on the nucleoside triphosphate-inorganic pyrophosphate exchange. (1963) *Proc.Natl.Acad.Sci.U.S.A* **49**, 226-229.

Goldberg IH and REICH E. Actinomycin inhibition of RNA synthesis directed by DNA. (1964) *Fed.Proc.* **23**, 958-964.

Gollamudi R, Ghalib MH, Desai KK, Chaudhary I, Wong B, Einstein M *et al.* Intravenous administration of Reolysin, a live replication competent RNA virus is safe in patients with advanced solid tumors. (2010) *Invest New Drugs* **28**, 641-649.

Gollob JA, Wilhelm S, Carter C, and Kelley SL. Role of Raf kinase in cancer: therapeutic potential of targeting the Raf/MEK/ERK signal transduction pathway. (2006) *Semin.Oncol.* **33**, 392-406.

Goodrum FD and Ornelles DA. p53 status does not determine outcome of E1B 55-kilodalton mutant adenovirus lytic infection. (1998) *J.Virol.* **72**, 9479-9490.

Gordon M and Baksh S. RASSF1A: Not a prototypical Ras effector. (2011) *Small Gtpases.* **2**, 148-157.

Grasberger BL, Lu T, Schubert C, Parks DJ, Carver TE, Koblish HK *et al.* Discovery and cocrystal structure of benzodiazepinedione HDM2 antagonists that activate p53 in cells. (2005) *J.Med.Chem.* **48**, 909-912.

Gujar SA, Marcato P, Pan D, and Lee PW. Reovirus virotherapy overrides tumor antigen presentation evasion and promotes protective antitumor immunity. (2010) *Mol.Cancer Ther.* **9**, 2924-2933.

Gujar SA, Pan DA, Marcato P, Garant KA, and Lee PW. Oncolytic virus-initiated protective immunity against prostate cancer. (2011) *Mol.Ther.* **19**, 797-804.

Guse K, Cerullo V, and Hemminki A. Oncolytic vaccinia virus for the treatment of cancer. (2011) *Expert.Opin.Biol.Ther.* **11**, 595-608.

Hainaut P and Hollstein M. p53 and human cancer: the first ten thousand mutations. (2000) *Adv.Cancer Res.* **77**, 81-137.

Hamad NM, Elconin JH, Karnoub AE, Bai W, Rich JN, Abraham RT *et al.* Distinct requirements for Ras oncogenesis in human versus mouse cells. (2002) *Genes Dev.* **16**, 2045-2057.

Hanel EG, Xiao Z, Wong KK, Lee PW, Britten RA, and Moore RB. A novel intravesical therapy for superficial bladder cancer in an orthotopic model: oncolytic reovirus therapy. (2004) *J.Urol.* **172**, 2018-2022.

Hansberger MW, Campbell JA, Danthi P, Arrate P, Pennington KN, Marcu KB *et al.* IkappaB kinase subunits alpha and gamma are required for activation of NF-kappaB and induction of apoptosis by mammalian reovirus. (2007) *J.Virol.* **81**, 1360-1371.

Harrington KJ, Karapanagiotou EM, Roulstone V, Twigger KR, White CL, Vidal L *et al.* Two-stage phase I dose-escalation study of intratumoral reovirus type 3 dearing and palliative radiotherapy in patients with advanced cancers. (2010a) *Clin.Cancer Res.* **16**, 3067-3077.

Harrington KJ, Vile RG, Melcher A, Chester J, and Pandha HS. Clinical trials with oncolytic reovirus: moving beyond phase I into combinations with standard therapeutics. (2010b) *Cytokine Growth Factor Rev.* **21**, 91-98.

Hashiro G, Loh PC, and Yau JT. The preferential cytotoxicity of reovirus for certain transformed cell lines. (1977) *Arch.Virol.* **54**, 307-315.

Heid CA, Stevens J, Livak KJ, and Williams PM. Real time quantitative PCR. (1996) *Genome Res.* **6**, 986-994.

Heinemann L, Simpson GR, Boxall A, Kottke T, Relph KL, Vile R *et al.* Synergistic effects of oncolytic reovirus and docetaxel chemotherapy in prostate cancer. (2011) *BMC.Cancer* **11**, 221-

Heise C, Hermiston T, Johnson L, Brooks G, Sampson-Johannes A, Williams A *et al.* An adenovirus E1A mutant that demonstrates potent and selective systemic anti-tumoral efficacy. (2000) *Nat.Med.* **6**, 1134-1139.

Henry DO, Moskalenko SA, Kaur KJ, Fu M, Pestell RG, Camonis JH *et al.* Ral GTPases contribute to regulation of cyclin D1 through activation of NF-kappaB. (2000) *Mol.Cell Biol.* **20**, 8084-8092.

Hermann L, Embree J, Hazelton P, Wells B, and Coombs RT. Reovirus type 2 isolated from cerebrospinal fluid. (2004) *Pediatr.Infect.Dis.J.* **23**, 373-375.

Heusch M, Lin L, Geleziunas R, and Greene WC. The generation of nfkb2 p52: mechanism and efficiency. (1999) *Oncogene* **18**, 6201-6208.

Hingorani P, Zhang W, Lin J, Liu L, Guha C, and Kolb EA. Systemic administration of reovirus (Reolysin) inhibits growth of human sarcoma xenografts. (2011) *Cancer* **117**, 1764-1774.

Hirasawa K, Nishikawa SG, Norman KL, Alain T, Kossakowska A, and Lee PW. Oncolytic reovirus against ovarian and colon cancer. (2002) *Cancer Res.* **62**, 1696-1701.

Ho WC, Fitzgerald MX, and Marmorstein R. Structure of the p53 core domain dimer bound to DNA. (2006) *J.Biol.Chem.* **281**, 20494-20502.

Holm GH, Zurney J, Tumilasci V, Leveille S, Danthi P, Hiscott J *et al.* Retinoic acid-inducible gene-I and interferon-beta promoter stimulator-1 augment proapoptotic responses following mammalian reovirus infection via interferon regulatory factor-3. (2007) *J.Biol.Chem.* **282**, 21953-21961.

Hori T, Kondo T, Kanamori M, Tabuchi Y, Ogawa R, Zhao QL *et al.* Nutlin-3 enhances tumor necrosis factor-related apoptosis-inducing ligand (TRAIL)-induced apoptosis through up-regulation of death receptor 5 (DR5) in human sarcoma HOS cells and human colon cancer HCT116 cells. (2010) *Cancer Lett.* **287**, 98-108.

Huang S, Qu LK, and Koromilas AE. Induction of p53-dependent apoptosis in HCT116 tumor cells by RNA viruses and possible implications in virus-mediated oncolysis. (2004) *Cell Cycle* **3**, 1043-1045.

Imada K. Immunodeficient mouse models of lymphoid tumors. (2003) *Int.J.Hematol.* **77**, 336-341.

Inoue J, Gohda J, Akiyama T, and Semba K. NF-kappaB activation in development and progression of cancer. (2007) *Cancer Sci.* **98**, 268-274.

Issaeva N, Bozko P, Enge M, Protopopova M, Verhoef LG, Masucci M *et al.* Small molecule RITA binds to p53, blocks p53-HDM-2 interaction and activates p53 function in tumors. (2004) *Nat.Med.* **10**, 1321-1328.

Izaurralde E and Mattaj IW. RNA export. (1995) *Cell* **81**, 153-159.

Jayasuriya AK, Nibert ML, and Fields BN. Complete nucleotide sequence of the M2 gene segment of reovirus type 3 dearing and analysis of its protein product mu 1. (1988) *Virology* **163**, 591-602.

Jeffers JR, Parganas E, Lee Y, Yang C, Wang J, Brennan J *et al.* Puma is an essential mediator of p53-dependent and -independent apoptotic pathways. (2003) *Cancer Cell* **4**, 321-328.

Jiang J, Hermann L, and Coombs KM. Genetic characterization of a new mammalian reovirus, type 2 Winnipeg (T2W). (2006) *Virus Genes* **33**, 193-204.

Johansson PJ, Sveger T, Ahlfors K, Ekstrand J, and Svensson L. Reovirus type 1 associated with meningitis. (1996) *Scand.J.Infect.Dis.* **28**, 117-120.

Karin M. Nuclear factor-kappaB in cancer development and progression. (2006) *Nature* **441**, 431-436.

Karin M and Ben-Neriah Y. Phosphorylation meets ubiquitination: the control of NF-[kappa]B activity. (2000) *Annu.Rev.Immunol.* **18**, 621-663.

Karin M, Cao Y, Greten FR, and Li ZW. NF-kappaB in cancer: from innocent bystander to major culprit. (2002) *Nat.Rev.Cancer* **2**, 301-310.

Kauffmann-Zeh A, Rodriguez-Viciana P, Ulrich E, Gilbert C, Coffer P, Downward J *et al.* Suppression of c-Myc-induced apoptosis by Ras signalling through PI(3)K and PKB. (1997) *Nature* **385**, 544-548.

Kennedy NJ and Davis RJ. Role of JNK in tumor development. (2003) *Cell Cycle* **2**, 199-201.

Kern SE, Kinzler KW, Bruskin A, Jarosz D, Friedman P, Prives C *et al.* Identification of p53 as a sequence-specific DNA-binding protein. (1991) *Science* **252**, 1708-1711.

Kim M, Egan C, Alain T, Urbanski SJ, Lee PW, Forsyth PA *et al.* Acquired resistance to reoviral oncolysis in Ras-transformed fibrosarcoma cells. (2007) *Oncogene* **26**, 4124-4134.

Kim M, Williamson CT, Prudhomme J, Bebb DG, Riabowol K, Lee PW *et al.* The viral tropism of two distinct oncolytic viruses, reovirus and myxoma virus, is modulated by cellular tumor suppressor gene status. (2010) *Oncogene* **29**, 3990-3996.

Kobayashi T, Antar AA, Boehme KW, Danthi P, Eby EA, Guglielmi KM *et al.* A plasmid-based reverse genetics system for animal double-stranded RNA viruses. (2007) *Cell Host.Microbe* **1**, 147-157.

Kobayashi T, Chappell JD, Danthi P, and Dermody TS. Gene-specific inhibition of reovirus replication by RNA interference. (2006) *J.Virol.* **80**, 9053-9063.

Kolwijck E, Massuger LF, Thomas CM, Span PN, Krasovec M, Kos J *et al.* Cathepsins B, L and cystatin C in cyst fluid of ovarian tumors. (2010) *J.Cancer Res.Clin.Oncol.* **136**, 771-778.

Kominsky DJ, Bickel RJ, and Tyler KL. Reovirus-induced apoptosis requires both death receptor- and mitochondrial-mediated caspase-dependent pathways of cell death. (2002a) *Cell Death.Differ.* **9**, 926-933.

Kominsky DJ, Bickel RJ, and Tyler KL. Reovirus-induced apoptosis requires mitochondrial release of Smac/DIABLO and involves reduction of cellular inhibitor of apoptosis protein levels. (2002b) *J.Virol.* **76**, 11414-11424.

Le Boeuf F and Bell JC. United virus: the oncolytic tag-team against cancer!. (2010) *Cytokine Growth Factor Rev.* **21**, 205-211.

Lech PJ and Russell SJ. Use of attenuated paramyxoviruses for cancer therapy. (2010) *Expert.Rev.Vaccines.* **9**, 1275-1302.

Lee PP, Yee C, Savage PA, Fong L, Brockstedt D, Weber JS *et al.* Characterization of circulating T cells specific for tumor-associated antigens in melanoma patients. (1999) *Nat.Med.* **5**, 677-685.

Leitner S, Sweeney K, Oberg D, Davies D, Miranda E, Lemoine NR *et al.* Oncolytic adenoviral mutants with E1B19K gene deletions enhance gemcitabine-induced apoptosis in pancreatic carcinoma cells and anti-tumor efficacy in vivo. (2009) *Clin.Cancer Res.* **15**, 1730-1740.

Lemieux R, Zarbl H, and Millward S. mRNA discrimination in extracts from uninfected and reovirus-infected L-cells. (1984) *J.Virol.* **51**, 215-222.

Levicar N, Nuttall RK, and Lah TT. Proteases in brain tumour progression. (2003) *Acta Neurochir.(Wien.)* **145**, 825-838.

Levine AJ, Wu MC, Chang A, Silver A, Attiyeh EF, Lin J *et al.* The spectrum of mutations at the p53 locus. Evidence for tissue-specific mutagenesis, selection of mutant alleles, and a "gain of function" phenotype. (1995) *Ann.N.Y.Acad.Sci.* **768**, 111-128.

Liemann S, Chandran K, Baker TS, Nibert ML, and Harrison SC. Structure of the reovirus membrane-penetration protein, Mu1, in a complex with is protector protein, Sigma3. (2002) *Cell* **108**, 283-295.

Liu X, Yue P, Khuri FR, and Sun SY. p53 upregulates death receptor 4 expression through an intronic p53 binding site. (2004) *Cancer Res.* **64**, 5078-5083.

Loken SD, Norman K, Hirasawa K, Nodwell M, Lester WM, and Demetrick DJ. Morbidity in immunosuppressed (SCID/NOD) mice treated with reovirus (dearing 3) as an anti-cancer biotherapeutic. (2004) *Cancer Biol.Ther.* **3**, 734-738.

Lolkema MP, Arkenau HT, Harrington K, Roxburgh P, Morrison R, Roulstone V *et al.* A phase I study of the combination of intravenous reovirus type 3 Dearing and gemcitabine in patients with advanced cancer. (2011) *Clin.Cancer Res.* **17**, 581-588.

Longley DB, Harkin DP, and Johnston PG. 5-fluorouracil: mechanisms of action and clinical strategies. (2003) *Nat.Rev.Cancer* **3**, 330-338.

Lyman MA, Aung S, Biggs JA, and Sherman LA. A spontaneously arising pancreatic tumor does not promote the differentiation of naive CD8+ T lymphocytes into effector CTL. (2004) *J.Immunol.* **172**, 6558-6567.

Ma L, Chen Z, Erdjument-Bromage H, Tempst P, and Pandolfi PP. Phosphorylation and functional inactivation of TSC2 by Erk implications for tuberous sclerosis and cancer pathogenesis. (2005) *Cell* **121**, 179-193.

Maginnis MS, Forrest JC, Kopecky-Bromberg SA, Dickeson SK, Santoro SA, Zutter MM *et al.* Beta1 integrin mediates internalization of mammalian reovirus. (2006) *J.Virol.* **80**, 2760-2770.

Malumbres M and Pellicer A. RAS pathways to cell cycle control and cell transformation. (1998) *Front Biosci.* **3**, d887-d912.

Malys N and McCarthy JE. Translation initiation: variations in the mechanism can be anticipated. (2011) *Cell Mol.Life Sci.* **68**, 991-1003.

Mandinova A and Lee SW. The p53 pathway as a target in cancer therapeutics: obstacles and promise. (2011) *Sci.Transl.Med.* **3**, 64rv1-

Marcato P, Dean CA, Giacomantonio CA, and Lee PW. Oncolytic reovirus effectively targets breast cancer stem cells. (2009) *Mol.Ther.* **17**, 972-979.

Marcato P, Shmulevitz M, Pan D, Stoltz D, and Lee PW. Ras transformation mediates reovirus oncolysis by enhancing virus uncoating, particle infectivity, and apoptosis-dependent release. (2007) *Mol.Ther.* **15**, 1522-1530.

Melcher A, Parato K, Rooney CM, and Bell JC. Thunder and lightning: immunotherapy and oncolytic viruses collide. (2011) *Mol.Ther.* **19**, 1008-1016.

Meley D, Spiller DG, White MR, McDowell H, Pizer B, and See V. p53-mediated delayed NF-kappaB activity enhances etoposide-induced cell death in medulloblastoma 1. (2010) *Cell Death.Dis.* **1**, e41-

Mendez II, Hermann LL, Hazelton PR, and Coombs KM. A comparative analysis of freon substitutes in the purification of reovirus and calicivirus. (2000) *J.Virol.Methods* **90**, 59-67.

Mendez II, Weiner SG, She YM, Yeager M, and Coombs KM. Conformational changes accompany activation of reovirus RNA-dependent RNA transcription. (2008) *J.Struct.Biol.* **162**, 277-289.

Meylan E and Tschopp J. Toll-like receptors and RNA helicases: two parallel ways to trigger antiviral responses. (2006) *Mol.Cell* **22**, 561-569.

Milner J and Medcalf EA. Cotranslation of activated mutant p53 with wild type drives the wild-type p53 protein into the mutant conformation. (1991) *Cell* **65**, 765-774.

Milner J, Medcalf EA, and Cook AC. Tumor suppressor p53: analysis of wild-type and mutant p53 complexes. (1991) *Mol.Cell Biol.* **11**, 12-19.

Miyashita T and Reed JC. Tumor suppressor p53 is a direct transcriptional activator of the human bax gene. (1995) *Cell* **80**, 293-299.

Momand J, Jung D, Wilczynski S, and Niland J. The MDM2 gene amplification database. (1998) *Nucleic Acids Res.* **26**, 3453-3459.

Muller M, Wilder S, Bannasch D, Israeli D, Lehlbach K, Li-Weber M *et al.* p53 activates the CD95 (APO-1/Fas) gene in response to DNA damage by anticancer drugs. (1998) *J.Exp.Med.* **188**, 2033-2045.

Nakano K and Vousden KH. PUMA, a novel proapoptotic gene, is induced by p53. (2001) *Mol.Cell* **7**, 683-694.

Nibert ML, Odegard AL, Agosto MA, Chandran K, and Schiff LA. Putative autocleavage of reovirus mu1 protein in concert with outer-capsid disassembly and activation for membrane permeabilization. (2005) *J.Mol.Biol.* **345**, 461-474.

Nibert ML, Schiff LA and Fields BN. (2001). *Fields Virology*. Knipe D M. and Howley P M. (eds). Lippincott-Raven Press: Philadelphia, pp. 1679-1728.

Norman KL, Coffey MC, Hirasawa K, Demetrick DJ, Nishikawa SG, DiFrancesco LM *et al.* Reovirus oncolysis of human breast cancer. (2002) *Hum.Gene Ther.* **13**, 641-652.

Norman KL, Hirasawa K, Yang AD, Shields MA, and Lee PW. Reovirus oncolysis: the Ras/RalGEF/p38 pathway dictates host cell permissiveness to reovirus infection. (2004) *Proc.Natl.Acad.Sci.U.S.A* **101**, 11099-11104.

Noser JA, Mael AA, Sakuma R, Ohmine S, Marcato P, Lee PW *et al.* The RAS/Raf1/MEK/ERK signaling pathway facilitates VSV-mediated oncolysis: implication for the defective interferon response in cancer cells. (2007) *Mol.Ther.* **15**, 1531-1536.

O'Donnell SM, Holm GH, Pierce JM, Tian B, Watson MJ, Chari RS *et al.* Identification of an NF-kappaB-dependent gene network in cells infected by mammalian reovirus. (2006) *J.Virol.* **80**, 1077-1086.

O'Mullane L and Eperon IC. The pre-mRNA 5' cap determines whether U6 small nuclear RNA succeeds U1 small nuclear ribonucleoprotein particle at 5' splice sites. (1998) *Mol.Cell Biol.* **18**, 7510-7520.

O'Shea CC, Johnson L, Bagus B, Choi S, Nicholas C, Shen A *et al.* Late viral RNA export, rather than p53 inactivation, determines ONYX-015 tumor selectivity. (2004) *Cancer Cell* **6**, 611-623.

Oberhaus SM, Smith RL, Clayton GH, Dermody TS, and Tyler KL. Reovirus infection and tissue injury in the mouse central nervous system are associated with apoptosis. (1997) *J.Virol.* **71**, 2100-2106.

Oda E, Ohki R, Murasawa H, Nemoto J, Shibue T, Yamashita T *et al.* Noxa, a BH3-only member of the Bcl-2 family and candidate mediator of p53-induced apoptosis. (2000) *Science* **288**, 1053-1058.

Ohlen C, Kalos M, Cheng LE, Shur AC, Hong DJ, Carson BD *et al.* CD8(+) T cell tolerance to a tumor-associated antigen is maintained at the level of expansion rather than effector function. (2002) *J.Exp.Med.* **195**, 1407-1418.

Ouattara LA, Barin F, Barthez MA, Bonnaud B, Roingeard P, Goudeau A *et al.* Novel human reovirus isolated from children with acute necrotizing encephalopathy. (2011) *Emerg.Infect.Dis.* **17**, 1436-1444.

Palombella VJ, Rando OJ, Goldberg AL, and Maniatis T. The ubiquitin-proteasome pathway is required for processing the NF-kappa B1 precursor protein and the activation of NF-kappa B. (1994) *Cell* **78**, 773-785.

Pandha HS, Heinemann L, Simpson GR, Melcher A, Prestwich R, Errington F *et al.* Synergistic effects of oncolytic reovirus and cisplatin chemotherapy in murine malignant melanoma. (2009) *Clin.Cancer Res.* **15**, 6158-6166.

Paul RW, Choi AH, and Lee PW. The alpha-anomeric form of sialic acid is the minimal receptor determinant recognized by reovirus. (1989) *Virology* **172**, 382-385.

Pesonen S, Kangasniemi L, and Hemminki A. Oncolytic adenoviruses for the treatment of human cancer: focus on translational and clinical data. (2011) *Mol.Pharm.* **8**, 12-28.

Pett DM, Vanaman TC, and Joklik WK. Studies on the amino and carboxyl terminal amino acid sequences of reovirus capsid polypeptides. (1973) *Virology* **52**, 174-186.

Prestwich RJ, Errington F, Ilett EJ, Morgan RS, Scott KJ, Kottke T *et al.* Tumor infection by oncolytic reovirus primes adaptive antitumor immunity. (2008) *Clin.Cancer Res.* **14**, 7358-7366.

Prestwich RJ, Errington F, Steele LP, Ilett EJ, Morgan RS, Harrington KJ *et al.* Reciprocal human dendritic cell-natural killer cell interactions induce antitumor activity following tumor cell infection by oncolytic reovirus. (2009a) *J.Immunol.* **183**, 4312-4321.

Prestwich RJ, Ilett EJ, Errington F, Diaz RM, Steele LP, Kottke T *et al.* Immune-mediated antitumor activity of reovirus is required for therapy and is independent of direct viral oncolysis and replication. (2009b) *Clin.Cancer Res.* **15**, 4374-4381.

Qiao J, Wang H, Kottke T, White C, Twigger K, Diaz RM *et al.* Cyclophosphamide facilitates antitumor efficacy against subcutaneous tumors following intravenous delivery of reovirus. (2008) *Clin.Cancer Res.* **14**, 259-269.

Rabinovich GA, Gabrilovich D, and Sotomayor EM. Immunosuppressive strategies that are mediated by tumor cells. (2007) *Annu.Rev.Immunol.* **25**, 267-296.

Ramos-Alvarez M and Sabin AB. Enteropathogenic viruses and bacteria; role in summer diarrheal diseases of infancy and early childhood. (1958) *J.Am.Med.Assoc.* **167**, 147-156.

Rangarajan A, Hong SJ, Gifford A, and Weinberg RA. Species- and cell type-specific requirements for cellular transformation. (2004) *Cancer Cell* **6**, 171-183.

Rasmussen L and Arvin A. Chemotherapy-induced immunosuppression. (1982) *Environ.Health Perspect.* **43**, 21-25.

Reddy GK and Bukowski RM. Sorafenib: recent update on activity as a single agent and in combination with interferon-alpha2 in patients with advanced-stage renal cell carcinoma. (2006) *Clin.Genitourin.Cancer* **4**, 246-248.

Reichard KW, Lorence RM, Cascino CJ, Peeples ME, Walter RJ, Fernando MB *et al.* Newcastle disease virus selectively kills human tumor cells. (1992) *J.Surg.Res.* **52**, 448-453.

Rezai K, Lokiec F, Grandjean I, Weill S, de CP, Bordier V *et al.* Impact of imatinib on the pharmacokinetics and in vivo efficacy of etoposide and/or ifosfamide. (2007) *BMC.Pharmacol.* **7**, 13-

Riolobos L, Valle N, Hernando E, Maroto B, Kann M, and Almendral JM. Viral oncolysis that targets Raf-1 signaling control of nuclear transport. (2010) *J.Virol.* **84**, 2090-2099.

Roberts PJ and Der CJ. Targeting the Raf-MEK-ERK mitogen-activated protein kinase cascade for the treatment of cancer. (2007) *Oncogene* **26**, 3291-3310.

Rodenhuis S. ras and human tumors. (1992) *Semin.Cancer Biol.* **3**, 241-247.

Rodgers SE, Barton ES, Oberhaus SM, Pike B, Gibson CA, Tyler KL *et al.* Reovirus-induced apoptosis of MDCK cells is not linked to viral yield and is blocked by Bcl-2. (1997) *J.Virol.* **71**, 2540-2546.

Rodriguez-Viciana P, Warne PH, Khwaja A, Marte BM, Pappin D, Das P *et al.* Role of phosphoinositide 3-OH kinase in cell transformation and control of the actin cytoskeleton by Ras. (1997) *Cell* **89**, 457-467.

Rommelaere J, Geletneky K, Angelova AL, Daeffler L, Dinsart C, Kiprianova I *et al.* Oncolytic parvoviruses as cancer therapeutics. (2010) *Cytokine Growth Factor Rev.* **21**, 185-195.

Rosen L, Hovis JF, Mastrota FM, Bell JA, and Huebner RJ. Observations on a newly recognized virus (Abney) of the reovirus family. (1960) *Am.J.Hyg.* **71**, 258-265.

Ryan KM, Ernst MK, Rice NR, and Vousden KH. Role of NF-kappaB in p53-mediated programmed cell death. (2000) *Nature* **404**, 892-897.

Ryan KM, O'Prey J, and Vousden KH. Loss of nuclear factor-kappaB is tumor promoting but does not substitute for loss of p53. (2004) *Cancer Res.* **64**, 4415-4418.

Sabin AB. Reoviruses. A new group of respiratory and enteric viruses formerly classified as ECHO type 10 is described. (1959) *Science* **130**, 1387-1389.

Sarinella F, Calistri A, Sette P, Palu G, and Parolin C. Oncolysis of pancreatic tumour cells by a gamma34.5-deleted HSV-1 does not rely upon Ras-activation, but on the PI 3-kinase pathway. (2006) *Gene Ther.* **13**, 1080-1087.

Schomer-Miller B, Higashimoto T, Lee YK, and Zandi E. Regulation of IkappaB kinase (IKK) complex by IKKgamma-dependent phosphorylation of the T-loop and C terminus of IKKbeta. (2006) *J.Biol.Chem.* **281**, 15268-15276.

Schonberg M, Silverstein SC, Levin DH, and Acs G. Asynchronous synthesis of the complementary strands of the reovirus genome. (1971) *Proc.Natl.Acad.Sci.U.S.A* **68**, 505-508.

Schreck R and Rapp UR. Raf kinases: oncogenesis and drug discovery. (2006) *Int.J.Cancer* **119**, 2261-2271.

Sei S, Mussio JK, Yang QE, Nagashima K, Parchment RE, Coffey MC *et al.* Synergistic antitumor activity of oncolytic reovirus and chemotherapeutic agents in non-small cell lung cancer cells. (2009) *Mol.Cancer* **8**, 47-

Sharpe AH, Chen LB, and Fields BN. The interaction of mammalian reoviruses with the cytoskeleton of monkey kidney CV-1 cells. (1982) *Virology* **120**, 399-411.

Shaw RJ and Cantley LC. Ras, PI(3)K and mTOR signalling controls tumour cell growth. (2006) *Nature* **441**, 424-430.

Sheikh MS, Burns TF, Huang Y, Wu GS, Amundson S, Brooks KS *et al.* p53-dependent and -independent regulation of the death receptor KILLER/DR5 gene expression in response to genotoxic stress and tumor necrosis factor alpha. (1998) *Cancer Res.* **58**, 1593-1598.

Shieh GS, Shiau AL, Yo YT, Lin PR, Chang CC, Tzai TS *et al.* Low-dose etoposide enhances telomerase-dependent adenovirus-mediated cytosine deaminase gene therapy through augmentation of adenoviral infection and transgene expression in a syngeneic bladder tumor model. (2006) *Cancer Res.* **66**, 9957-9966.

Shields JM, Pruitt K, McFall A, Shaub A, and Der CJ. Understanding Ras: 'it ain't over 'til it's over'. (2000) *Trends Cell Biol.* **10**, 147-154.

Shmulevitz M, Pan LZ, Garant K, Pan D, and Lee PW. Oncogenic Ras promotes reovirus spread by suppressing IFN-beta production through negative regulation of RIG-I signaling. (2010) *Cancer Res.* **70**, 4912-4921.

Shuman S. Capping enzyme in eukaryotic mRNA synthesis. (1995) *Prog.Nucleic Acid Res.Mol.Biol.* **50**, 101-129.

Siebenlist U, Franzoso G, and Brown K. Structure, regulation and function of NF-kappa B. (1994) *Annu.Rev.Cell Biol.* **10**, 405-455.

Skup D and Millward S. Reovirus-induced modification of cap-dependent translation in infected L cells. (1980) *Proc.Natl.Acad.Sci.U.S.A* **77**, 152-156.

Smakman N, van den Wollenberg DJ, Borel R, I, Hoeben RC, and Kranenburg O. Sensitization to apoptosis underlies KrasD12-dependent oncolysis of murine C26 colorectal carcinoma cells by reovirus T3D. (2005) *J.Virol.* **79**, 14981-14985.

Smakman N, van den Wollenberg DJ, Elias SG, Sasazuki T, Shirasawa S, Hoeben RC *et al.* KRAS(D13) Promotes apoptosis of human colorectal tumor cells by ReovirusT3D and oxaliplatin but not by tumor necrosis factor-related apoptosis-inducing ligand. (2006a) *Cancer Res.* **66**, 5403-5408.

Smakman N, van der Bilt JD, van den Wollenberg DJ, Hoeben RC, Borel R, I, and Kranenburg O. Immunosuppression promotes reovirus therapy of colorectal liver metastases. (2006b) *Cancer Gene Ther.* **13**, 815-818.

Smith CC, Nelson J, Aurelian L, Gober M, and Goswami BB. Ras-GAP binding and phosphorylation by herpes simplex virus type 2 RR1 PK (ICP10) and activation of the Ras/MEK/MAPK mitogenic pathway are required for timely onset of virus growth. (2000) *J.Virol.* **74**, 10417-10429.

Smith JA, Schmechel SC, Williams BR, Silverman RH, and Schiff LA. Involvement of the interferon-regulated antiviral proteins PKR and RNase L in reovirus-induced shutoff of cellular translation. (2005) *J.Virol.* **79**, 2240-2250.

Smith KD, Mezhir JJ, Bickenbach K, Veerapong J, Charron J, Posner MC *et al.* Activated MEK suppresses activation of PKR and enables efficient replication and in vivo oncolysis by Deltagamma(1)34.5 mutants of herpes simplex virus 1. (2006) *J.Virol.* **80**, 1110-1120.

Smith RE, Zweerink HJ, and Joklik WK. Polypeptide components of virions, top component and cores of reovirus type 3. (1969) *Virology* **39**, 791-810.

Sobell HM. Actinomycin and DNA transcription. (1985) *Proc.Natl.Acad.Sci.U.S.A* **82**, 5328-5331.

Staveley-O'Carroll K, Sotomayor E, Montgomery J, Borrello I, Hwang L, Fein S *et al.* Induction of antigen-specific T cell anergy: An early event in the course of tumor progression. (1998) *Proc.Natl.Acad.Sci.U.S.A* **95**, 1178-1183.

Steele L, Errington F, Prestwich R, Ilett E, Harrington K, Pandha H *et al.* Pro-inflammatory cytokine/chemokine production by reovirus treated melanoma cells is PKR/NF-kappaB mediated and supports innate and adaptive anti-tumour immune priming. (2011) *Mol.Cancer* **10**, 20-

Stewart TJ and Abrams SI. How tumours escape mass destruction. (2008) *Oncogene* **27**, 5894-5903.

Strano S, Dell'Orso S, Di AS, Fontemaggi G, Sacchi A, and Blandino G. Mutant p53: an oncogenic transcription factor. (2007) *Oncogene* **26**, 2212-2219.

Strong JE, Coffey MC, Tang D, Sabinin P, and Lee PW. The molecular basis of viral oncolysis: usurpation of the Ras signaling pathway by reovirus. (1998) *EMBO J.* **17**, 3351-3362.

Strong JE and Lee PW. The v-erbB oncogene confers enhanced cellular susceptibility to reovirus infection. (1996) *J.Virol.* **70**, 612-616.

Strong JE, Tang D, and Lee PW. Evidence that the epidermal growth factor receptor on host cells confers reovirus infection efficiency. (1993) *Virology* **197**, 405-411.

Strozyk E, Poppelmann B, Schwarz T, and Kulms D. Differential effects of NF-kappaB on apoptosis induced by DNA-damaging agents: the type of DNA damage determines the final outcome. (2006) *Oncogene* **25**, 6239-6251.

Sturzenbecker LJ, Nibert M, Furlong D, and Fields BN. Intracellular digestion of reovirus particles requires a low pH and is an essential step in the viral infectious cycle. (1987) *J.Virol.* **61**, 2351-2361.

Takai S, Kimura K, Nagaki M, Satake S, Kakimi K, and Moriwaki H. Blockade of neutrophil elastase attenuates severe liver injury in hepatitis B transgenic mice. (2005) *J.Virol.* **79**, 15142-15150.

Takai Y, Sasaki T, and Matozaki T. Small GTP-binding proteins. (2001) *Physiol Rev.* **81**, 153-208.

Takaoka A, Hayakawa S, Yanai H, Stoiber D, Negishi H, Kikuchi H *et al.* Integration of interferon-alpha/beta signalling to p53 responses in tumour suppression and antiviral defence. (2003) *Nature* **424**, 516-523.

Thanos D and Maniatis T. NF-kappa B: a lesson in family values. (1995) *Cell* **80**, 529-532.

Thornborrow EC, Patel S, Mastropietro AE, Schwartzfarb EM, and Manfredi JJ. A conserved intronic response element mediates direct p53-dependent transcriptional activation of both the human and murine bax genes. (2002) *Oncogene* **21**, 990-999.

Tovar C, Rosinski J, Filipovic Z, Higgins B, Kolinsky K, Hilton H *et al.* Small-molecule MDM2 antagonists reveal aberrant p53 signaling in cancer: implications for therapy. (2006) *Proc.Natl.Acad.Sci.U.S.A* **103**, 1888-1893.

Traenckner EB, Pahl HL, Henkel T, Schmidt KN, Wilk S, and Baeuerle PA. Phosphorylation of human I kappa B-alpha on serines 32 and 36 controls I kappa B-alpha proteolysis and NF-kappa B activation in response to diverse stimuli. (1995) *EMBO J.* **14**, 2876-2883.

Twigger K, Vidal L, White CL, De Bono JS, Bhide S, Coffey M *et al.* Enhanced in vitro and in vivo cytotoxicity of combined reovirus and radiotherapy. (2008) *Clin.Cancer Res.* **14**, 912-923.

Tyler KL, Barton ES, Ibach ML, Robinson C, Campbell JA, O'Donnell SM *et al.* Isolation and molecular characterization of a novel type 3 reovirus from a child with meningitis. (2004) *J.Infect.Dis.* **189**, 1664-1675.

Tyler KL, Squier MK, Rodgers SE, Schneider BE, Oberhaus SM, Grdina TA *et al.* Differences in the capacity of reovirus strains to induce apoptosis are determined by the viral attachment protein sigma 1. (1995) *J.Virol.* **69**, 6972-6979.

Urano T, Emkey R, and Feig LA. Ral-GTPases mediate a distinct downstream signaling pathway from Ras that facilitates cellular transformation. (1996) *EMBO J.* **15**, 810-816.

Urbanelli L, Trivelli F, Ercolani L, Sementino E, Magini A, Tancini B *et al.* Cathepsin L increased level upon Ras mutants expression: the role of p38 and p44/42 MAPK signaling pathways. (2010) *Mol.Cell Biochem.* **343**, 49-57.

van England M, Nieland LJ, Ramaekers FC, Schutte B, and Reutelingsperger CP. Annexin V-affinity assay: a review on an apoptosis detection system based on phosphatidylserine exposure. (1998) *Cytometry* **31**, 1-9.

Vassilev LT, Vu BT, Graves B, Carvajal D, Podlaski F, Filipovic Z *et al.* In vivo activation of the p53 pathway by small-molecule antagonists of MDM2. (2004) *Science* **303**, 844-848.

Vidal L, Pandha HS, Yap TA, White CL, Twigger K, Vile RG *et al.* A phase I study of intravenous oncolytic reovirus type 3 Dearing in patients with advanced cancer. (2008) *Clin.Cancer Res.* **14**, 7127-7137.

Vousden KH and Lane DP. p53 in health and disease. (2007) *Nat.Rev.Mol.Cell Biol.* **8**, 275-283.

Wang F, Ma Y, Barrett JW, Gao X, Loh J, Barton E *et al.* Disruption of Erk-dependent type I interferon induction breaks the myxoma virus species barrier. (2004) *Nat.Immunol.* **5**, 1266-1274.

Wang G, Barrett JW, Stanford M, Werden SJ, Johnston JB, Gao X *et al.* Infection of human cancer cells with myxoma virus requires Akt activation via interaction with a viral ankyrin-repeat host range factor. (2006) *Proc.Natl.Acad.Sci.U.S.A* **103**, 4640-4645.

Weissbach H, Redfield B, O'Connor T, and Chirigos MA. Studies on the disposition of actinomycin D-3H in virus-infected and tumor-bearing mice. (1966) *Cancer Res.* **26**, 1832-1838.

Wennier S, Li S, and McFadden G. Oncolytic virotherapy for pancreatic cancer. (2011) *Expert.Rev.Mol.Med.* **13**, e18-

White CL, Twigger KR, Vidal L, De Bono JS, Coffey M, Heinemann L *et al.* Characterization of the adaptive and innate immune response to intravenous oncolytic reovirus (Dearing type 3) during a phase I clinical trial. (2008) *Gene Ther.* **15**, 911-920.

Whiteside ST, Epinat JC, Rice NR, and Israel A. I kappa B epsilon, a novel member of the I kappa B family, controls RelA and cRel NF-kappa B activity. (1997) *EMBO J.* **16**, 1413-1426.

Whiteside TL. Immune suppression in cancer: effects on immune cells, mechanisms and future therapeutic intervention. (2006) *Semin.Cancer Biol.* **16**, 3-15.

Wittinghofer A. Signal transduction via Ras. (1998) *Biol.Chem.* **379**, 933-937.

Wuerzberger-Davis SM, Chang PY, Berchtold C, and Miyamoto S. Enhanced G2-M arrest by nuclear factor-{kappa}B-dependent p21waf1/cip1 induction. (2005) *Mol.Cancer Res.* **3**, 345-353.

Wyllie AH, Kerr JF, and Currie AR. Cell death: the significance of apoptosis. (1980) *Int.Rev.Cytol.* **68**, 251-306.

Yamamoto T, Ohno T, Wakahara K, Nagano A, Kawai G, Saitou M *et al.* Simultaneous inhibition of mitogen-activated protein kinase and phosphatidylinositol 3-kinase pathways

augment the sensitivity to actinomycin D in Ewing sarcoma. (2009) *J.Cancer Res.Clin.Oncol.* **135**, 1125-1136.

Yamaoka S, Courtois G, Bessia C, Whiteside ST, Weil R, Agou F *et al.* Complementation cloning of NEMO, a component of the IkappaB kinase complex essential for NF-kappaB activation. (1998) *Cell* **93**, 1231-1240.

Yang WQ, Lun X, Palmer CA, Wilcox ME, Muzik H, Shi ZQ *et al.* Efficacy and safety evaluation of human reovirus type 3 in immunocompetent animals: racine and nonhuman primates. (2004) *Clin.Cancer Res.* **10**, 8561-8576.

Yin J, Pollock C, Tracy K, Chock M, Martin P, Oberst M *et al.* Activation of the RalGEF/Ral Pathway Promotes Prostate Cancer Metastasis to Bone. (2007) *Mol.Cell Biol.* **21**, 7538-50.

Yoon SS, Carroll NM, Chiocca EA, and Tanabe KK. Cancer gene therapy using a replication-competent herpes simplex virus type 1 vector. (1998) *Ann.Surg.* **228**, 366-374.

Yu J and Zhang L. Apoptosis in human cancer cells. (2004) *Curr.Opin.Oncol.* **16**, 19-24.

Yujiri T, Ware M, Widmann C, Oyer R, Russell D, Chan E *et al.* MEK kinase 1 gene disruption alters cell migration and c-Jun NH2-terminal kinase regulation but does not cause a measurable defect in NF-kappa B activation. (2000) *Proc.Natl.Acad.Sci.U.S.A* **97**, 7272-7277.

Zarbl H, Skup D, and Millward S. Reovirus progeny subviral particles synthesize uncapped mRNA. (1980) *J.Virol.* **34**, 497-505.

Zhang G, Gurtu V, Kain SR, and Yan G. Early detection of apoptosis using a fluorescent conjugate of annexin V. (1997) *Biotechniques* **23**, 525-531.

Appendix A: List of Primers

Bax-rt-fwd: 5’-TCAGGATGCGTCCACCAAGAAG-3’

Bax-rt-fwd: 5’-TGTGTCCACGGCGGCAATCATC-3’

DR4-rt-fwd: 5’-AGAGAGAAGTCCCTGCACCA-3’

DR4-rt-fwd: 5’-GTCACTCCAGGGCGTACAAT-3’

DR5-rt-fwd: 5’-CACCAGGTGTGATTCAGGTG-3’

DR5-rt-fwd: 5’-CCCCACTGTGCTTTGTACCT-3’

GAPDH-rt-fwd: 5’-GAGTCAACGGATTTGGTCGT-3’

GAPDH-rt-fwd: 5’-TTGATTTTGGAGGGATCTCG-3’

Noxa-rt-fwd: 5’-CTTGGAAACGGAAGATGGAA-3’

Noxa-rt-fwd: 5’-CACAGTAGGCCAGCGGTAAT-3’

PUMA-rt-fwd: 5’-GACGACCTCAACGCACAGTA-3’

PUMA-rt-fwd: 5’-CACCTAATTGGGCTCCATCT-3’

p21-rt-fwd: 5’-GACACCACTGGAGGGTGATC-3’

p21-rt-fwd: 5’-CAGGTCCACATGGTCTTCCT-3’

TRAIL-rt-fwd: 5’-TTCACAGTGCTCCTGCAGTC-3’

TRAIL-rt-fwd: 5’-CAGCAGGGGCTGTTCATACT-3’

SMP-PCR-F: 5’-CTGACTCGAGAAGGTATATTGCTGTTGACAGTGAGCG-3’

SMP-PCR-R: 5’-CTGACAATTCCGAGGCAGTAGGCA -3’

Appendix B: Acknowledgement of Journals and Copyright Permission

1. Chapter 1, Figure 1.1, 1.2 and 1.3

Modified from RNA Virus: Host Signaling Responses to reovirus Infection, Da Pan, Paola Marcato, Maya Shmulevitz, Patrick W.K. Lee, edited by Decheng Yang, copyright@ 2009 by World Scientific Publishing Co. Pte. Ltd.

Requests and responses for permission to reproduce the figures:

Request -1:

To whom it may concern,

I am a phD student at Dalhousie University in Halifax, Nova Scotia, Canada. I am currently finishing up my phD dissertation and would like to reuse some figures that were published in our book chapter in your book (RNA viruses-Host gene response to infections). It would be a great help if I were to be able to use them and I am unsure of the process to attain permission. If you could direct me in the proper procedures, it would be a great help. Thank you in advance.

Sincerely,

Da Pan

Response-1:

Dear Da Pan

Thanks for your email to us. Please let me have the details of those figures which you plan to reuse from your book chapter from 'RNA Viruses'.

Kind regards

Tu Ning

Request-2:

Dear Tu,

Thank you for replying me and thank you for your help in advance.

I was the first author of the Chapter 26, Section IV of the book "Double-Stranded RNA Virus", "Host Signaling Responses to reovirus Infection". pp627-653. I will be reusing all the figures in the chapter (Figs 1, 2 and 3) in my thesis and they would be my Fig1.1, 1.2 and 1.3.

Regards,

Da Pan

Response-2:

Dear Da Pan

We would be pleased to grant you the permission of reproducing the Fig 1-3 from chapter 26 of our title 'RNA Virus: Host Signaling Responses to reovirus Infection". pp627-653 in your thesis, provided that full acknowledgment given to the original source with the following format:

Title of the Work, Author (s) and/or Editor(s) Name (s), Copyright @ year and name of the publisher

Kind regards

Tu Ning

2. Chapter 3, Figure 3.1-3.12 and chapter 5, Figure 5.2, 5.3 and 5.5

Figures 3.1-3.12 modified from: Stabilisation of p53 enhances reovirus-induced apoptosis and virus spread through p53-dependent NF-κB activation. Da Pan, Lu-Zhe Pan, Richard Hill, Paola Marcato, Maya Shmulevitz, Lyubomir T Vassilev and Patrick W.K. Lee, Br J Cancer. 2011 doi: 10.1038/bjc.2011.325. [Epub ahead of print].

Figures 5.3, 5.2 and 5.5 modified from: **Ras** transformation mediates **reovirus** oncolysis by enhancing virus uncoating, particle infectivity, and apoptosis-dependent release. Paola Marcato, Maya Shmulevitz, Da Pan, Don Stoltz and Patrick W.K. Lee, Mol Ther. 2007 15(8): 1522-30. Epub 2007 Apr 24.

Requests and responses for permission to reproduce the figures:

Request -1:

To whom it may concern,

I am a phD student at Dalhousie University in Halifax, Nova Scotia, Canada. I am currently finishing up my phD dissertation and would like to reuse some figures that were published in our paper in your journal. It would be a great help if I were to be able to use them and I am unsure of the process to attain permission. If you could direct me in the proper procedures, it would be a great help. Thank you in advance.

Sincerely,

Da Pan

Response-1:

Dear Sir/Madam,

Thank you for your *Nature* permissions request. Please provide details of the figures you would like to use and where they can be found on Rightslink so I can help you get permission for this use.

Kind regards,

Charlotte Kinnah

Request-2:

Thank you for replying me concerning the letters of copyright permission.

I will need permissions to reuse the figures or/and content from three papers published by Nature Publishing Group.

1) Published by **Molecular Therapy** (ISSN 1525-0016)

The title of the paper is:

Ras Transformation Mediates Reovirus Oncolysis by Enhancing Virus Uncoating, Particle Infectivity, and Apoptosis-dependent Release (doi:10.1038/sj.mt.6300179)

Authors: Marcato P, Shmulevitz M, Pan D, Stoltz D and Lee PW.

I will need to use Fig. 1, Fig. 3a and Fig. 5 for my thesis.

2) Published by **Molecular Therapy** (ISSN 1525-0016)

The title of the paper is: Oncolytic virus-initiated protective immunity against prostate cancer (doi:10.1038/mt.2010.297)

Authors: Gujar SA, Pan D, Marcato P, Garant KA, Lee PW.

I will need Fig. 1 for my thesis.

3) Published by **British Journal of Cancer** (ISSN 0007-0920)

The title of the paper is: Stabilisation of p53 enhances reovirus-induced apoptosis and virus spread through p53-dependent NF-*k*B activation (doi:10.1038/bjc.2011.325)

Authors: Pan D, Pan LZ, Hill R, Marcato P, Shmulevitz M, Vassilev LT, Lee PW.

I will need the whole article for my thesis.

Thank you in advance for your help and please let me know whether you need more information.

Sincerely,

Da Pan

Response-2:

Dear Dr. Pan,

Thank you for the details. Permission is not required for this use as authors retain the right to reproduce figures in other works created by them. All that is required is an acknowledgement of the journal and Nature Publishing Group. Please refer to the Molecular Therapy http://www.nature.com/mt/for_authors.html and British Journal of Cancer http://www.nature.com/bjc/authors/index.html author information for your reference.

Kind regards,

Charlotte Kinnah